ABSTRACT

MAGNETIC MINERALS AND PROPERTIES OF THE MELROSE STOCK

By

Dewey Dennis Sanderson

An integrated petrologic-magnetic rock property study was conducted on the Melrose Stock, an early Cretaceous Basin and Range intrusive in eastern Nevada. The stock was delineated into a monzonite and a quartz monzonite pluton with evidence that the former was emplaced first.

The magnetite content and magnetic properties of remanence and susceptibility are about twice as great in the monzonite as in the quartz monzonite. Both rock units contain a major soft remanent component, placing the reliability of the remanent measurements and their paleomagnetic significance in doubt, even with alternating field demagnetization. However, the remanence indicates that the horst of which the intrusive is a part has undergone structural rotation of approximately 15°. The difference between the paleo-pole positions of the two plutons suggests an interval of time between their emplacement and crystallization.

Only one-third of the NRM remained after magnetic cleaning to 100 oersteds. Storage tests revealed that in 100 days up to 50 percent of the NRM was a soft VRM. This, however, was easily removed with approximately

20 oersteds of demagnetization.

The opaque mineral assemblage of the two rock types is essentially identical, approximately 90 percent magnetite and 10 percent ilmenite. The compositions are near the stoichiometric values. Within a one mile wide zone adjacent to the intrusive margin, the titanium is tied up in sphene rather than ilmenite because of the influence of the carbonate host rock assimilated during crystallization. The ilmenite which formed deep within the magma chamber exhibits abundant exsolution of hematite.

A technique (the association coefficient) developed to quantitatively determine the microscopic distribution of the magnetite with relation to the constituent minerals in the rock suggests that the magnetite formed throughout much of the crystallization by three processes: direct precipitation, oxidation and alteration. Oxidation refers to magnetite formed as one ferromagnesian mineral is converted to another under oxidizing conditions during the normal sequence of crystallization. Magnetite by alteration (deuteric and hydrothermal) is formed by late stage fluids reacting with the ferromagnesian minerals as in chloritization and serpentinization. relative amounts of magnetite formed by direct precipitation, oxidation, and alteration in this order are 65, 25, and 10 percent in the quartz monzonite and 45, 30, and 25 percent in the monzonite. The association study is used as a

Dewey Dennis Sanderson qualitative index to changes in the oxidation state of the crystallizing magma with respect to rock type, time and space.

The magnetite grain size distribution of the quartz monzonite is coarser than the monzonite. Furthermore, the magnetite grains associated with the ferromagnesian minerals are notably coarser than the grains associated with the nonferromagnesian mineral fraction. The factors of time and availability of iron by oxidation have influenced the variation of the magnetite grain size. The difference in the grain size distribution of the two rock types is expressed as a more stable remanence of the monzonite than the quartz monzonite.

The magnetic susceptibility of the two rock types
was effectively delineated by in situ and core specimen
measurements. The in situ coil yields better quality
data as well as the capacity to better resolve magnetic
units than laboratory measurements on core specimens.
To obtain a representative value of magnetic susceptibility, a site density of approximately one site per square
mile was found to be sufficient for an intrusive the size
of the Melrose Stock (12 square miles). The number of sites
is more critical than the number of measurements per site
when establishing representative susceptibilities.

MAGNETIC MINERALS AND PROPERTIES OF THE MELROSE STOCK

By

Dewey Dennis Sanderson

A THESIS

Submitted to
Michigan State University
in partial fulfillment of the requirements
for the degree of

DOCTOR OF PHILOSOPHY

Department of Geology

675830

ACKNOWLEDGMENTS

I wish to express my sincerest gratitude to Dr. William J. Hinze, my thesis advisor, for his guidance, advice, suggestions and time during the course of this study. In addition, his contribution to my learning while at East Lansing is most gratefully acknowledged.

Dr. Thomas A. Vogel gave generously of his time throughout the course of the study and reviewing the manuscript; his help is greatly appreciated.

Special thanks are extended to Mr. John D. Corbett for making this study possible while he was employed by the Anaconda Company.

The author wishes to thank Drs. Harold Stonehouse, James Trow and Hugh Bennett for their comment and evaluation of the manuscript.

My wife, Sharon, deserves special recognition and thanks for her patience and understanding and for her time spent in typing the drafts of this thesis.

TABLE OF CONTENTS

Chapter														Page
I.	INTROD	UCTION	•	•	•	•	•	•	•	•	•	•	•	1
	1.1	Objec	tive	8	•	•	•	•	•	•	•	•	•	1
		Geolo						•	•	•		•	•	3
		Rock							•		•	•	•	8
II.	PETROL	OGIC P	ROPE	RTI	ES	•	•	•	•	•	•	•	•	11
	2.1	Petro	logy	' •	•	•	•	•	•	•	•	•	•	11
			.1						•	•	•	•	•	11
		2.1	. 2	Mod	lal	Ana	lys	is	•	•	•	•	•	12
		2.1	.3	Mic	cros	cor	oic	Des	cri	.pti	on	•	•	17
	2.2	Appar					e I	ist	rit	outi	on			
		of 1	Magn	eti	lte	•	•	•	•	•	•	•	•	22
	2.3	Opaqu	в Ре	tro	olog	ЭY	•	•	•	•	•	•	•	32
			.1						•	•	•	•	•	32
		2.3	. 2	Mag	met	tite	- (Iln	neni	.te	•	•	•	33
		2.3	. 3	Sph	ene	₽.	•	•	•	•	•	•	•	37
		2.3	.4	Her	nat:	ite	•	•	•	•	•	•	•	42
	2.4	Assoc	iati	.on	Coe	effi	cie	ent	•	•	•	•	•	50
		_	.1					-	•	•	•	•	•	50
			. 2						•	•	•	•	•	51
			.3								•	•	•	53
		2.4	.4			gic neti							•	
						icie			•			•	_	58
		2.4	• 5					-	-	ret	ati	lon	•	6 2
	2.5	The I	nter	sti	iti	al-J	[nc]	lu si	lon	Ind	lex	•	•	75
	2.6	Magne			nd 1	the	Fer	ron	nagr	nesi	lan	Mir	1 —	97
		878												₩ '/

Chapter											Page
III.	MAGNET	IC SUSCEP	TIBILII	Y.	•	•	•	•	•	•	95
	3.1	Introduc	tion .	•	•	•	•	•	•	•	95
		3.1.1	Purpos	se .	•	•	•	•	•	•	95
		3.1.2	Source	s of	Va	ria	tio	n.	•	•	96
		3.1.3	Source Measur	remen	t V	ari	ati	ons	•	•	97
	3.2	Discussi	on of F	Resul	.ts	•	•	•	•	•	99
		3.2.1	Normal	l ver	sus	Lo	gri	thm:	ic		
			Dist	tribu	itio	n.	•	•	•	•	99
			Inters	site	Var:	iat	ion	s.	•	•	100
		3.2.3	In Sit	tu .	•	•	•	•	•	•	104
		3.2.4	In Sit	•	•	•	•	•	•	•	107
	3.3	Sampling	• • •	•	•	•	•	•	•	•	114
	3 1	Suscepti	hilitu	bac	+ha	Co	0 M A	+	۸£		
	J.4		trusive								119
		Cite III	CT GDT AG	•	•	•	•	•	•	•	113
	3.5	Suscepti	bility	and	Mag	net:	ite	•	•	•	125
IV.	REMANE	NT MAGNET	IZATION	1 .	•	•	•	•	•	•	132
	4.1	Introduc	tion .		_	_	_		_		132
	4.2	Introduc NRM Resu	lts.	•	•	•	•	•	•	•	133
							•				
			NRM Da								133
		4,2,2	NRM Di	Lrect	ion	3.	•	•	•	•	141
	4.3	Alternat	ing Fie	eld D	e ma	gne	tiz	atio	on	•	145
		4.3.1	Prelin	ninar	v De	e m a	an e	tiza	a –		
				1 .	_		_				145
		4.3.2	Demagr	etiz	ati	on a	at	Opt:	imi	m	
				els.							158
		4.3.3	Remane	ent I	nte	nsi	tie	s.	•	•	163
	4.4	Storage	Tests .		•	•	•	•	•	•	167
		4 4 1	Storag	TA DY	.000	dur	_				167
			Result							•	168
		4.4.2	Demagr	osti =		• •	. ÷	• •	-64	•	100
		4,4,3									175
			Samp	ples	•	•	•	•	•	•	175
	4.5	Q-Ratios	• • •	•	•	•	•	•	•	•	185
	4.6	Paleomag	netism,	•	•	•	•	•	•	•	191
V.	SUMMAR	Υ						_		_	197

Chapte	Br																P age	
REFERI	ENCI	ES	CI	TED	•	•	•	•	•	•	•	•	•	•	•	•	204	
APPENI	DIX	A	•	•	•	•	•	•	•	•	•	•	•	•	•	•	208	
(Gene	Bre	al !	Rema	arkı	B O	n M	lagı	neti	c P	rop	ert	ies	•	•	•	208	
APPENI	DIX	В	•	•	•	•	•	•	•	•	•	•	•	•	•	•	215	
	Opac	que	e M	ine	ral	Sp	eci	.es	and	Th	eir	Re	lat	ive				
									•				•	•	•	•	215	
APPEN	DIX	С	•	•	•	•	•	•	•	•	•	•	•	•	•	•	217	
1	NRM	Re	e s u	lts	bv	Si	te		•	•	•		•		•		217	

LIST OF TABLES

Table	•	E	age
2-1.	Modal analysis minimums, maximums, and means of the Melrose Stock	•	21
2-2.	Percentage of opaque grains greater than 50 microns in diameter	•	30
2-3.	Probability model for association coefficients	•	55
2-4.	Source of excess magnetite associated with the ferromagnesian minerals in percent of total magnetite content	•	69
2-5.	Percent magnetite to total magnetite content formed by alteration, oxidation reaction, and direct precipitation	l •	74
3-1.	Magnetic susceptibility sampling matrix in percent deviation from the grand mean of the quartz monzonite pluton	•	115
3-2.	Magnetic susceptibility sampling matrix in percent deviation from the grand mean of the monzonite pluton	•	116
4-1.	Comparison of NRM data of Sites 1-17 with reduction to field and laboratory orientations	•	140
4-2.	NRM results of 29 sites grouped in various combinations	•	142
4-3.	50 oersted demagnetization results of 29 sites grouped in various combinations	•	160
4-4.	100 oersted demagnetization results of 28 sites grouped in various combinations	•	161
4-5.	Remanent magnetization intensities (x10 ⁻⁴ emu/cc)	•	164

rable													Page
4-6.	Remanent inter	nsi	ty :	rat	ios	•	•	•	•	•	•	•	166
4-7.	Results of Sto	ora	g e	tes	t.	•	•	•	•	•	•	•	174
4-8.	Paleomagnetic poles determined from the 19												
	NRM results.	•	•	•	•	•	•	•	•	•	•	•	194
A-1.	Opaque Data.	•	•	•	•	•	•	•	•	•	•	•	215
A-2.	NRM Data		•	•		•	•	•	•	•	•	•	217

LIST OF FIGURES

Figure		Page
1-1.	Index map of east-central Nevada showing location of the Melrose Stock. Modified after G.G. Snow	5
1-2.	Generalized geologic map and site locations of the Melrose Stock (after G.G. Snow)	7
2-1.	Partial modal analyses of rocks of the Melrose Stock. Rock composition fields of the U.S. Geological Survey are shown	13
2-2.	Modal analyses of rocks from the Melrose Stock	15
2-3.	Rock types of the Melrose Stock based upon modal analyses	16
2-4a.	Apparent grain size distribution within the monzonite pluton. 1) opaques associated with the quartz-feldspar fraction. 2) opaques associated with the ferromagnesian fraction.	25
2-4b.	Apparent opaque grain size distribution within the monzonite pluton. 1) opaques associated with the quartz-feldspar fraction. 2) opaques associated with the ferromagnesian fraction	26
2-5a.	Apparent opaque grain size distribution within the quartz monzonite pluton. 1) opaques associated with the quartz-feld-spar fraction. 2) opaques associated with the ferromagnesian fraction	27
2-5b.	Apparent opaque grain size distribution within the quartz monzonite pluton. 1) opaques associated with the quartz-feld-spar fraction. 2) opaques associated with	
	the ferromagnesian fraction	28

Figure		P	age
2-6a,b.	Electron microprobe microphotograph of an ilmenite grain with hematite exsolution and a sphene reaction rim, a, sample current; b, titanium fluorescence	•	35
2-6c, d.	Electron microprobe microphotograph of an ilmenite grain with hematite exsolu- tion and a sphene reaction rim. c, cal- cium fluorescence; d, iron fluorescence.	•	3 6
2-7.	Distribution of sphene	•	39
2—8.	Distribution of hematite exsolution within ilmenite	•	44
2—9.	Distribution of exsolution bearing ilmenite with respect to site elevation	•	4 6
2-10.	Opaque mineral zones within the stock reflecting the geometry of the magma chamber. Line A-A' is the location of profile of Figure 2-11	•	48
2-11.	Cross-section of the Melrose Stock show- ing the observed opaque mineral zoning. See Figure 2-9 for location of profile .	•	49
2-1 2.	Schematic diagram of data collection procedure for the association coefficients of W with respect to minerals X,Y, and Z. Graticule of ocular shown on each W grain. Counts are made at the points indicated by arrows. The resulting point counts, associations, and association coefficients are		
5-1 3.	shown in the accompanying table Frequency of occurrence of the association coefficients of the constituent minerals by rock type for magnetite	•	52 63
2-14.	by rock type for magnetite	3	73
2-1 5.	Distribution of the interstitial-inclusion index for the quartz monzonite and monzonite rock types		76

Figure		Page
2-16.	Interstitial-inclusion index spatial distribution	. 77
2-17,	Variation of the interstitial-inclusion in- dex with elevation within the quartz mon- zonite pluton	. 79
2-18.	Variation of quartz content with elevation within the quartz monzonite pluton	81
2-19,	Variation of the interstitial-inclusion index with elevation within the monzonite pluton	. 83
2-20.	Variation of quartz content with elevation within the monzonite pluton	85
2-21,	Diagramatic sketch of the high and low interstitial-inclusion index zones with-in the monzonite pluton and the interpreted cross section of the pluton	86
2-22,	Relationship of magnetite content to ferro-magnesian content according to rock type	. 88
² -23,	Variation of the hornblende association coefficient with ferromagnesian content within the quartz monzonite pluton	90
2-2 4 .	The relationship of the hornblende association coefficient with elevation within the quartz monzonite pluton. Excludes data of sites showing appreciable hydrothermal alteration of the ferromagnesian minerals	91.
² -25,	Magnetite content versus percent hornblende to percent ferromagnesian content with respect to rock type	92
3-1,	Distribution of individual in situ magnetic susceptibility measurements in the monzon-ite pluton on linear and logrithmic scales	101
3-2.	Distribution of individual in situ mag- netic susceptibility measurements in the quartz monzonite pluton on linear and	102
	logrithmic scales	102

Figure		Page
3-3,	Site susceptibility extremes versus site means of in situ measurements. Unity slope line separates maximum and minimum values. Included are the intercept, slope, standard error of the estimate, and correlation coefficient for each of the data groups.	103
3-4.	Site susceptibility extremes versus site means of in situ measurements after rejection of anomalous data. Unity slope line separates maximum and minimum values. Included are the intercept, slope, standard error of the estimate, and correlation coefficient for each of the data groups	106
3-5,	Site susceptibility extremes versus site means of core specimen measurements. Unity slope line separates maximum and minimum values. Included are the intercept, slope, standard error of the estimate, and correlation coefficient for each of the data groups	108
3-6.	Site susceptibility extremes versus site means of core specimen measurements after rejection of anomalous data. Unity slope line separates maximum and minimum values. Included are the intercept, slope, standard error of the estimate, and correlation coefficient for each of the data groups	109
3-7.	Magnetic susceptibility distributions of in situ and core specimen measurements by rock type	111
3-8.	Spatial distribution of in situ magnetic susceptibility and aeromagnetic lows	120
3-9.	In situ magnetic susceptibility versus distance from the south contact of the Melrose Stock	121
3-10.	Variation of in situ magnetic suscepti- bility with elevation within the mon- zonite pluton	123

Figure		E	Page
3–11.	Variation of in situ magnetic suscepti- bility with elevation within the quartz monzonite pluton	•	124
3-12.	Volume of magnetite as a function of ele- vation within the quartz monzonite pluton.	•	126
3-13.	Distribution of magnetite content by site with respect to rock type	•	127
3-14.	Magnetic susceptibility versus magnetite content. The expected susceptibility-magnetite relationship (Mooney and Bleifuss, 1953) is indicated by the solid line. The best fit line through the data is indicated by the dashed line		128
4-1.	NRM site circles of confidence according to time of collection. a) 1968 specimens, 18 months of storage; b) 1970 specimens, 1 month of storage	•	134
4-2a,	NRM of Site 10, directions and intensities. Equal area projection	•	136
4-2b.	NRM of Site 21, directions and intensities. Equal area projection	•	137
4 -3,	NRM site circles of confidence before (a) and after (b) rejection of anomalous data	•	138
4-4.	NRM directions of 29 sites grouped in various combinations. Circles of confidence shown for the 1970 monzonite sites and the 1970 quartz monzonite sites.	•	143
4-5a.	A.f. demagnetization results of Site VN-4	•	147
4-5b.	A.f. demagnetization results of Site VN-10		
4-5c.	A.f. demagnetization results of Site VN-13	•	149
4-5d.	A.f. demagnetization results of Site VN-19	•	150

Figure		Page
4-5 e.	A.f. demagnetization results of Site VN-20	151
4-5f.	A.f. demagnetization results of Site VN-22	152
4 –5g.	A.f. demagnetization results of Site VN-25	153
4-5h.	A.f. demagnetization results of Site VN-30	154
4-5i,	A.f. demagnetization results of Site VN-31	155
4-6.	Mean site directions for NRM, 50, 100, 150, 200, and 300 oersteds demagnetization of Sites 4, 10, and 13, those collected in 1968. Equal area projection	156
4-7.	Mean site directions for NRM, 50, 100, 150, 200, and 300 oersteds demagnetization of Sites 19, 20, 22, 25, 30, and 31, those collected in 1970. Equal area projection.	157
4-8.	NRM, 50, and 100 oersted demagneti- zation directions of the monzonite and quartz monzonite collected in 1968 and 1970. Numbers refer to Tables 4-2, 4-3, and 4-4 and are located at the NRM po- sitions. Equal area projection	162
4 -9.	Migration of remanent magnetization upon storage in the laboratory	169
4-10.	Intensity of VRM acquired during storage in the laboratory	170
4-11.	Intensity of VRM acquired for two specimens from Site 32 during storage in the laboratory	171
4-12.	Plot of VRM acquisition with respect to time	173
4-13a.	Storage test and demagnetization of specimen VN-30A-A	176

Figure		Page
4-13b.	Storage test and demagnetization of specimen VN-32A-2	177
4-13c.	Storage test and demagnetization of specimen VN-32B	178
4-13d.	Storage test and demagnetization of specimen VN-41B	179
4-13 e .	Storage test and demagnetization of specimen VN-41C	180
4-13£,	Storage test and demagnetization of specimen VN-41D	181
1-13g,	Storage test and demagnetization of specimen VN-47A	182
l-13h,	Storage test and demagnetization of specimen VN-47D	183
4-14.	Distribution of Q ratios by rock type	187
4-15,	Q ratios versus distance from south contact in the monzonite pluton	190
4-16.	Paleomagnetic pole positions of the 1970 NRM along with rotations of the poles corresponding to rotations of the Melrose	
_	Stock horst	193
A-1.	Compositional relationships of the major	211

CHAPTER I

INTRODUCTION

1.1 Objectives

The magnetic properties of rocks are a function of their compositions, origin, and geological history. Consequently, magnetic rock properties can be extremely useful geological tools. The primary use of rock magnetism studies is in delineating paleomagnetic field directions. As a result studies have concentrated on rocks which are known to exhibit relatively stable remanent magnetism. Particular emphasis has been placed upon investigations Of volcanic, basic intrusive, and sedimentary rocks. In Contrast, acidic to intermediate composition intrusive igneous rocks have received limited attention despite their wide spread occurrence and geological importance because The general instability of their remanent magnetism. Paleomagnetic data obtained from granite intrusives have been reported by Currie and others (1963), Opdyke and Wensink (1966), Gromme (1967), May (1968), and Hanna (19₆₉₋₁₉₇₀₎.

A quartz monzonite intrusive, the Melrose Stock, in the Dolly Varden Mountains of eastern Nevada is the

investigation. The general objective of this study is to determine the mineralogic, petrologic, and geometric controls on the magnetic rock properties and their spatial variations in this Basin and Range type pluton. This will be investigated through an intensive study of the opaque mineralogy, remanent magnetism and magnetic susceptibility. The specific objectives of this investigation are:

- 1) To determine the variations of magnetic susceptibility and remanent magnetization between and within the lithologies of the intrusive;
- 2) To relate the paragenesis, occurrence, distribution, association, composition, and texture of the magnetic minerals to the susceptibility and remanence:
- 3) To determine the effect of the intrusive's geometry on the magnetic susceptibility and remanence;
- 4) To use the magnetic minerals and their properties to decipher the intrusive's cooling and emplacement history;
- 5) To assess the effects of weathering on the magnetic properties of surface samples;
- 6) To use paleomagnetism to detect structural rotation in the Melrose Stock.

Achievement of these objectives will provide a more

variations in the magnetic properties of the Melrose Stock in particular and of the Basin and Range type intrusive in general. In addition, the study will demonstrate how magnetic rock properties can be used to solve geologic problems, will provide information on sampling requirements for a magnetic rock properties study and finally will provide the magnetic interpreter with magnetic rock property data, their variation and significance for an intrusive this type.

1 2 Geology of the Area

The Dolly Varden Mountains have been studied by only

few investigators. A rather comprehensive study of the

mountains was conducted by Geoffrey G. Snow as a Ph.D.

secretation at the University of Utah in 1963. Previously

Ported studies by J.M. Hill (1916) on the general geology

ore deposits of the range represents the only other

Published work. The Dolly Varden Mountains are mentioned

y Zirkel (1876) and Emmons (1877) as part of reconnai
ance geologic surveys. There has been periodic work done

in the area by mining and petroleum companies, but the

results of their projects are not available. The petrology

of the Melrose Stock is the result of this investigation

and the general geology reported herein is based on the

observations of Snow.

The Dolly Varden Range is a horst in the Basin and

Range Province in east-central Nevada (Figure 1-1). The nearly north-south trending range rises over 2,000 feet above the surrounding alluvial filled valleys. Even though the area is semi-arid with less than 10 inches of rain a Year, vegetation and wildlife are plentiful. The mountains provide a wide spectrum of geologic features to observe and study. Rock types include a sedimentary sequence, an intrusive complex, both flow and pyroclastic volcanics and locally metamorphosed sediments. Tectonic activity has resulted in a number of structural relationships.

The oldest exposed rocks in the range are of Mississip-Pian age, but these comprise only 5 percent of the sedimen-Tary column. Pennsylvanian rocks are not present. Nearly lacktriangle lacktriangle 000 feet of Permian limestones, dolomites, sandstones and siltstones are exposed throughout the range and only 100 Eet of Triassic limestone attest to a Mesozoic deposi-Cional record. A hiatus from Triassic to Oligicene time Places Tertiary volcanics unconformably on the sediments and the intrusive. The volcanics are composed of flows, I Snimbrites and pyroclastics of varying composition. Mio-Cene or Pliocene age deposits include minor and local vol-Canics and fresh water sediments. Youngest of the deposits are the Quaternary lake deposits, presumably related to Former Lake Bonneville. The Melrose Stock, which occupies the core of the range, has an exposure of approximately 12 square miles. A potassium-argon age determination on biotite from the monzonite places the age of the intrusive

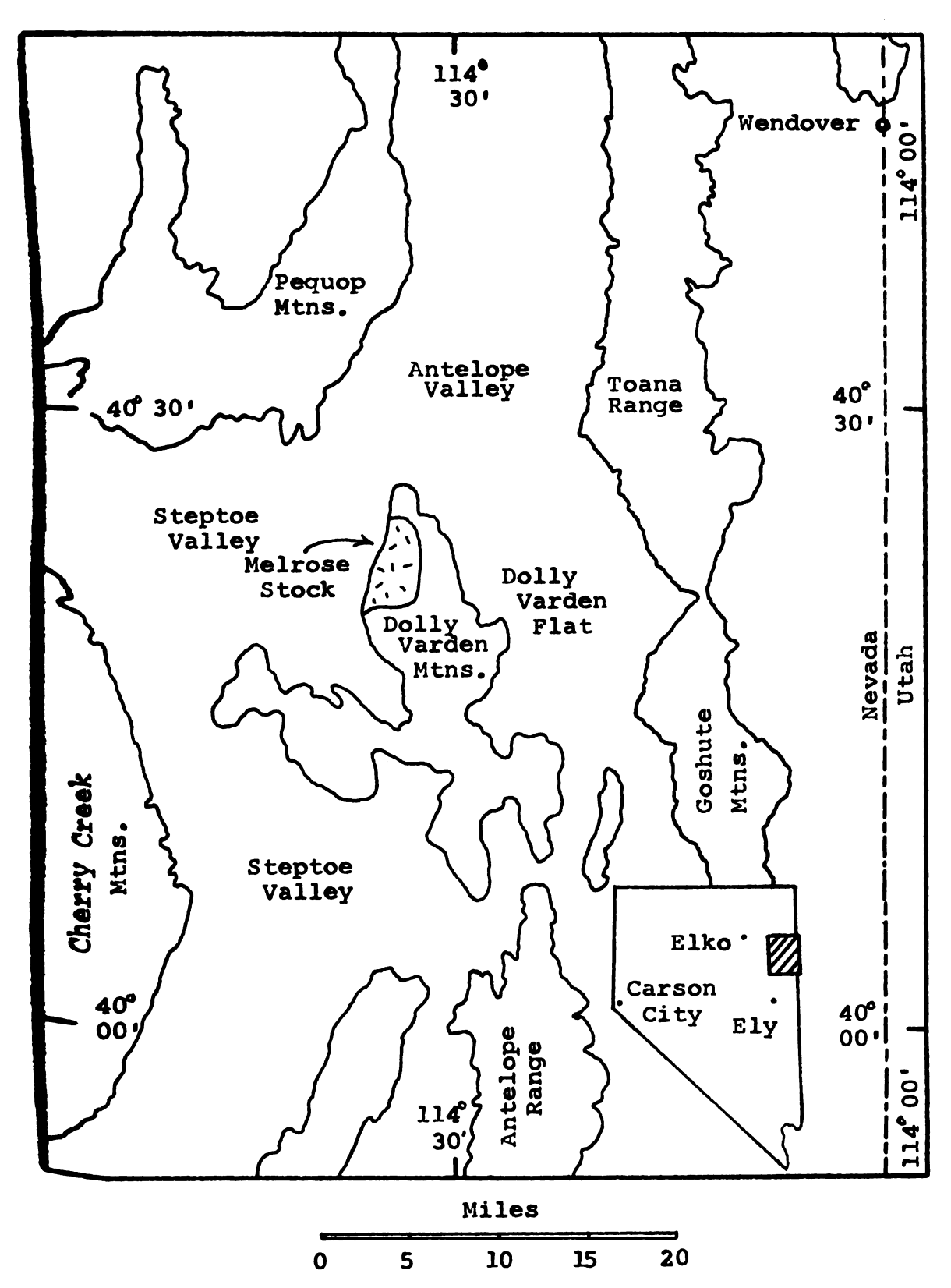


Figure 1-1. Index map of east-central Nevada showing location of the Melrose Stock. Modified after G.G. Snow.

at 125 m.y. or early Cretaceous (Armstrong, 1963).

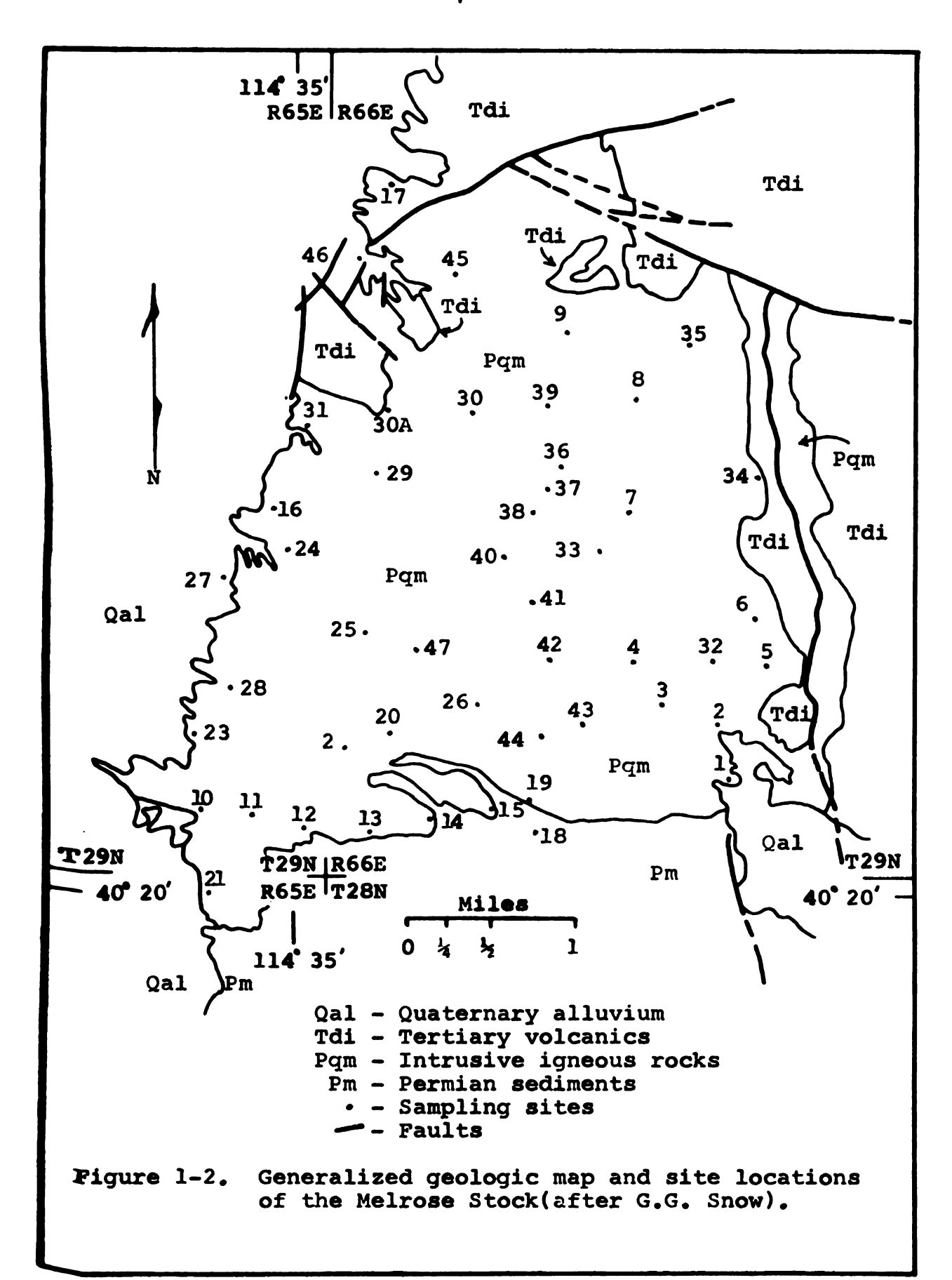
The relationship of the stock to the surrounding host rocks is quite varied as seen in Figure 1.2. The southern margin of the stock is in contact both concordantly and discordantly with Permian limestones that have been tipped on end. The sediment-intrusive contact is sharp and the effects of heating from the intrusive do not extend more than a few feet into the sediments. Recrystallization of the limestone along the contact is not significant and there is only minor silicification of the host rock. The west side of the intrusive is truncated by a basin and range fault which runs the length of the range though it is covered by alluvium along much of its extent. The north and east sides of the stock are overlain unconformably by Tertiary ignimbrite. The ignimbrite has apparently covered much of the stock which had been layed bare by post-Laramide uplift and erosion. Core, recovered from drill holes approximately a mile to the east of the intrusive and at a depth Of nearly 1,000 feet below the surface, reveals Tertiary Flow breccia lying unconformably on the intrusive. Out-Liers of quartz-monzonite found to the east of the drill holes are believed to be apophyses of the intrusive.

Unpublished aeromagnetic maps indicate the intrusive

to be much larger than its outcrop exposure. Snow's con
Clusion that the intrusive's roof is quite irregular appears

to be correct from observations of the magnetic map. The

basin fault downdrops a portion of the stock west of the



range at least 780 feet for a well to that depth in the alluvium and west of the fault does not penetrate the quartz monzonite. This fact is also substantiated by the aexomagnetics. On a regional scale the Melrose Stock is on a magnetic high trend which can be traced from the Uinta Mountains, through Bingham Canyon and Gold Hill to the Dolly Varden Mountains (Zietz and others, 1968).

The rocks in the stock are of intermediate composition, porphyritic (0-15 percent phenocrysts) granitic rocks.

Most commonly the rocks are from medium to coarse grained.

Xenoliths from a few centimeters to a few tens of centimeters are rather common throughout much of the intrusive.

In hand specimen, variations exist in color and composition

Which permit the rocks to be easily divided into two types,

a quartz-monzonite and a monzonite. The contact between

the two units is transitional over a distance of about 10

Feet. The monzonite constitutes about 25 percent of the

exposed area of the stock.

1.3 Rock Sampling

A total of 48 sites was sampled during the summers

1968 and 1970. The site locations are shown in Figure

1-2. Hand samples were collected from all sites, oriented

10res from 35 sites, and 5 additional sites have cores taken

10 munoriented hand specimens. A fairly uniform, site

10 msity was established over the stock. The location of

11 tes was based on geophysical rather than geologic grounds.

Drilling of the oriented cores was carried out with a portable drill unit similar to that described by Doell and Cox (1967). Drilling of a three inch core generally took about five minutes. The time required to obtain 6-8 cores ranged from one-half to one hour. Breakage during drilling resulting from incipient fractures and weathering amounted to at least 2 to 3 cores per site. The size of a collection site was in part dictated by the extent of the Outcrop which generally ranged from 20 to 70 feet in the maximum dimension. The cores were uniformally selected over the entire area of the outcrop.

Brunton compass and an orienter made of copper. The construction of the orienter is a slotted barrel mounted orthogonally to a square plate upon which the compass is placed.

The precision of the orienter is estimated at 2 degrees.

From one to three specimens were cut from each core and then all specimens were stored with the same orientation in the ambient field of the laboratory from the time of preparation to measurement. Thin sections were made from the trimmings of the cores. Polishing of the thin sections permitted them to be used for reflected and transmitted microscope and electron microprobe investigations. In addition, opaque section mounts were made for all of the sites from the core trimmings.

The following convention was adopted for specimen indentification. Example: VN-14D-2. The VN is the code

number in that area. The letter D refers to the fourth core drilled at Site 14 and 2 indicates that it is the second specimen from the end of the core nearest the outcrop surface.

CHAPTER II

PETROLOGIC PROPERTIES

2.1 Petrology

2.1.1 Introduction

A significant aspect of this investigation is to establish the relationship of the magnetic mineral suite to the constituent minerals in the rocks and to determine this relationship as expressed in the magnetic properties. The relation of the magnetic minerals to the host minerals in the rock has not been previously investigated in the manner presented in this chapter. Previous observations of other rock suites have given the stimulus to carefully observe the magnetic minerals in their environment for what they can reveal about the history of the intrusive.

The data reported in this chapter will be used to draw Conclusion, regarding the magnetic properties and history Of the Melrose Stock.

The petrologic investigation of this research project involved the measurement of a number of physical quantities including modal volumes, size distributions and intergranular relationships. The latter gave rise to two parameters developed by this investigator in an attempt to study in

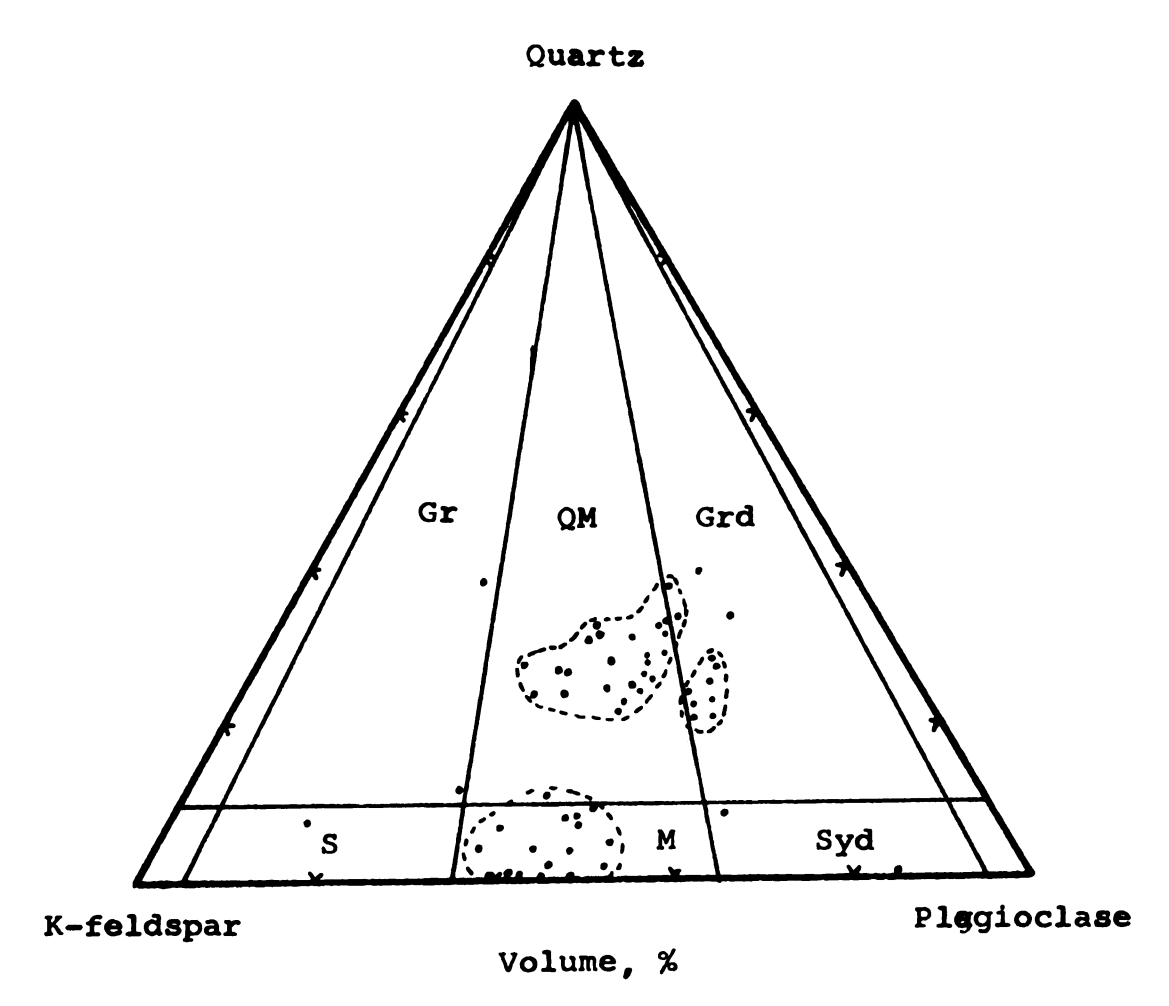
detail the magnetic mineral suite.

2.1.2 Modal Analysis

Modal analyses were carried out at a magnification of 140X with a total of 1,000 point counts per thin section, permitting constituent minerals to be determined relatively accurately. This relatively high point count was made to accurately determine the modal volumes of the ferromagnesian minerals because of their special interest in this study. The modal volume of opaque minerals was determined in conjunction with the association study of approximately 9,000 counts per thin section.

Knowing the amounts of the ferromagnesians and magnetite will permit the evaluation of their association with each other, how each is reflected in the magnetic properties, and to what extent the geometry of the magma chamber influenced the formation of these minerals.

The results of the modal analyses are shown in Figure 2-1. The results of the modal analyses fall into two distinct groups, a quartz-rich and a quartz-poor, with a subgrouping in the quartz-rich group. The quartz-poor group falls into the monzonite field with the amount of K-feldspar slightly greater than the plagioclase. The data which do not fall into the general grouping may be explained in the following manner. The specimen in the syenite field may well represent the influence of the proximity of the limestone-intrusive contact which is only



Gr - Granite Syd - Syenodiorite
QM - Quartz Monzonite S - Syenite
Grd - Granodiorite M - Monzonite

Figure 2-1. Partial modal analyses of rocks of the Melrose Stock. Rock composition fields of the U.S. Geological Survey are shown.

100 feet away. The two data points in the syenodiorite field are rather coarse grained and therefore may not be representative of the rock.

The other major group is in the quartz-monzonite field with the minor subgrouping in the granodiorite field. The data point well in the granite field is from Site 14 and may represent a specimen from a granitic dike, one of the accessory rock types in the intrusive.

A plot of the constituent minerals on a ternary diagram is shown in Figure 2-2. In this representation two fields exist with no evidence of further subdivisions as in Figure 2-1. The upper group of data in Figure 2-2 corresponds to the quartz-monzonite sites of Figure 2-1, the lower to monzonite sites. The monzonite group has about 5 percent more ferromagnesian minerals and 10 percent more feldspars than the quartz-monzonite, but the significant difference is in the quartz content. The monzonite is evidently a more basic phase of the stock which is supported by the fact that it has augite as one of the ferromagnesian minerals. Furthermore, a Michel-Levy determination of plagioclase composition shows values of An₃₆ and An₄₀ for the quartz-monzonite and monzonite plagioclases respectively. There is a 93 percent probability that this difference is real.

The lithologies delineated in Figure 2-1 are shown in Figure 2-3. A dashed line separates the general areas of these three rock types. The monzonite is confined to the

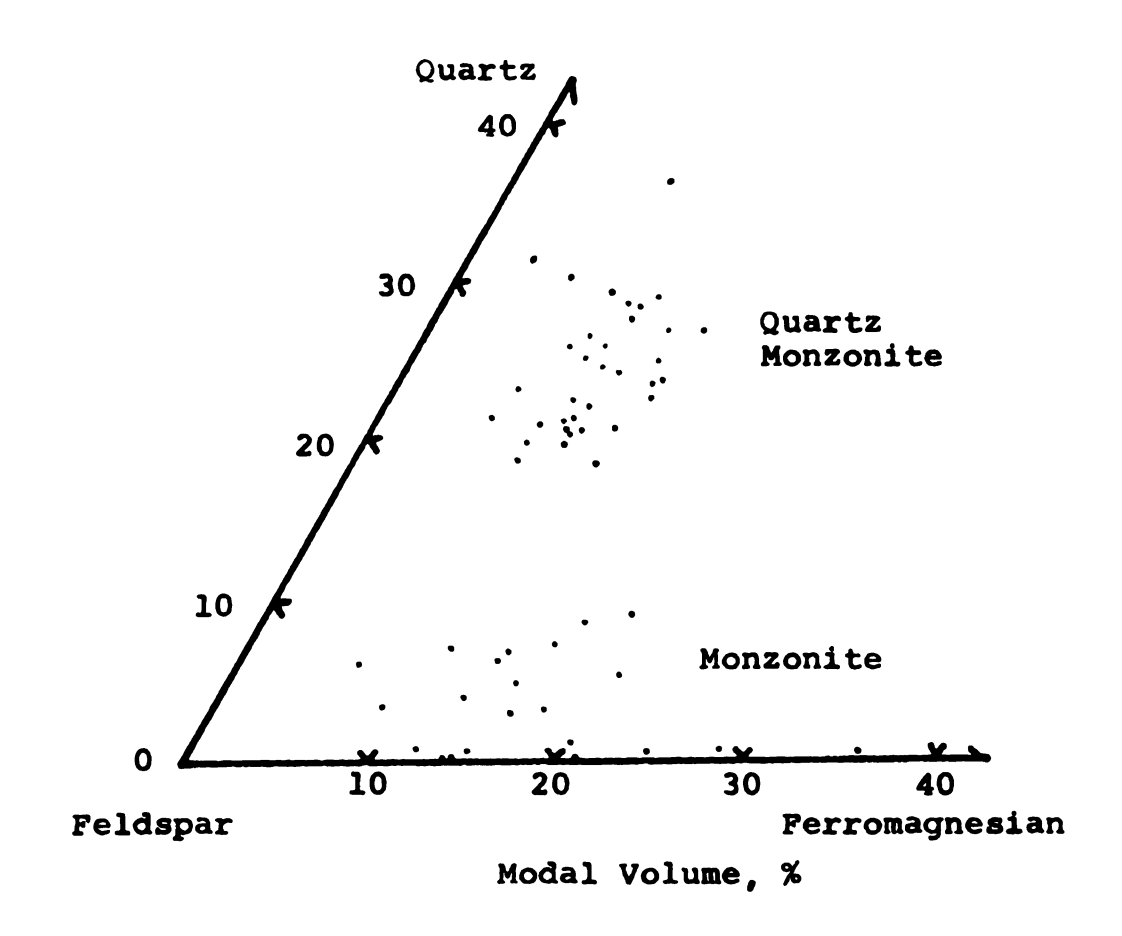
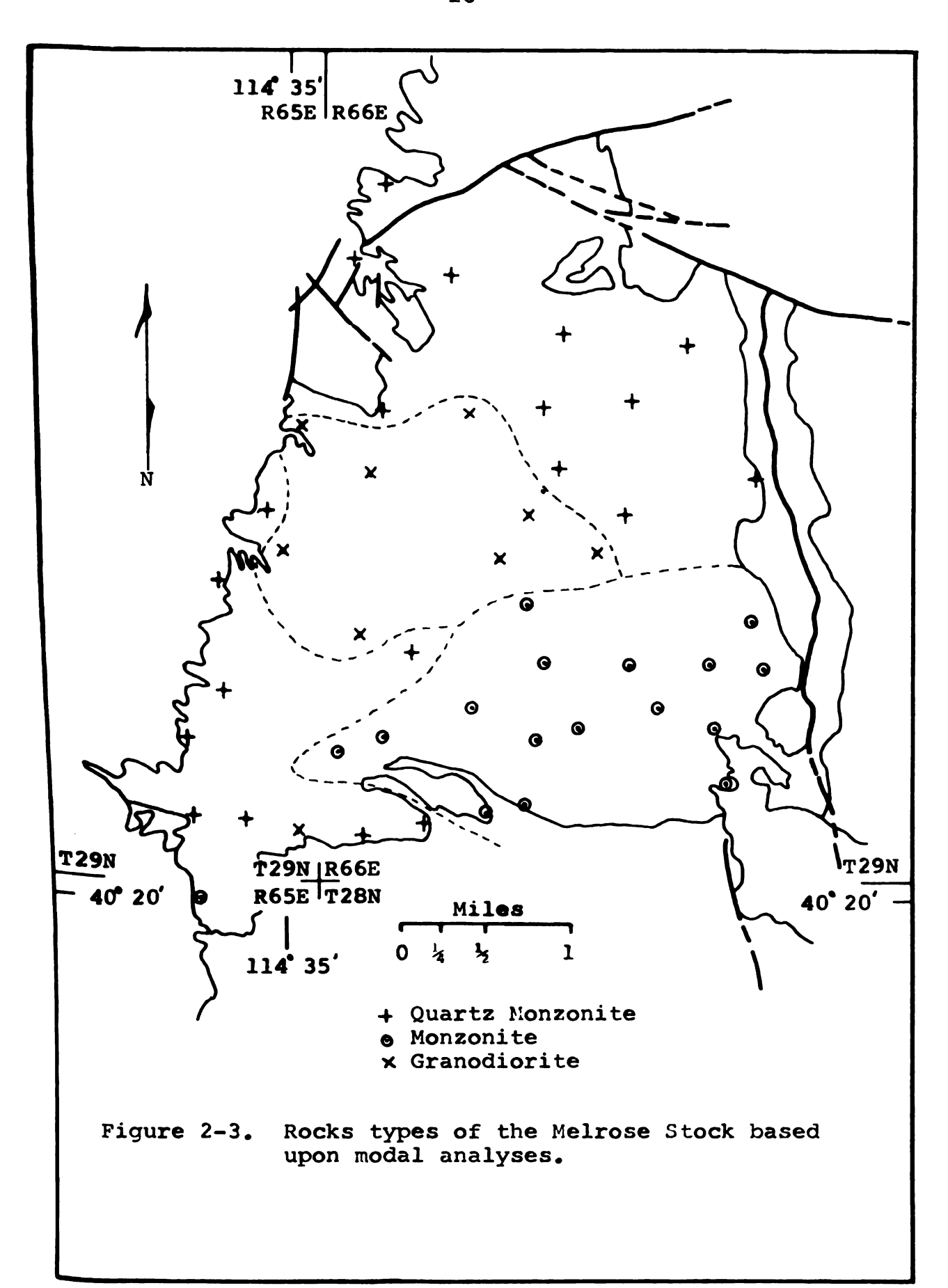


Figure 2-2. Modal analyses of rocks from the Melrose Stock.



southeast portion of the exposed intrusive. The one site of monzonite in the southwest corner of the intrusive may be connected to the main monzonite mass in the subsurface. The spatial grouping of the granodiorite sites lends support to the distinct subgroup as shown on the ternary plot of Figure 2-1.

For the purposes of this study only the quartz monzonite and monzonite rock types will be delineated. The
sites having compositions in the granodiorite field are
grouped with the quartz monzonite. This is done because
both are quartz rich and have no augite. The magnetic
properties appear to reflect differences in the quartz and
augite content and not in feldspar ratios. No field contact is apparent between the granodiorite and quartz monzonite.

2.1.3 Microscopic Description

A description of the various minerals will provide a picture of the events which took place during solidification of the magma. The opaque minerals appear to have formed throughout much of the cooling history, and consequently the character of the constituent minerals will shed light on the genesis of the opaque suite. The following description applies to both rock types.

Plagioclase exists as both matrix material and large crystals, but the crystals are not as large as the microcline phenocrysts. The tabular plagioclase crystals, ranging to

about 5 millimeters in length show albite, pericline and carlsbad twinning in order of decreasing abundance. In the ground mass of many specimens it is difficult to differentiate the feldspars from each other because of the general absence of twinning in the plagioclase. Alteration of the plagioclase to calcite, epidote and albite is very common. Many plagioclase crystals display a cataclastic fracturing as if late stage emplacement or movement fractured them.

K-feldspar occurs as orthoclase and microcline, much of which has excellently developed perthite. Myremekitic texture is common. Most of the K-feldspar appears in the matrix and is highly poikilitic to most of the other minerals. Carlsbad twinning is observed in the phenocrysts. Microcline gridding is common, but it is poorly preserved due to the pervasive argillic alteration. The effects of fracturing in the plagioclase seems to have its equivalent in the K-feldspar as kinking of the cleavage planes indicating stresses were imposed on the grains late in the cooling history of the intrusive. In a few thin sections the K-feldspar is secondary, apparently related to hydrothermal activity.

The quartz is generally quite free of inclusions as contrasted to the K-feldspar. It appears to have formed primarily before the orthoclase because only approximately one-fourth of it can be considered interstitial. The grains are generally composite, but not to the extent of being mosaic. In a few thin sections, however, a portion of the

quartz is obviously mosaic and related to hydrothermal activity. A few specimens reveal the quartz grains to be highly fractured.

The anhydrous, ferromagnesian mineral augite is nearly completely restricted to the monzonite. A few of the quartz monzonite and monzonite specimens show traces of augite.

Due to the point counter used in the study having a capacity for tallying only six minerals, augite was counted with the hornblende. Its modal volume varies from 20 to 90 percent of the hornblende volume in the sites where it occurs in appreciable amounts. Augite averages approximately one-half of the hornblende in the monzonite sites as determined by counts of the hornblende-augite ratio in a few thin sections. Much of the augite is intimately associated with the hornblende apparently as the result of the incongruent conversion of augite before equilibrium was reached.

Hornblende grains show a wide degree of alteration; a fine mixture of chlorite, biotite and epidote fill some hornblende pseudomorphs, while others are fresh and show excellent twinning. This variation can be seen in a single thin section and indicates hydrothermal alteration along minute avenues in the rock. The altered amphibole is generally poikilitic, especially with magnetite. There are instances of the hornblende showing peritectic conversion to biotite.

Biotite is characteristically poikilitic and in the

monzonite occurs in distinctively larger crystals. It does not show as much alteration as the hornblende, but where it is altered, the product is chlorite. Biotite does not appear to be as closely associated with hornblende as the augite is to hornblende.

The plagioclase content is nearly the same in each rock type. The quartz-monzonite has approximately 15 percent less K-feldspar than the monzonite. This effect is more than offset by the great difference in the quartz content. The monzonite has twice as much hornblende as the quartz monzonite while the amount of biotite in each remains nearly the same. Because roughly one-half of the hornblende content in the monzonite is augite, the hydrous ferromagnesian content in both rocks is approximately the same. The magnetite is twice as abundant in the monzonite.

The accessory minerals in decreasing order of abundance are magnetite, ilmenite, sphene, apatite, zircon and corundum. The minerals appearing as alteration products are sericite, calcite, epidote, biotite, chlorite, quartz, albite, leucoxene, and hematite. The accessory minerals relating to the opaque mineralogy will be discussed individually in later sections.

A compilation of the modal analyses is given in Table 2-1. Listed for each of the constituent minerals and magnetite (including other opaque accessories) is the minimum and maximum values measured with their respective arithmetic means according to rock type.

Modal analysis minimums, maximums, and means of the Melrose Stock Table 2-1.

	Quar	Quartz Monzonite	nite	×	Monzonite	
	Nin.	Mas:	Mean	Min.	Max.	Mean
Plag.	27	48	38	14	25	36
K-spar	1.5	39	26	O	53	41
Otz.	18	37	24	0	თ	4
Horn.	7	æ	ĸ	9	17	12
Bio.	1	10	9	H	21	ഹ
Mgt.	0	2	F	н	м	2

2.2 Apparent Grain Size Distribution of Magnetite

The size of the magnetic minerals was measured in an attempt to understand more fully the behavior of the magnetic properties. Knowledge of the grain size distribution will help predict the stability of the remanent magnetism. If the bulk of the magnetite grains is in the size fraction greater than roughly 50 microns, the remanent magnetization will have a low coercivity and hence a soft remanence.

The measurement of grain size cannot be taken as absolute since a thin section gives values of grain sizes which only approach the true size. However, if a comparison is made on a relative basis, then valid conclusions can be drawn from the data.

The size distribution count was divided into two categories, those opaque grains associated with quartz and feldspar (nonferromagnesian) and those allied with the ferromagnesian minerals. The two categories represent zones where iron is present and deficient. In this manner an insight into the growth history of the magnetite grains will become clearer. The size of the magnetite grains is expected to reflect the "supply" of iron available where their growth was taking place. Zones in which the iron "supply" was limited, as well as the time for growing, will show a smaller size of magnetite grains. The ferromagnesian minerals are a likely source of iron if it is available through some reactions.

The following criterion was used to define the association of a magnetite grain to a group. If a grain was included or had more than half of its area embayed by a given category (ferromagnesian vs nonferromagnesian), it was counted for that group. There was also a problem of dealing with composite magnetite grains. Composite grains were treated as single grains when 15 percent of their contacts were in common. The rational for this was that the magnetic properties are a function of grain size and hence a cluster of small grains together would tend to express the magnetic properties of a large grain. In order to express the properties of large grains, the cluster has to be crystallographically continuous across the boundaries of the individual grains. In other words, it is assumed that when more than 15 percent of the perimeters are in contact, one grain nucleated on another as an overgrowth and are structurally continuous, though not necessarily in the same crystallographic orientation. The value of 15 percent was arbitrarily chosen. Magnetite grains altered along fractures can be divided into many magnetically independent grains. Exsolution of titanomagnetite or ilmenite in a magnetite grain will also split up an apparently homogeneous grain. This must be taken into account as reported by Larson and others (1969), but this did not have to be applied to the samples of the Melrose Stock, because the magnetite was free of exsolution.

The above distribution of magnetite represents a

frequency of occurrence based on the number of grains encountered and not volume for that percentage. For example, if 96 percent and 4 percent of the magnetite grains were in the 0-5 and 5-10 micron groups respectively, the percent volume of magnetite in each fraction is approximately the same. A larger size fraction, though having a small portion of the magnetite in numbers of grains, can be the major contributor to the magnetic properties.

A total of ten thin sections were measured for size distributions, five from each rock type. From 500 to 800 grains were counted on each thin section. A magnification of 280X was used with a graticule having 5 micron divisions as a standard of reference. The number of grains in the field of view falling into each of seven size groups was recorded. The seven size groups are 0-5, 5-10, 10-25, 25-50, 50-100, 100-200, and greater than 200 microns. Grains of 1.0-1.5 microns were at the limit of resolution. Going to a higher magnification would have increased the resolution to some extent, but the large grains would have more than covered the field of view making their determination difficult.

The results of the measurements are shown in Figures 2-4 and 2-5. The histograms represent the percentage of the grains encountered which fell into each of the seven size groups.

All of the histograms have a maximum in the smallest size fraction and then drop off sharply in succeeding

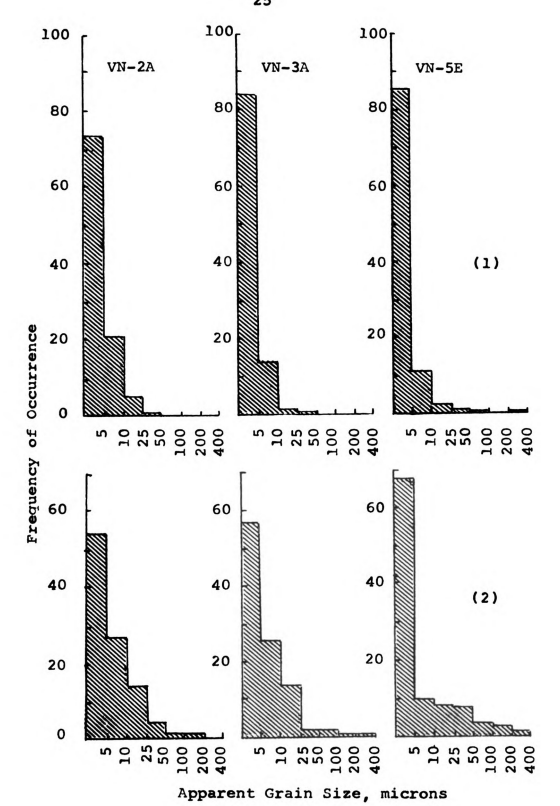
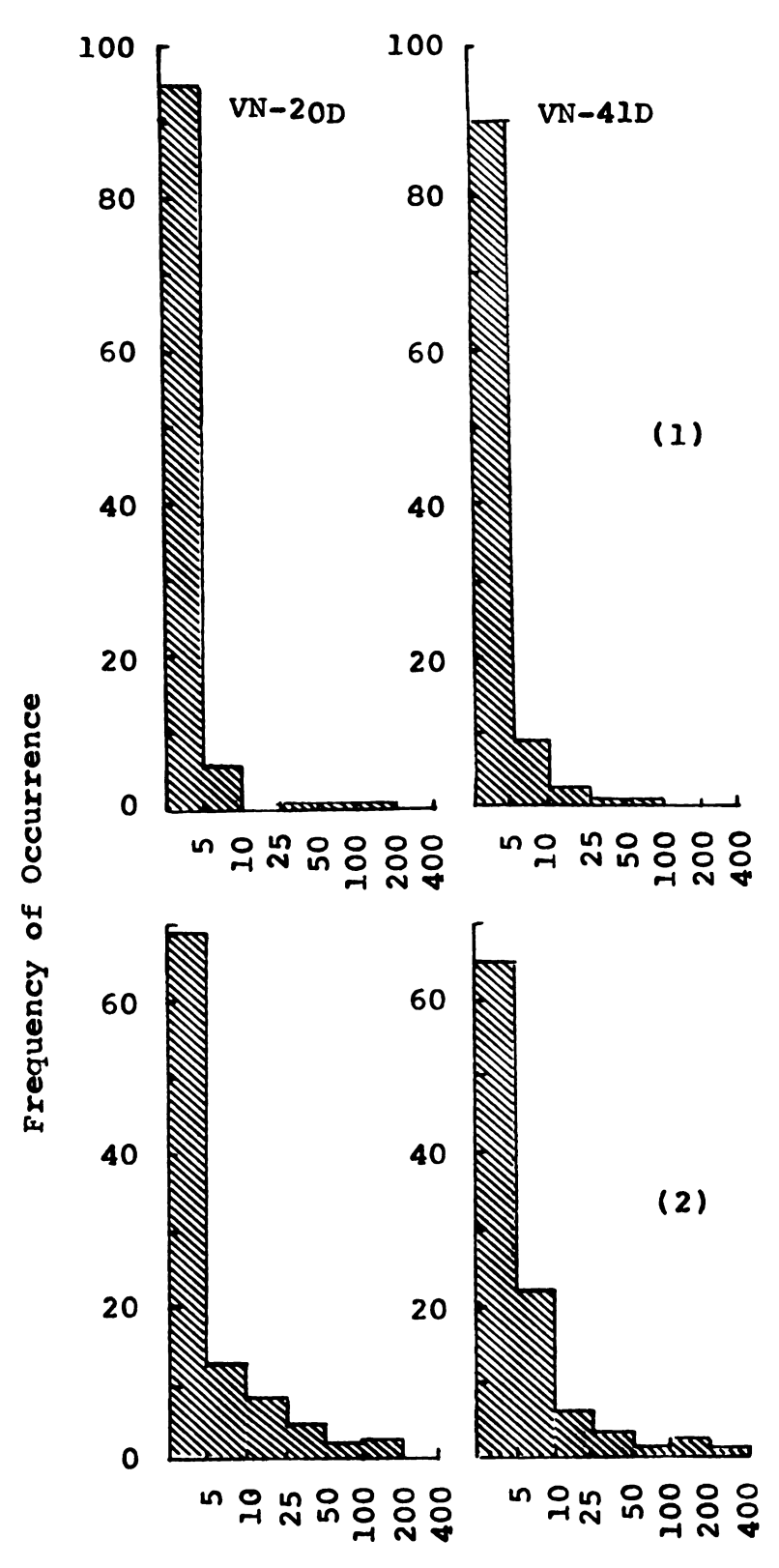


Figure 2-4a. Apparent grain size distribution within the monzonite pluton. 1) opaques associated with the quartz-feldspar fraction. 2) opaques associated with the ferromagnesian fraction.



Apparent Grain Size, microns

Figure 2-4b. Apparent opaque grain size distribution within the monzonite pluton. 1) opaques associated with the quartz-feldspar fraction. 2) opaques associated with the ferromagnesian fraction.

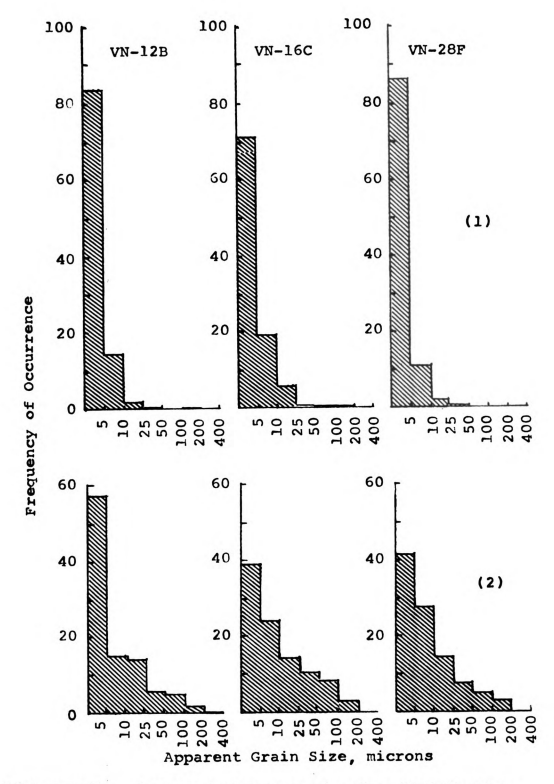
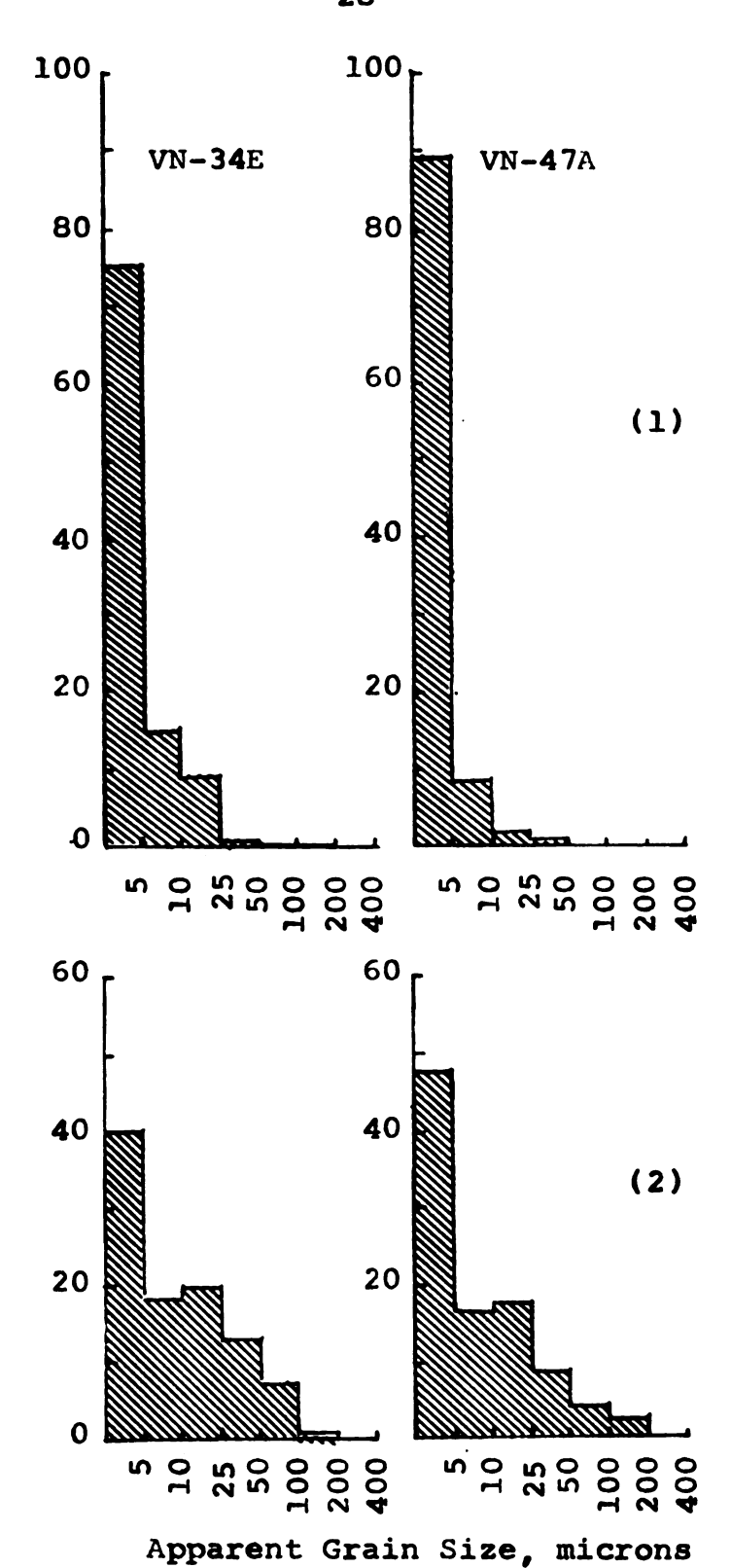


Figure 2-5a. Apparent opaque grain size distribution within the quartz monzonite pluton. 1) opaques associated with the quartz-feld-spar fraction. 2) opaques associated with the ferromagnesian fraction.



Pigure 2-5b. Apparent opaque grain size distribution within the quartz monzonite pluton. 1) opaques associated with the quartz-feld-spar fraction. 2) opaques associated with the ferromagnesian fraction.

intervals. The size distribution is expected to display a bell shaped curve, consequently the results indicate the right hand portion of such a curve. Without greater resolution, it cannot be determined whether the smallest size fraction measured actually represents the most abundant grains size group. Similar one-tailed distributions have been recorded by Larson and others (1969).

In general, for both the quartz monzonite and monzonite the grain size of the opaques associated with the nonferromagnesian silicates is smaller than those related to the ferromagnesian minerals. Within the nonferromagnesian group, 99 percent or more of the opaque grains fall in the size fraction of less than 50 microns (See Table 2-2). Grain sizes falling in the largest size group make up less than 1 percent of the grains. The ferromagnesian group on the other hand has much more magnetite in the coarser fraction (>50,4), more than ten times the number of grains as the nonferromagnesian group.

The difference which was noted between the two categories suggests an influence of the ferromagnesian minerals on the size of the magnetite grains. Because the large grains are ten times as abundant about the ferromagnesian minerals as contrasted to the quartz and feldspar, the iron silicates favored or enhanced the formation of larger magnetite grains. Perhaps these minerals served as the source of iron for the opaque oxides. This point is discussed in greater depth in the association study.

Table 2-2. Percentage of opaque grains greater than 50 microns in diameter.

	*Opaque Ass	ociation
Rock Type	Nonferromagnesian	Ferromagnesian
Quartz Monzonite Monzonite	0.4 0.4	8.8 4.4

^{*}Based on 5 thin sections from each rock type

A visual comparison of the histograms (Figures 2-4, 2-5) of each rock type shows that the magnetite in the quartz-feldspar category has approximately the same fraction distribution, but the magnetite associated with the ferromagnesians in the quartz monzonite is noticably coarser than the magnetite in the monzonite. The quartz monzonite and monzonite respectively have 8.8 and 4.4 percent of the opaque grains in the size fraction greater than 50 microns.

The larger grain size of the magnetite in the quartz monzonite indicates that the magnetite had a longer time to grow and/or that more iron was available for rapid growth of the crystals. The viscosity of the monzonite would have been expected to be less than that of the quartz monzonite so that the growth potential of the magnetite grains would be enhanced in the monzonite. However, the results do not support this idea. The forthcoming section on mineral associations shows the monzonite to have had a shorter crystallization history than the quartz monzonite which suggests a shorter duration for the magnetite to grow in the monzonite than in the quartz monzonite. It is believed that a longer time span of crystallization permitted growth of larger magnetite crystals in the quartz monzonite, perhaps in part due to the deeper burial. hydrous phase content should help to promote the growth of larger magnetite grains, but it is not known which magma had the greater hydrous phase content.

The results of the magnetite grain size distribution study suggest that the stability of the remanent magnetization will be inversely proportional to the ferromagnesian mineral content, because the large magnetite grains (>50 m) show a preference to the ferromagnesian minerals. Furthermore, the higher percentage of large magnetite grains in the quartz monzonite indicates that the monzonite should have a more stable remanence than the quartz monzonite.

Nagata (1961) has shown the coercivity, hence the remanent stability, of magnetite grains increases appreciably for grains less than 50 microns in size.

2.3 Opaque Petrology

2.3.1 Introduction

An integral part of this study was the investigation of the opaque mineral suite, its connection to the genesis of the constituent minerals and their relationship to each other. To these ends, a total of 42 opaque mounts from as many sites, 25 mounts from the quartz monzonite and 17 mounts from the monzonite, were examined at 450%. The opaque species, their relative abundance by visual estimates, their textures and relationships to each other were recorded. The study primarily focused on the iron-titanium oxides, but the occurrence of sphene was also noted for this mineral may aid in the evaluation of the magnetic minerals. The origin of sphene and the exsolution within the ilmenite are considered as evidence for zoning within the intrusive.

The following opaque species were identified: magnetite, ilmenite, hematite, goethite, maghemite, pyrite and chalcopyrite. Distinguishing between sphene and goethite occasionally posed a problem.

2.3.2 Magnetite and Ilmenite

The two primary opaque oxides of the Melrose Stock are magnetite and ilmenite with hematite, goethite and maghemite as alteration products. The two major opaques do not show a significant difference in their relative abundance with regards to rock type. The monzonite has 12 percent ilmenite, 85 percent magnetite and the remainder as alteration products and the quartz monzonite has 10 percent ilmenite, 85 percent magnetite and the remainder as alteration products. Tabulations of the sites with sphene coronas and composite ilmenite-magnetite grains revealed no preference to rock type.

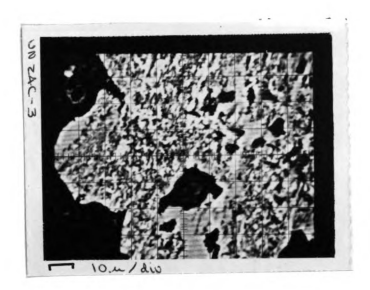
Magnetite is present in all opaque sections and is always the dominant opaque. Microprobe results indicate the magnetite to be pure magnetite with no apparent exsolution. The polish of the magnetite grains varies considerably, but in general it shows moderate to heavy pitting, as a result of surface alteration to goethite which was removed during polishing. The grains are anhedral to euhedral with a tendency for the euhedral grains to be more closely associated with the nonferromagnesian minerals. The habit of magnetite varies from single grains

to clusters of several grains. No evidence of exsolution was noted in the magnetite, but hematite was commonly seen in the magnetite along structural planes. This occurrence of hematite is interpreted as a result of hydrothermal alteration which is also associated with the alteration of other minerals in the specimen. In several instances, ilmenite and magnetite occur together as abutting grains. The shape of the combined unit, which is often quite regular, suggests that the grains existed previously as a grain of a single species. This abutting relationship is evidence of an advanced stage of exsolution of an original titanomagnetite according to Buddington and Lindsley (1963). Two sample mounts displayed local alteration of magnetite to maghemite. Sphene coronas occur around both magnetite and ilmenite, however, they were more frequent around ilmenite.

The few grains of ilmenite analyzed with the microprobe show them to be pure ilmenite. Exsolution was observed in some of the ilmenite grains and is shown in
Figure 2-6a. The remaining photos of the sequence are
referred to in section 2.3.3.

Ilmenite generally displayed its prismatic shape in cross section as contrasted to the magnetite which was more equidimensional. The polished surface of the ilmenite grains was more homogeneous than the pitted magnetite.

Commonly the ilmenite was altered to goethite, but this alteration attacked the grains from the perimeter inwards.



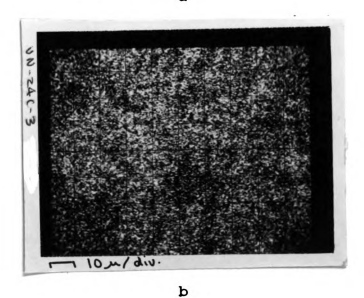
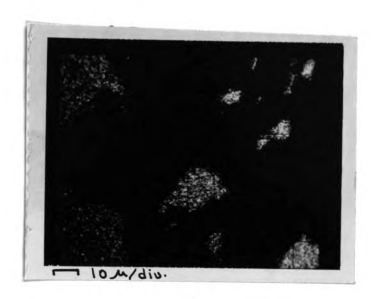


Figure 2-6a,b. Electron microprobe microphotograph of an ilmenite grain with hematite exsolution and a sphene reaction rim. a) sample current, b) titanium fluorescence.



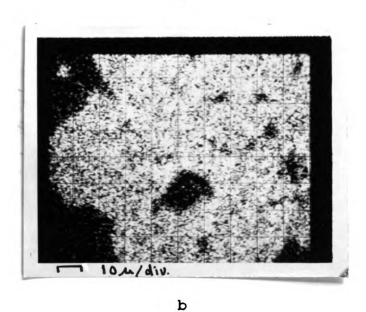


Figure 2-6c,d. Electron microprobe microphotograph of an ilmenite grain with hematite exsolution and a sphene reaction rim. c) calcium fluorescence, d) iron fluorescence. This is in contrast to the magnetite. Pseudomorphs of goethite after ilmenite were occasionally seen. In several instances the nearly complete alteration of ilmenite to sphene was seen with only a skeletal ilmenite remnent.

Ilmenite in many sites has what appears to be well formed exsolution lamellae of hematite. These blebs, approximately 0.5 microns in width, and 2.0 microns in length parallel the long axis of the ilmenite grains. Minor amounts of hematite occur as an alteration product of ilmenite.

The lack of apparent difference in the opaque assemblage of the rock types suggests that the chemical and physical condition of the two phases was similar, at least in the later stages of crystallization. The two lithologies cannot be differentiated on the basis of their opaque assemblage. There are, however, differences in the opaque assemblage, but these reflect influences due to the geometry of the magma.

A tabulation of the opaque data is given in the Appendix B.

2.3.3 Sphene

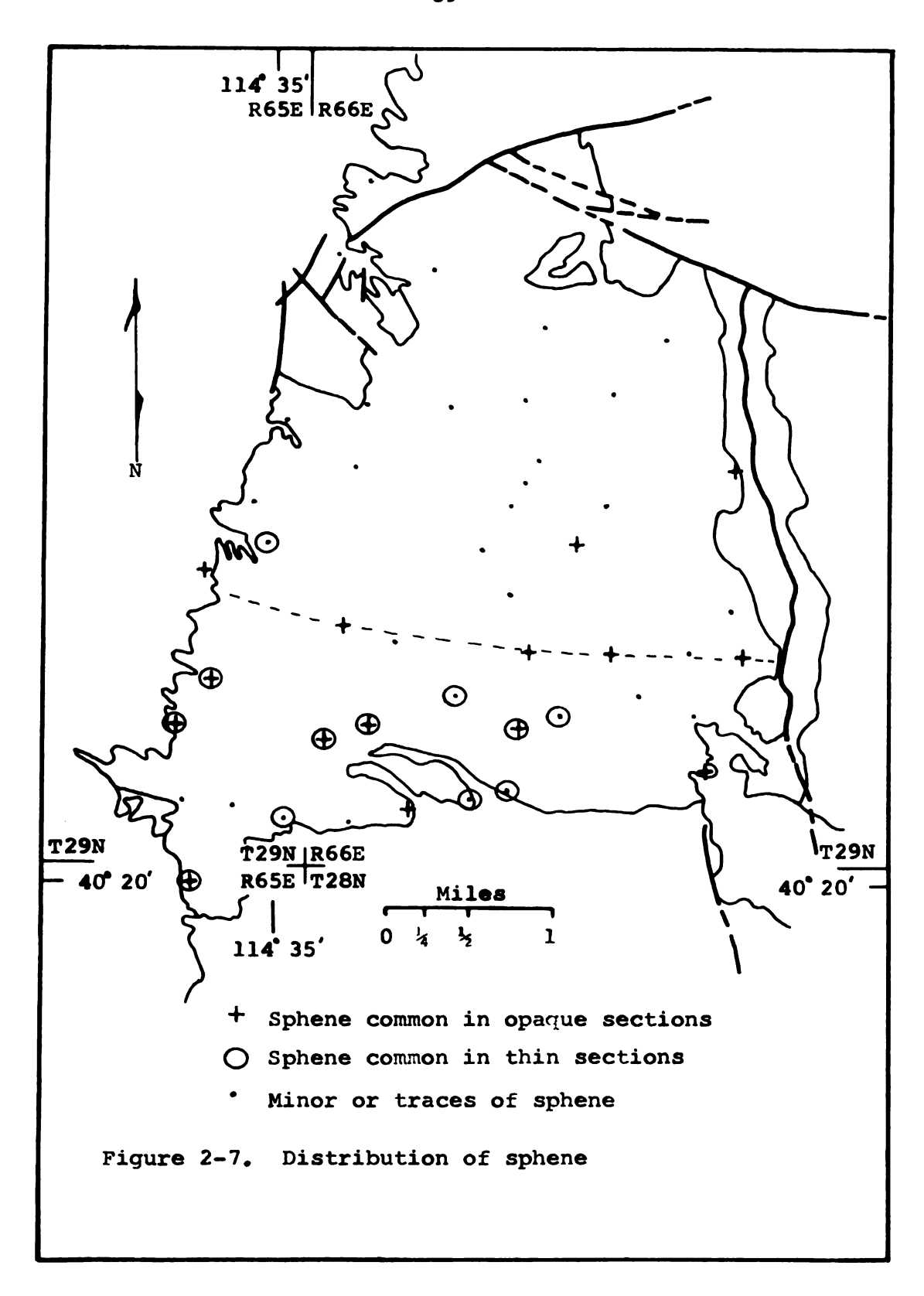
Sphene was selected for investigation because it appears to be related to the ilmenite and to the geometry of the intrusive. The occurrence of sphene was noted in a qualitative way. The sphene content was classified into three categories: trace, minor and common. In terms of

actual modal volume, the common grouping approximates one percent.

There is a lack of correlation of sphene content with lithology. However, the plotting of the areal distribution of sphene may reveal patterns related to the geometry of the intrusive.

The sites in which sphene was noted as common are plotted in Figure 2-7. In addition to the data obtained from the opaque mounts, results of the thin section measurements are also included. This was done as a check of the opaque mount data because of the possible errors of identifying sphene as goethite. In thin sections there is no problem in distinguishing between the two minerals. Figure 2-7 shows that sphene, where common, is limited to the southern part of the intrusive, an observation supported by both the opaque and thin section data. The fact that data from both samples at each site do not substantiate each other is not surprising because the two types of sections are not always from the same core. Hence, they may be sampling some of the heterogeneity existing at a given site.

It is believed that the margin of the intrusive might have been an influence on the formation of sphene. A marginal zone of approximately 5,000 feet width reflects the influence of the host rock on the opaque mineralogy of the intrusive. If the vertical margin did have a control on sphene formation, the interior and northern portions of



the stock were apparently greater than 5,000 feet from a margin or contact. It is then inferred that at least 5,000 feet of rock have been removed from the stock and additionally that the stock is much larger than its present exposure.

The occurrence of the abundant sphene is believed to be the result of limestone assimilation in the crystall-izing melt. The effects of assimilation are expected to decrease towards the interior of the magma chamber resulting in a halo or rim confined to the periphery of the intrusive body. The formation of sphene requires CaO, SiO₂ and TiO₂ under the proper pressure-temperature conditions. The reaction

3 FeTiO $_3$ + 3CaSiO $_3$ + $^{1}_{2}$ O $_2$ \rightarrow Fe $_3$ O $_4$ + 3CaTiSiO $_5$ as suggested by Verhoogen (1962) can well explain the observations in the Melrose Stock. Wollastonite (CaSiO $_3$) probably was not present as a reactant but more likely as CaO from the dissociated limestone and SiO $_2$ from the melt. The oxidizing conditions necessary to drive the reaction to the right would be enhanced by the limestone dissociation, H $_2$ O derived from the sediment, and H $_2$ O already present in the melt. The TiO $_2$ has a large affinity for CaO as shown by the very large negative free energy (-77.1 kcal at 298 K) of the reaction.

The common sphene coronas about both ilmenite and magnetite plus the sphene pseudomorphs after ilmenite give strong support to the proposed reaction. The

microprobe photos of Figure 2-6a through d show, in addition to the exsolution, a portion of an ilmenite grain with a sphene corona.

Photos "b", "c" and "d" are of the same area as "a", however, they are made of the x-ray fluorescence of the elements, titanium, calcium and iron. Titanium covers the complete photograph (b) with nearly the same intensity, but a faint outline of the ilmenite grain can be distinquished where the ilmenite concentration is slightly greater. The calcium and iron photos (c and d respectively) are reverse images of each other, where the iron concentration is high, the calcium content is low and vice versa. The detail of the exsolution cannot be resolved in these x-ray fluorescence photos. This series of photos substantiates the reaction in which sphene is formed at the expense of ilmenite. Further evidence of the proposed reaction would be obtained from the ratio of ilmenite to magnetite which would be expected to decrease near the margins of the intrusive. The reaction produces magnetite at the expense of ilmenite. A plot of relative ilmenite content in all sites from the south contact shows no trend. This is not particularly disturbing because near the contact not all sites have abundant sphene. This may reflect inhomogeneities resulting from the stoping of limestone blocks. In other words, the effects due to the limestone assimilation are probably not pervasive but more abundant as subzones near the contact.

The average ilmenite content of the sites possessing common or abundant sphene in thin sections and opaque sections relative to all of the opaques is 8 percent and the content in those sections having minor or a trace of sphene is 14 percent. This inverse relationship, even though there is overlapping of values of the two groups, does support the idea of the sphene forming at the expense of the ilmenite.

The conditions necessary for formation of ilmenite from direct precipitation or by removal of titanium from a pyroxene structure requires a reducing atmosphere early in the crystallization history. The formation of sphene necessitates a change to an oxidizing or high partial pressure of oxygen later in the cooling history. The change in the "atmosphere" of the magma reflects the normal concentration of the hydrous phase as crystallization procedes and the dissociation of the sedimentary host rock releasing CO₂ and H₂O₄.

It appears that the geometry of the magma has influenced the assemblage of magnetic minerals, but the effect is not great enough that variations of magnetic susceptibility due to the proposed reaction can be meaningfully delineated. However, the influence of the host rock does provide an insight into the geometry of the magma chamber.

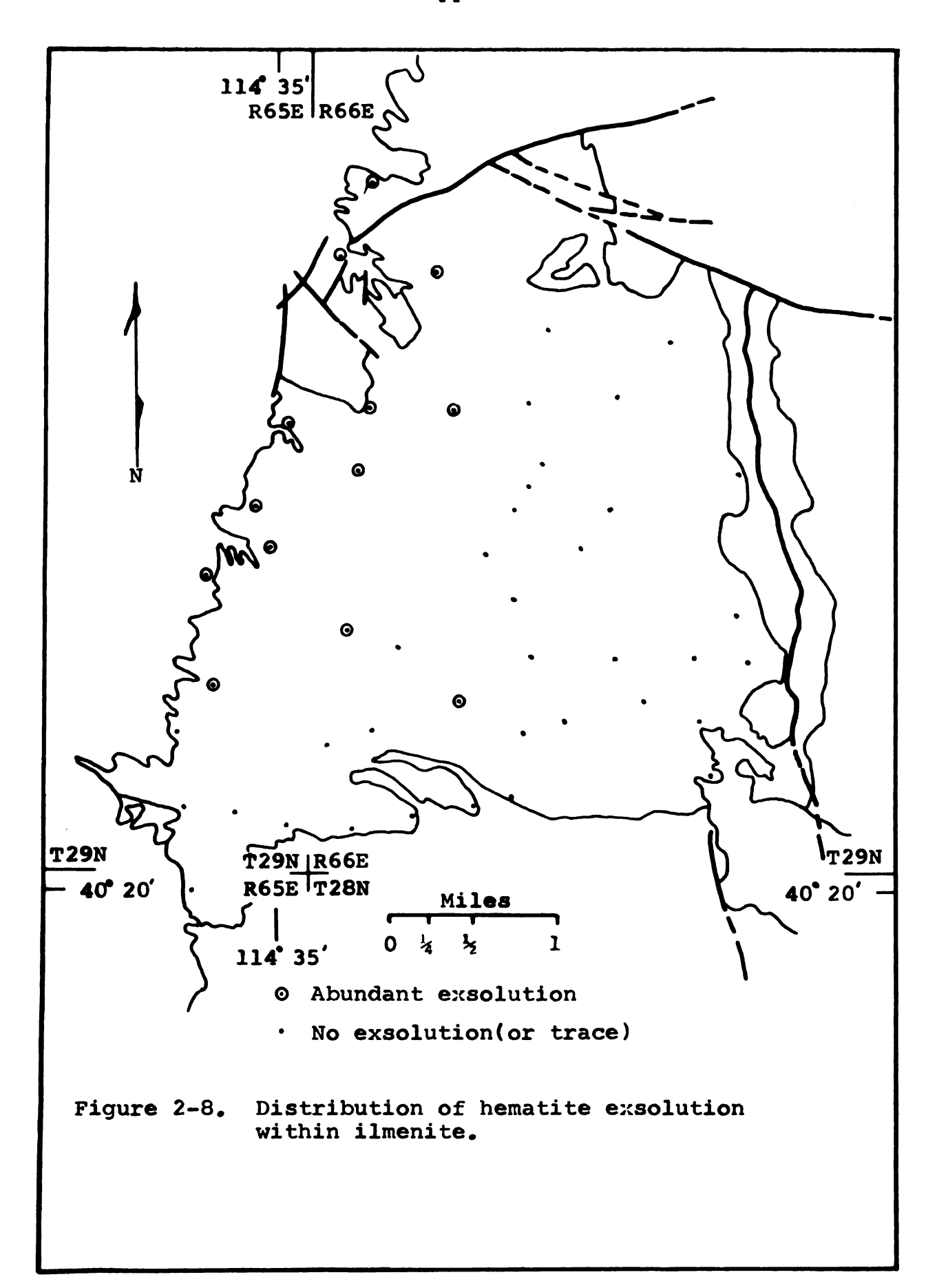
2.3.4 Hematite

The occurrence of hematite can provide useful

information regarding the paragensis of the opaque minerals as well as of the intrusive. Normally the presence of hematite indicates an oxidizing condition, perhaps as a condition resulting from the abundance of intergranular fluids, primarily water. However, hematite can also form as a product of the unmixing of a hemo-ilmenite through a slow cooling history. The habit of hematite to the other opaque mineral may indicate something of the past events of the Melrose Stock.

As mentioned earlier, the hematite occurs in both the magnetite and ilmenite. The hematite associated with the magnetite is undoubtedly due to late stage alteration. The hematite associated with the ilmenite is open to question regarding interpretation based on petrographic observation. The two alternative origins, of the hematite oxidation and exsolution, shall be considered.

The sites having the apparent hematite exsolution within the ilmenite are distributed along the western border of the range as shown in Figure 2-8. The proximity to the basin and range fault on the west side of the range may indicate a cause and effect relationship. The fault may have served as a major avenue along which fluids migrated, and altered the rocks of the intrusive, thus suggesting that the blebs of hematite are a result of alteration or oxidation. A number of abandoned prospects are found on the west side of the range indicating areas of alteration and minor mineralization. The distribution of sites having

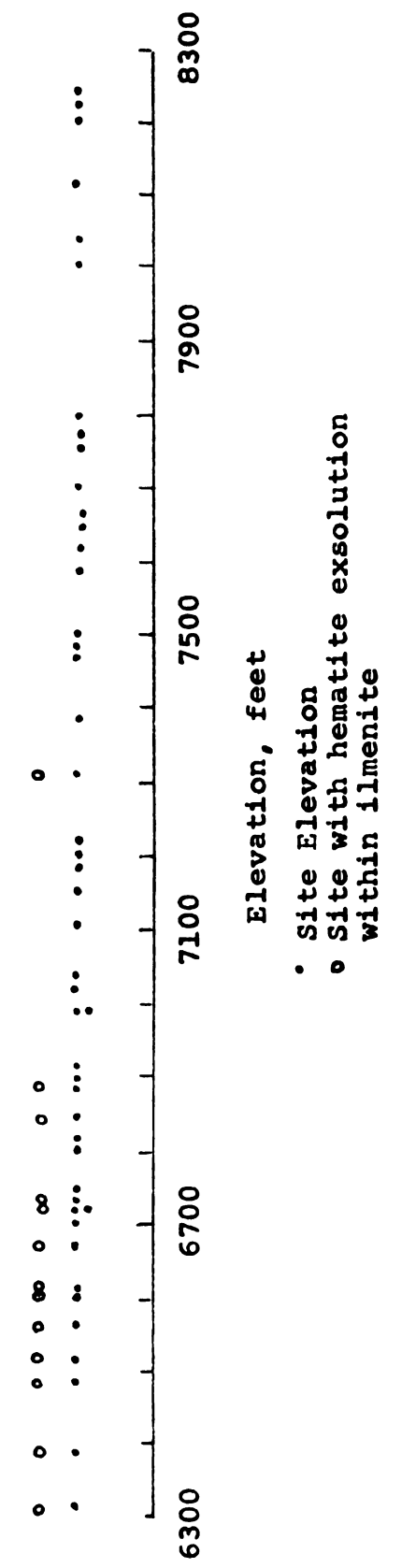


hematite after magnetite also fall along the western margin of the range. The evidence supports the contention that the hematite is derived by alteration.

There is also evidence supporting the view that the hematite blebs are in fact exsolution lamellae. The blebs appear to be discrete entities within the ilmenite grains with no apparent avenues or partings to the perimeter of the grains as evidenced in the alteration of magnetite. If the lamellae are true exsolution, the hematite would be expected to have formed deep in the intrusive where temperatures and slow cooling rates permitted exsolution.

Support to the latter hypothesis can be obtained by studying the distribution of hematite within the intrusive. A measure of depth within the magma chamber is obtained from the distance to a known contact (as on the south) and the site's elevation. In general (Figure 2-8), sites displaying the hematite lamellae are in excess of one mile from the known margin of the intrusive. The exception is Site 26 which is in the monzonite. The site elevation effect is tested by plotting vertically the site elevation positions and denoting the presence of hematite lamellae. The results are shown in Figure 2-9. There is a remarkable correlation between the presence of hematite lamellae and sites of low elevation. The occurrence of the apparent exsolution is found deep within the magma chamber.

Not all sites with the apparent exsolution show magnetite alteration to hematite. This would tend to support

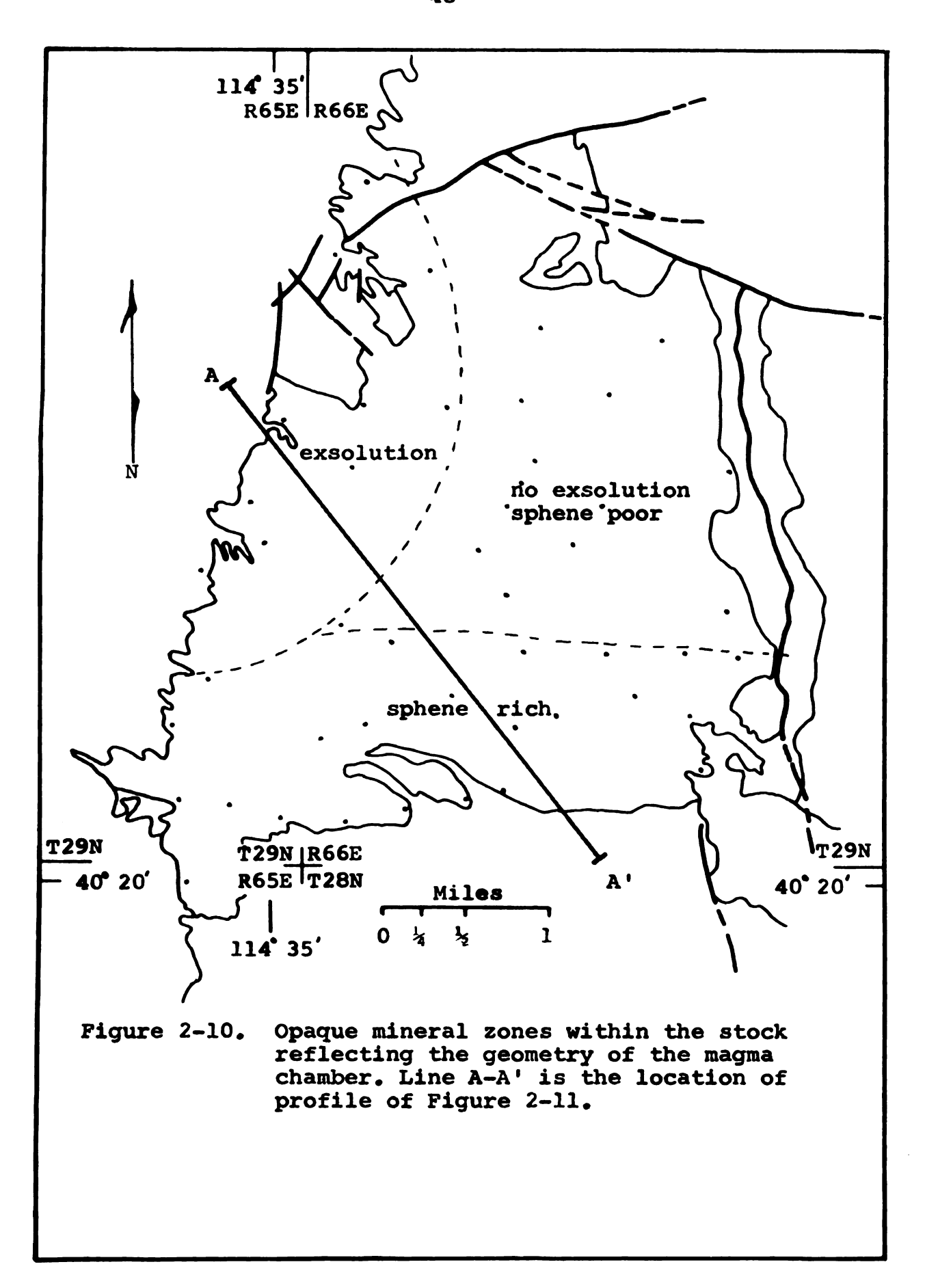


Distribution of exsolution bearing ilmenite with respect to site elevation. Figure 2-9.

the view of the exsolution for the alteration, had it occurred, should have affected both the magnetite and ilmenite. Furthermore the alteration of ilmenite would be expected to yield one or more titanium bearing minerals.

The evidence seems to more strongly suggest the blebs of hematite to be true exsolution rather than due to oxidation. Neither alternative can be rejected based on existing evidence. The possibility cannot be ruled out that the western portion of the intrusive may have been subjected to both the effects of slow cooling and alteration.

If the exsolution hypothesis is accepted, a broad zoning of the intrusive can be postulated based on the distribution of sphene and the exsolution within the ilmenite (Figure 2-10). An outer rim exists which is nearly a mile in thickness; this zone reflects the influence of the assimilation of the calcareous host rocks by the magma. An inner, deep seated zone is present and is in excess of a mile from a margin or roof. The interior zone would provide a favorable environment for the unmixing of an hemo-ilmenite. The other zone may be intermediate to the above zones, or it may possibly be a result of the roof of the intrusive in that portion of the stock being low in calcium. Figure 2-11 illustrates the general nature of the zoning on a northwest-southeast profile drawn through the Dolly Varden Mountains.



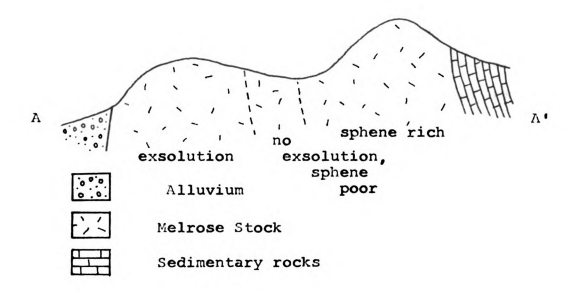


Figure 2-11. Cross-section of the Nelrose Stock showing the observed opacue mineral zoning. See Figure 2-9 for location of profile.

2.4 Association Coefficients

2.4.1 Introduction

In observations of rocks in thin section, relationships are commonly noted that are more intimate than would
be expected if the distribution of the minerals were purely
random. Observations on the suite of thin sections from the
Melrose Stock appear to show a preferential distribution
or association of magnetite to the ferromagnesian silicates.
A method was developed to quantify this observation. The
method developed will allow a quantitative determination
of the spatial distribution of the minerals about magnetite
grains. If a preferred association is suggested, or even
if it is not, then a better insight will be gained into
the crystallization history of the magnetite in particular
and the rock in general.

Though the method developed has been used in this study for the association of an accessory mineral with respect to the constituent minerals of the host rock, it could also be used to study other mineral grain assemblages in various types of rocks. When determining the association of a constituent mineral, it is advisable to modify the technique slightly to include associations of a mineral with itself. Quantitative investigations on intergranular relationships have been studied by Flinn (1969) and Kretz (1969).

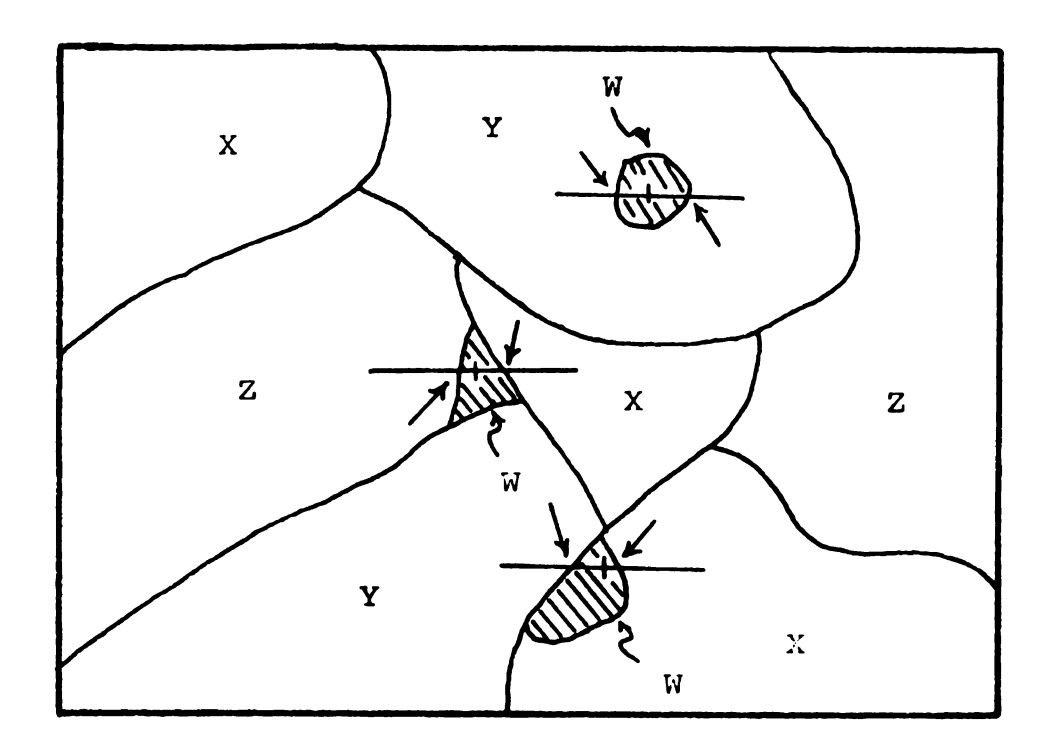
In the rocks of the Melrose Stock it is suspected that a portion of the magnetite associated with the

ferromagnesian minerals may be genetically related to the iron silicates. If the results of the association study suggest this to be statistically valid, then appropriate reactions can be postulated for the observed relationships. This will permit suggestions as to the relative changes of the oxygen fugacity in the magma chamber with respect to time and space.

2.4.2 Procedure

To establish the "neighborhood" about a particular mineral, a point count is carried out in the manner as depicted in Figure 2-12. The figure shows a schematic diagram of a photomicrograph of a rock with four minerals, W,X,Y, and Z. If the association of W with respect to X,Y and Z is desired and a W grain falls under the crosshair of the ocular, then a tally is given to each of the minerals which are at the points where the graticule line exits the W grain. For the uppermost W grain this yields two tallies for the Y. For the lowermost W grain the combination of two points is an X and a Y grain, so consequently, one tally is given to each of their entries. The subtotals of the respective minerals and their total for the hypothetical example are also shown in Figure 2-12.

In practice the number of magnetite grains which fall under the crosshairs during a normal point count is rather small. To increase the number of opaque grains encountered a graticule with 20 points in a line was used. In this



Mineral	х	Y	Z
Count(ST)	2	3	1
Total(T)		6	
Mode(M)	.33	.33	.33
Association(A)	.33	1.5	0.5
Assoc. Coef.(AC)	1.0	1.5	0.5

Figure 2-12. Schematic diagram of data collection procedure for the association coefficients of W with respect to minerals X, Y, and Z. Graticule of ocular shown on each W grain. Counts are made at the points indicated by arrows. The resulting point counts, associations, and association coefficients are shown in the accompanying table.

manner the probability of having the crosshairs falling on an opaque grain is increased twenty fold and in addition it gives weight to grains proportional to their volume. Thus, if a large grain falls under three adjacent crosshairs, three counts are given to each of the minerals bordering the opaque grain.

Approximately 30-40 minutes were spent on each thin section. Counting was expedited by traversing with the analyzer out so that it was easy to note when an opaque fell under a crosshair. The analyzer was used when a grain was encountered. From 150 to 400 counts were tallied in the 30 to 40 minutes.

Experimentation with random spacings and directions of traverse lines reveals no significant difference with the results obtained with a uniform grid system. Where no preferred orientation of the grains exists it is safe to use the uniform grid pattern and, furthermore, it is more expedient than the random grid. If there was a preferred orientation of the minerals, then a random grid system would be necessary.

2.4.3 Association Model

A probability model has been chosen and parameters derived from the expected distribution of mineral grain assemblages assuming a random distribution. Values of the parameters deviating from the expected norms are interpreted as being an indication of a non-random distribution.

Two assumptions are made in the application of this model to a geologic situation; first, the probability (P) of finding a given mineral at a point on a thin section is equal to that mineral's mode (M) and second, if a thin section has a great number of grains, the probability of observing any combination of two grains in contact is an independent event (equal to the product of the two respective probabilities).

Table 2-3 shows a simple hypothetical model with four minerals (W,X,Y, and Z). A similar model could be set up for any number of minerals. The object is to determine the association of W to X, Y, and Z. The first column in the table shows the possible combinations of the minerals bounding W at the two points where the graticule line exits W. The corresponding probabilities and point counts for these combinations are found in the remaining columns. To illustrate the model, suppose that X has a modal volume of 50 percent (i.e., P_x is 0.5). The probability of observing an (X,X) combination, an X grain at each point where the graticule line exits W, should be 0.25. In 100 observations, 25 (X,X) combinations should occur and this would yield 50 tallies for mineral X. Similarly, if the mode of Y is 40 percent (X is still 50 percent), 40 of 100 grains recorded should be (X,Y) combinations. This brings 40 counts to each X and Y. In this example the subtotals of X, Y and Z are respectively 100, 80 and 20 with a total of 200. The simplification of the

Probability model for association coefficients. Table 2-3.

	7	Pe	Point Counts	
Combinations	Frobability	×	Y	2
(x'x)	P _x P _x	2(P _x P _x)100		
(x,x), (x,x)	2P _k P _y	2(P _x P _y)100	2(P _x P _y)100	
(x,z), (z,x)	2P _x P _e	2(P _x P _z)100		2(P _x P _x)100
(X,Y)	P, P,		2(P, P,)100	
(X,Z), (Z,Y)	2Py P₹		2(Py P.)100	2(P, P,)100
(Z,Z)	P. P.			2(P2 P3)100
Subtotal(ST)	1.0	2(P)100	2(P)100	2(P)100
Total(T)			200	

sums shown in the table is a result of the following relationship:

1)
$$P_x + P_y + P_z = 1.0$$
.

The association of W with respect to X is defined as the ratio of the subtotal of X (ST_y) to the total T.

2)
$$A_{x} = \frac{ST_{x}}{T}$$

where A_{X} is the fraction of W associated with X. In the case of a random distribution, the association of W to X is the mode of X. Thus,

3)
$$A_{x} = \frac{ST_{x}}{T} = \frac{2P_{x}}{2} = P_{x}$$

Normalization of the association parameter with the mineral's mode (M as a fraction of 1.0) gives the association coefficient (AC),

4)
$$AC_{x} = \frac{A_{x}}{M_{x}} = 1.0.$$

With a random arrangement of grains the AC has a value of 1.0. The AC's for Y and Z are calculated in an identical manner.

As an example, consider the association coefficients calculated from the data of Figure 2-11 assuming the three minerals are present in equal amounts. The results of these calculations are also given in Figure 2-11.

Departures of AC values from 1.0 indicate a departure of the mineral grain assemblage from a random distribution.

Departure of AC values below 1.0 indicate a deficiency

asso 1.0

nine

ily

YC .

pos

and

abo

it:

th

le

1

C

I

association of two minerals whereas values greater than 1.0 indicate a preferential association. When certain minerals display a preferential association, this necessarily means that a deficiency association will be present in one or more of the other minerals. The deviation of the AC values from 1.0 has the limits given by the values 0.0 and 1.0/M, where M is the mineral's mode. The range of possible values for a particular AC is not symmetrical about 1.0. The smaller the mode of a mineral, the greater its AC upper limit. The deviation of an AC from 1.0 is a probability measure. The greater the departure from 1.0 the chances are less that the event will happen, or at least it being random.

A Chi-square test can be used to test the significance of a measured set of AC values from their expected values of 1.0. Using the AC values for the test yields a more conservative estimate of the significance than using the expected and observed point count data. The difference in the test probably reflects the normalization of the data to small numbers as contrasted to the original data.

From the association parameter (A) it is a simple matter to estimate the amount of a mineral associated with another mineral which would have to be explained by some association other than a random one. The excess association, the amount greater than the expected, is given by the expression

5) $(A-M) \times 100\%$.

This expression will be negative if the mode (M) exceeds the association and could be termed a negative excess association. The summation of the excess association will be zero. Disregarding the limited data, for the purposes of illustration, the following remarks can be made regarding Figure 2-12. Mineral X has no preferential association with W. Mineral Z has a deficiency preferential association with W and as a result shows less association with W. Mineral Y is the only mineral to show an excess association with W, by an amount of 17 percent ((0.50-0.33) x 100%). Thus, 17 percent of W's modal volume is preferentially associated with Y. Mineral Z has a 17 percent negative excess association. The sum of the three excess associations equals zero.

From the association parameter it is a simple matter to determine the amount of a mineral associated with another which would have to be explained by some other association than a random one. From the results of the example given in Figure 2-12, the excess association of W related to Y is 17 percent and this amount would have to be explained by means other than a random association.

2.4.4 Geologic Influences on the Magnetite Association Coefficient

The association coefficient can give valuable information concerning interrelationships of minerals. The purpose of this section is to explore some of the

possibilities which can explain excess associations of magnetite to the constituent minerals. Of course, many of the possibilities will be applicable to other association studies. The association parameter and coefficient were developed on a theoretical basis without reference to geologic processes that may affect their values. The geologic environment has notable differences from the mixing of balls together and analyzing them for associations, although in a sedimentary environment this may not be far from true.

The following discussion will primarily be concerned with associations that might arise in an intrusive igneous rock. The description will be concerned with associations divided into two categories, genetic and nongenetic. The former includes associations of the opaque minerals with other minerals which have a common chemical component.

Nongenetic associations arise out of circumstances which prevail in the magmatic environment where there is no chemical correspondence. These shall be considered first.

The formation of an igneous rock is not in most cases the mixing of preformed crystals. Rather, the formation is a long termed event in which various minerals form in response to the physical-chemical conditions of the system. As a result, minerals of different species will be precipitated at different times and in some cases subsequently resorbed. Some minerals may have the bulk of their modes crystallized before the arrival of another mineral.

instance, the early crystallization of mineral A and the late arrival of B precludes the possibility of having B included in A. This would limit the association of B with respect to A. On the other hand, if A and B are the last minerals to crystallize, then there is a high probability for a strong association of one to the other.

An association might arise which can be termed an imposed association. This association results from the viscosity of the melt being sufficiently high to cause the inclusion of one mineral in another because of their inability to repel each other as one or both grow. Furthermore, various minerals may differ in their power of crystallization to push away adjacent magnetite grains. In addition, the strength of crystallization is likely to be related to crystallographic direction. The two factors, viscosity and power of crystallization, should be kept in mincl when evaluating the association coefficient.

If magnetite is introduced into a fractured rock, there may be certain minerals having a greater capacity of Eractures per unit volume and hence, these would have a larger capacity to host the magnetite. An inherited association may arise from two minerals, A and B being originally associated, and a later mineral, C, forming at the expense of B. This would leave A in association with C. Certain minerals may act as hosts for the nucleation of other minerals and hence would display an association. In some cases this may be argued as a genetic

association, in others as a nongenetic.

Genetic associations can be broken down into formative and destructive associations. A formative association in this study refers to the association of magnetite to another mineral as a result of an incongruent reaction.

The candidate minerals for this relationship are the ferromesian silicates. Under suitable oxidizing and P-T conditions, the incongruent melting of a ferromagnesian provide Fe⁺² and Fe⁺³ necessary for magnetite (Czamanske, 1970). Magnetite formed in this manner will be referred to as an oxidation reaction.

Another formative association results from exsolution, a phenomenon that occasionally produces magnetite in formagnesian silicates. In such a case the association would be readily apparent and the association study would not provide new information.

Destructive associations indicate minerals formed subsequent to the normal crystallization sequence, namely deuteric and hydrothermal alterations. Magnetite released during chloritization and serpentinization are examples of destructive association.

Mechanisms tending to destroy associations are differential movement in crystallizing magma and chemical reactions which remove one of two minerals originally associated.

These processes lead to incorrect interpretation of association coefficients.

The foregoing discussion suggests several ways that

C

minerals may become associated and undoubtedly other possible for the associated and undoubtedly

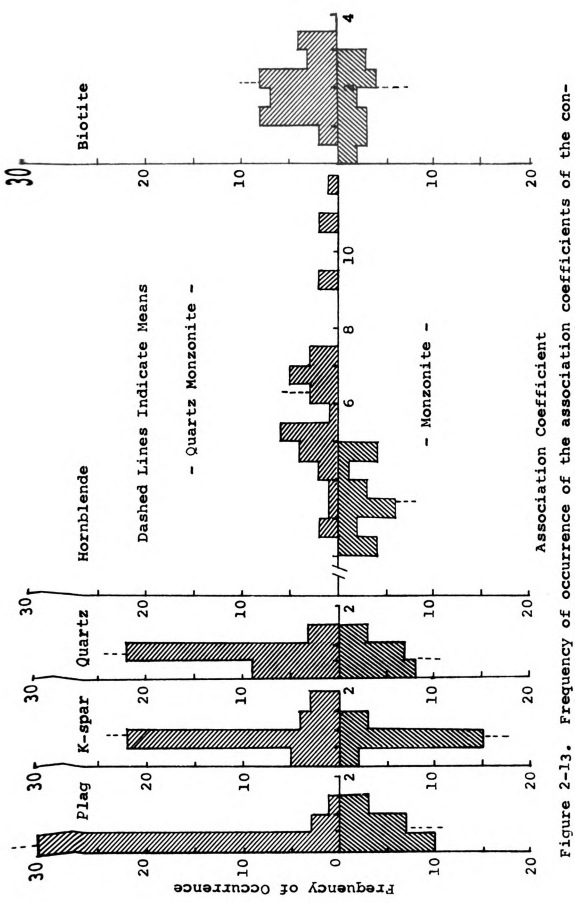
2 _ 4 _ 5 Results and Interpretation

The AC determinations of 34 thin sections from the Quartz monzonite and 20 from the monzonite are shown in Figure 2-13. The ten histograms show a breakdown of the AC values for each of the five constituent minerals for each rock type. The common abscissa is used to aid in comparison between rock types. The dashed line on each histogram represents the arithmetic mean for the respective AC groups.

The first striking feature of the histograms is the notable variation of the AC values for the constituent mineral within a rock unit. A Chi-square test on the deviation of the AC's from 1.0 shows that the quartz monzonite distribution is significantly different from an expected random distribution at the 99 percent level, whereas the monzonite has about a 10 percent chance of being randomly distributed.

Focusing attention on the results of the quartz monzonite, the feldspars and quartz have less magnetite association as contrasted to the ferromagnesian minerals.

Plagioclase has only one-third of the expected magnetite
association. The quartz and K-feldspar have very nearly



Frequency of occurrence of the association coefficients of the constituent minerals by rock type for magnetite.

the expected associations of magnetite. The distribution of AC values for hornblende shows no overlap with the iron-free silicates. The spread of hornblende AC values is the greatest of the constituent minerals. The biotite displays a reasonably compact distribution which has twice the expected proportion of magnetite.

There are three histograms in the monzonite group

which show noteworthy contrast with the quartz monzonite.

The monzonite plagioclase has, on the average, twice the amount of magnetite associated with it as in the quartz

monzonite. A change is noted in the association coefficient of K-feldspar from a slight excess in the quartz monzonite to a slight deficiency in the monzonite. The average association coefficient of hornblende in the quartz monzonite is roughly twice that observed in the monzonite and the association coefficient of quartz and biotite are approximately equal in the two rock types.

The proximity of the magnetite and ferromagnesian silicates to each other as indicated by the association coefficient shows that iron is concentrated into microzones. It is a problem at times trying to decide which came first, the ferromagnesian silicate or the magnetite. The inclusion of one mineral in another is not diagnostic that the inclusion came first as supported by the phenomenom of exsolution. Exsolution in the normal sense has been recorded for the ferromagnesian-magnetite assemblage, but it is not common and the textural relationships

observed during this study do not indicate exsolution.

The Questions then posed are, did the magnetite grains, which in many cases are included, serve as centers for ferro-silicate growth by being sources of Fe, did the magnetite and ferromagnesians form together, or did the magnetite form from the ferromagnesians? Ferromagnesian mineral grains hosting several magnetite grains (a common occurrence) are not likely to have formed by the dissociation of magnetite grains.

The idea that the magnetite and ferromagnesian min
FIGURE Formed contemporaneously will receive special atten
tion. The relationship of ferromagnesian silicates and

non-titanium oxides has been studied by Carmichael (1963,

1967) and Carmichael and Nicholls (1967). Their main in
tis the effect of ferromagnesian compositions on

of precipitation of the magnetite and vice versa.

Carmichael and Nicholls (1967). Their main in
tis the effect of ferromagnesian compositions on

of precipitation of the magnetite and vice versa.

Carmichael (1970) focuses attention on the possibility of

magnetic and vice versa.

Carmichael (1970) focuses attention on the possibility of

magnetic and vice versa.

Carmichael (1963) focuses attention on the possibility of

magnetic and vice versa.

Carmichael (1964) focuses attention on the possibility of

magnetic and vice versa.

Carmichael (1970) focuses attention on the possibility of

magnetic and vice versa.

Carmichael (1963) focuses attention on the possibility of

magnetic and vice versa.

Carmichael (1963) focuses attention on the possibility of

magnetic and vice versa.

Carmichael (1963) focuses attention on the possibility of

magnetic and vice versa.

Carmichael (1963) focuses attention on the possibility of

magnetic and vice versa.

Carmichael (1963) focuses attention on the possibility of

magnetic and vice versa.

Carmichael (1963) focuses attention on the possibility of

magnetic and vice versa.

The AC results and petrographic observations suggest
a portion of the magnetite formed during the inconent reactions of the ferromagnesian silicates. Instead
having the end product an iron free silicate which
ld imply highly oxidizing conditions, it is suggested

the reactions may be somewhat less extreme:

- Orthopyroxene + 0, → Clinopyroxene + Magnetite
- ∠ Clinopyroxene + 0, → Hornblende + Magnetite
- Biotite + Magnetite.
- A 1 three reactions require an oxidizing atmosphere.

The Fe would be available from the solid solution of (Mg^{+2}, Fe^{+2}) and/or $(Mg^{+2}, Fe^{+2}, Al^{+3})$ in the pyroxenes from $(Mg^{+2}, Fe^{+2}, Al^{+3}, Fe^{+3})$ in the hornblende. A Postion of the Fe^{+2} from the silicates has to be oxidized to Fe^{+3} in order to create magnetite. It is to be noted that H_2O is needed for both the reaction of clinopyroxene to hornblende and to produce the oxidizing atmosphere. Commanske did note a decrease in Fe/Fe + Mg ratio in amphiboles and biotites in his work, though he did not attribute this to a ferromagnesian to ferromagnesian mineral tion. Unfortunately no chemical analyses are available from this investigation to determine the change in Fe/(Fe + Mg) ratios from the augite to the hornblende to the biotite.

The suggestion that magnetite formed by oxidation of the orthopyroxenes is speculative since there is no evidence of orthopyroxenes. The reaction of augite to horn-blende is seen in the monzonite as well as the change of hornblende to biotite, though this latter reaction appears to be subordinate. These reactions could well explain the

hasociation of the magnetite to the ferromagnesians.

The greater amount of magnetite with the hornblende

Than with the biotite suggests that more of the magnetite

Than with the biotite suggests that more of the magnetite

Than with the biotite suggests that more of the magnetite

Than with the biotite formed crystallized than when the

Diotite formed. Magnetite once created would be stable

Than of remain in its relative position in the rock, provided

There was little movement in the magma. If the greatest

Than of the biotite formed by incongruent reaction of

Than blende under oxidizing conditions, a higher association of magnetite to biotite would be expected as a result

Than of magnetite to biotite would be expected as a result

Than of magnetite when the hornblende was constituted. Because the AC of hornblende is three times that

Diotite, it is reasonable to conclude that much of the

Diotite formed by direct precipitation as contrasted to

A number of thin sections show significant hydrotheralteration of the hornblende resulting in the release

agnetite. It appears that sites with AC values greater
than 6.0 (the quartz monzonite) represent areas of late

at alteration of the hornblende. In thin section biotite does not appear to have been as susceptible to alteration as the hornblende and its AC histogram reflects this

observation.

The observations of the thin sections and the AC reLts suggest that the magnetite has formed by three proLesses. The amount of magnetite associated with the nonLeromagnesian mineral is that which has apparently formed

direct precipitation. A portion of the magnetite associ ated with the ferromagnesian mineral is also a result → ■ direct precipitation. However, the volume of magnetite Sociated with this group which exceeds their modes is ⇐ tributed to oxidation and hydrothermal alteration. For mineral biotite, the average AC value of each rock The is about 2.0. Since biotite does not show appreciable In Section of Magnete to biotite is interpreted as due to an oxidation re-➡ < tion. Hornblende shows a bimodal frequency distribution
</p> Peak which is believed to represent the association arising from alteration of the hornblende late in the intrusive's history. Average values of 5.0 and 7.0 for the quartz Ronite and 3.0 and 5.0 for the monzonite can be estimated from the histograms of Figure 2-13. The lower of the values were used to calculate the volume of magnetite Created by the oxidation reaction and the higher value to determine the magnetite formed by alteration. Results of excess magnetite associated with the ferromagnesian min Table 2-4.

The results reveal that in both rock types about onefourth of the magnetite can be attributed to oxidation

reactions during the course of crystallization. In areas

where there has been hydrothermal alteration, about onetenth of the volume of magnetite in the quartz-monzonite

and one-quarter in the monzonite is thought to have formed
by alteration. In the unaltered rock the largest portion

Source of excess magnetite associated with the ferromagnesian minerals in percent of total magnetite content, Table 2-4.

	Perc	Percent Excess Magnetite	lagnetite	Total	Total
	Oxidation	ion	Alteration	Oxidation	Oxidation
	Biotite	Hornblende	Hornblende Hornblende		Alteration
Quartz Monzonite	9	20	10	26	36
Monzonite	9	24	24	30	54

approximately three-fourths of the magnetite is interpreted as being from direct precipitation. In rocks that he we been altered, approximately one-third to one-half of magnetite in the quartz monzonite and monzonite rectively has a genetic association.

In a broad sense the histograms represent an encoding the intrusive's cooling history. Comparison of the stograms of different rock types, or even within a unit, help identify dissimilar cooling histories which might too subtle to qualitatively detect. With the aid of servations made during the petrographic study, it is lieved that a reasonably clear picture can be drawn of crystallization sequence of the two primary rock types in the Melrose Stock.

The quartz monzonite will be considered first. Figure

2—1 3 illustrates that the magnetite has only minor association with the plagioclase. This arises when the plagioclase crystallizes as one of the earliest formed minerals.

However, there are some inclusions of magnetite within plagioclase indicating that a portion of the plagioclase formed after precipitation of the magnetite. The K-feldspar, excluding the phenocrysts, was constituted late in the rock's history for it is primarily interstitial and consequently is poikilitic to much magnetite. The numerical results support this point, because the association coefficients are greater than 1.0. Surprisingly, the quartz appears to have formed before much of the K-feldspar for

is usually equidimensional and not relegated to an interstitial position. It is suggested, in view of the AC lues for quartz and textural observations of the thin ections, that the quartz and magnetite were crystallizing concurrently, but the magnetite exhausted itself before the quartz.

From the evaluation of the excess magnetite association of hornblende, it appears that a portion of the magnetite formation can be correlated with the commencement cessation of the period of hornblende formation.

The extural relationships indicate that the hornblende formed cessation of the crystallization sequence. Biotite for the cessation of the crystallization sequence.

The association coefficients and textural relation—

The ps suggest a slightly different paragenesis in the mon
Consite. The plagioclase in the monzonite shows a closer

ciation with the magnetite. This feature is considered

crise from the magnetite crystallizing contemparaneously

the plagioclase to a greater degree than in the quartz

monzonite. A slight deficiency in the association of magnetite with K-feldspar could have resulted from the K-feld
precipitating at a higher temperature. The relative

amount of magnetite associated with the hornblende is less

than in the quartz monzonite, although in absolute volume

the opposite is the case. The precipitation of biotite

and quartz with magnetite is believed to be nearly the

same as in the quartz monzonite.

The two lithologic units do not have great dissimi
I writies in their cooling histories since they do not show

sharp field contact between them and both display similar

paque assemblages. A Chi-square test of the AC assemblages of the two rock types shows a 25 percent chance of

real difference which is, of course, not significant.

I is not believed that this invalidates suggesting the

pove minor differences. It is postulated that the main

ference of the plutons was in their po₂ which was higher

the quartz monzonite as evidenced by the greater assomethor the quartz monzonite to hornblende. This can very reason

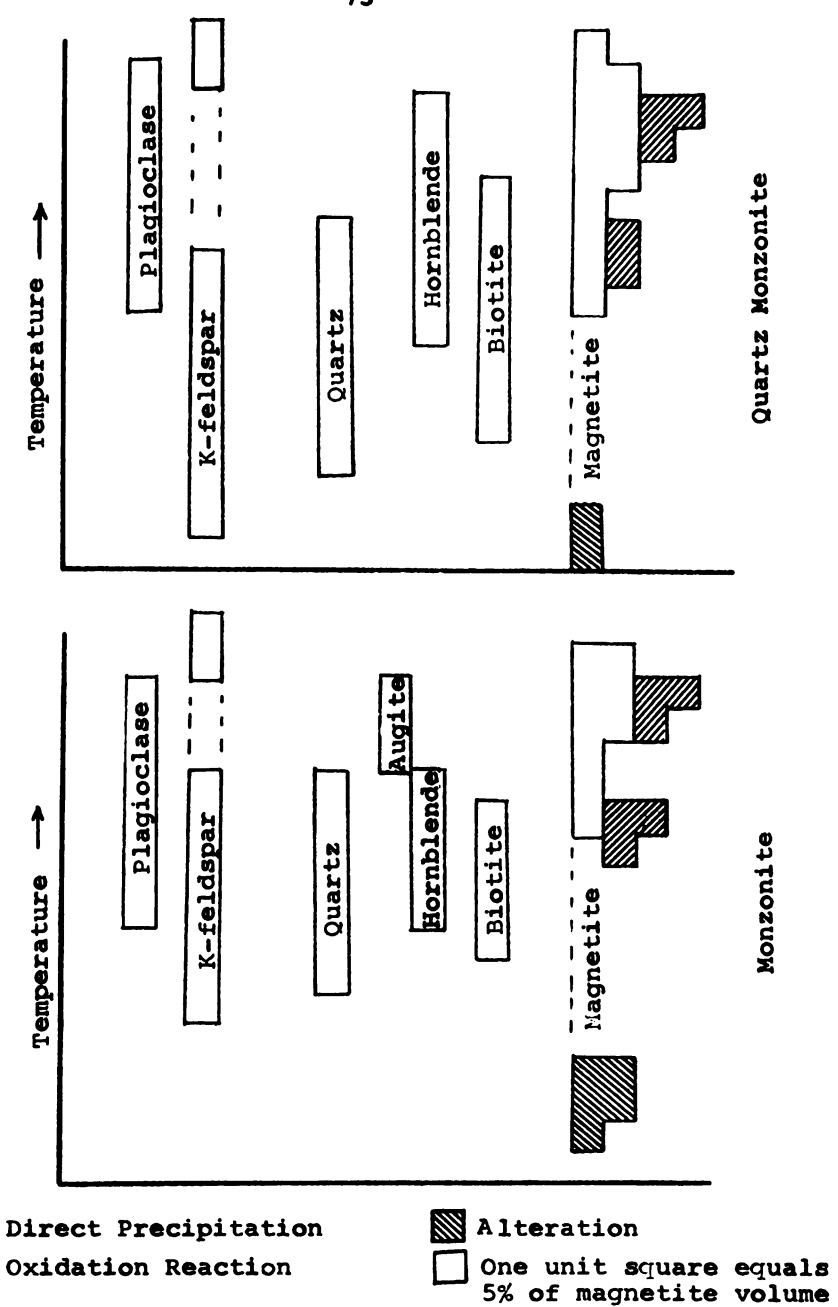
by be explained by a higher concentration of H₂O in the

reages in the monzonite would indicate that it had a

shorter crystallization history than the quartz monzonite.

The foregoing interpretation of the association coefficients of magnetite with respect to the constituent minerals and the petrographic relationship of the constituent minerals suggests a sequence of crystallization as illusted in Figure 2-14 for each rock type. The graphical representation of the magnetite crystallization includes the relative amounts of magnetite formed by direct precipitation, oxidation reaction and alteration. The separation in the K-feldspar bar indicates early formation of the Phenocrysts. Table 2-5 gives the numerical values of the magnetite formed by the three processes as depicted in Figure 2-14.





Proposed crystallization sequence of the Melrose Stock and the mode of magnetite formation based on association coefficients and petrographic observations.

Percent magnetite to total magnetite content formed by alteration, oxidation reaction, and direct precipitation. Table 2-5.

	Alteration	Oxidation Reaction	Direct Precipitation
Quartz Monzonite	10	25	65
Monzonite	25	30	45

*To Nearest 5 Percent

2.5 The Interstitial-Inclusion Index

The interstitial-inclusion index (III), which is an outgrowth of the association study, measures the average number of mineral species about a magnetite grain. It does not indicate the number of grains bordering a magnetite grain. Higher values of the index indicate an interstitial tendency of the magnetite whereas lower values suggest an included nature of the magnetite. The lowest value of the III (all the magnetite is included) is 1.0 and the maximum value is 5.0 (each magnetite is coordinated by the five constituent minerals). The III obviously cannot give the true number of species neighbors since a thin section is limited to two dimensions, but on a relative basis the parameter can be of value.

Figure 2-15 is a compilation of the frequency of OCCUrrence of the III's for the monzonite and quartz monzonite. The histograms are quite similar in range of values and an apparent bimodal distribution. To gain an insight into the possible cause of the apparent bimodal distributions, those sites with III > 2.2 and III < 2.0 for the quartz monzonite and III < 1.9 and III > 2.1 for the monzonite are plotted in Figure 2-16. The reason for eliminating the intermediate values at this point is to help delinate possible patterns. There does not appear to be a strong spatial pattern, though there may be a slight clustering of low values on the west side of the stock and high values on the east. The results of Figure 2-16 prompted

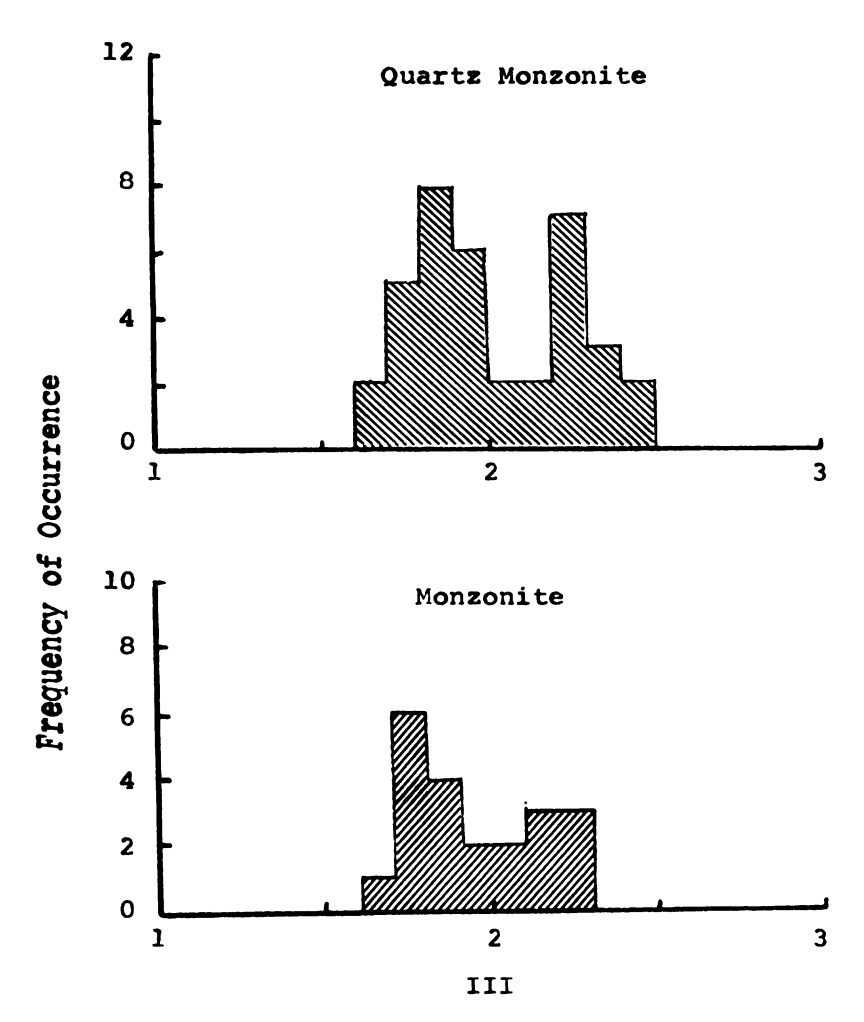
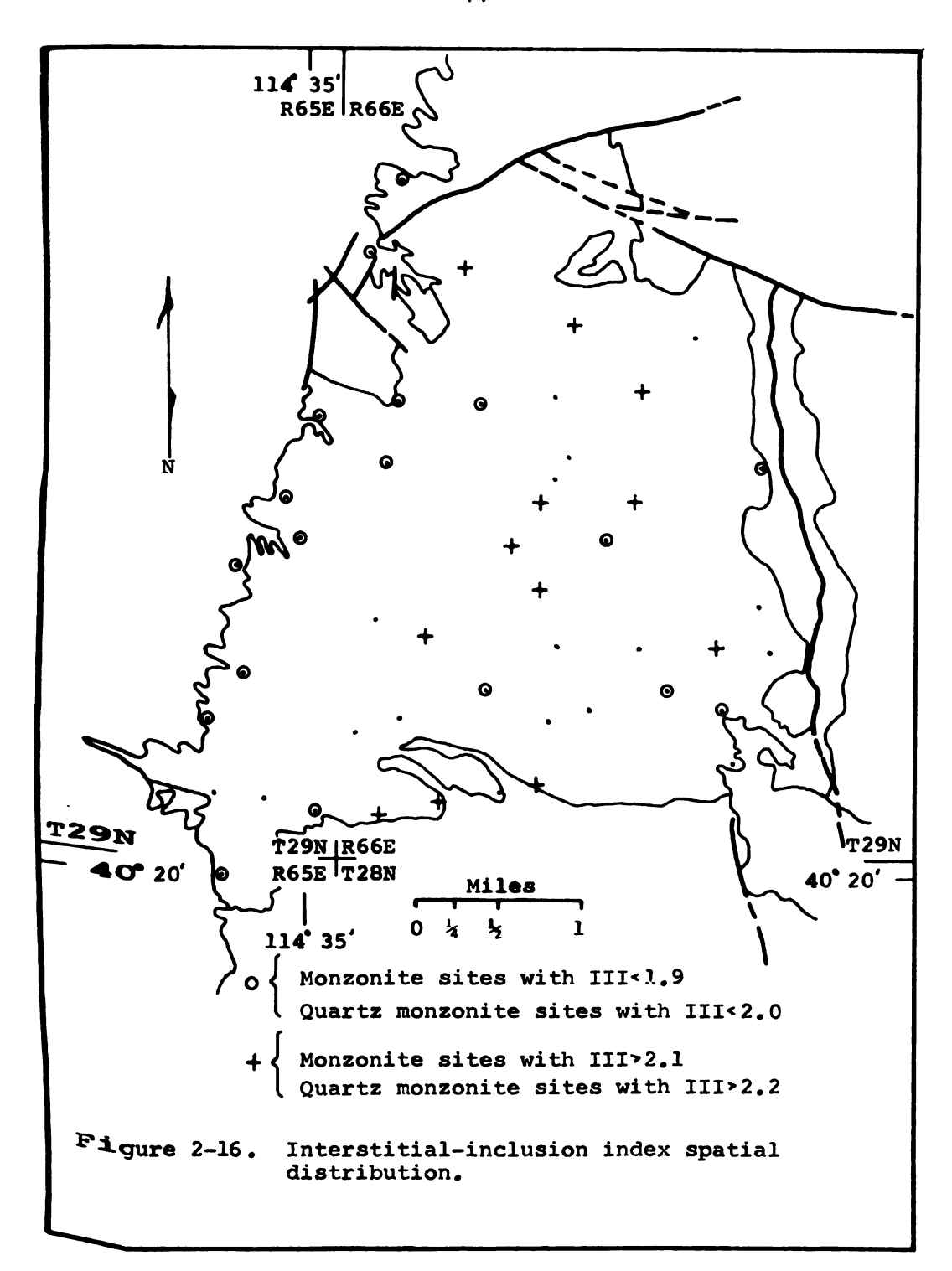


Figure 2-15. Distribution of the interstitial-inclusion index for the quartz monzonite and monzonite rock types.



plotting of the III's as a function of site elevation for each rock type (Figures 2-17 and 2-19).

The III increases with elevation in the quartz mon-**ZOnite**, though there is much scatter. There are three possible origins for the direct relationship of III to elevation in the quartz monzonite. A change in grain size of the magnetite with respect to elevation within the magma Chamber can give rise to a different coordination capacity with the constituent minerals. If the magnetite increased in size with elevation then there would be a greater probability of having more minerals coordinated with it. This assumes that the constituent minerals remain roughly con-Stant in size with elevation, an assumption which appears to be true on the basis of observation. The percentage Of grains whose size is greater than 50 microns (data from Figure 2-5) indicates the size to be increasing with de-Creasing elevation. This contradicts the consideration of grain size as being the influence on the variability of the III.

A second origin for the direct relationship is that
the trend may suggest the degree to which the magnetite
formed by oxidation reaction and direct precipitation.

Magnetite forming by an oxidation reaction would have a
greater likelihood of being included and hence a lower III.
Conversely, magnetite forming by direct precipitation is
more likely to be pushed to an interstitial position and
consequently display a higher III. However, there does

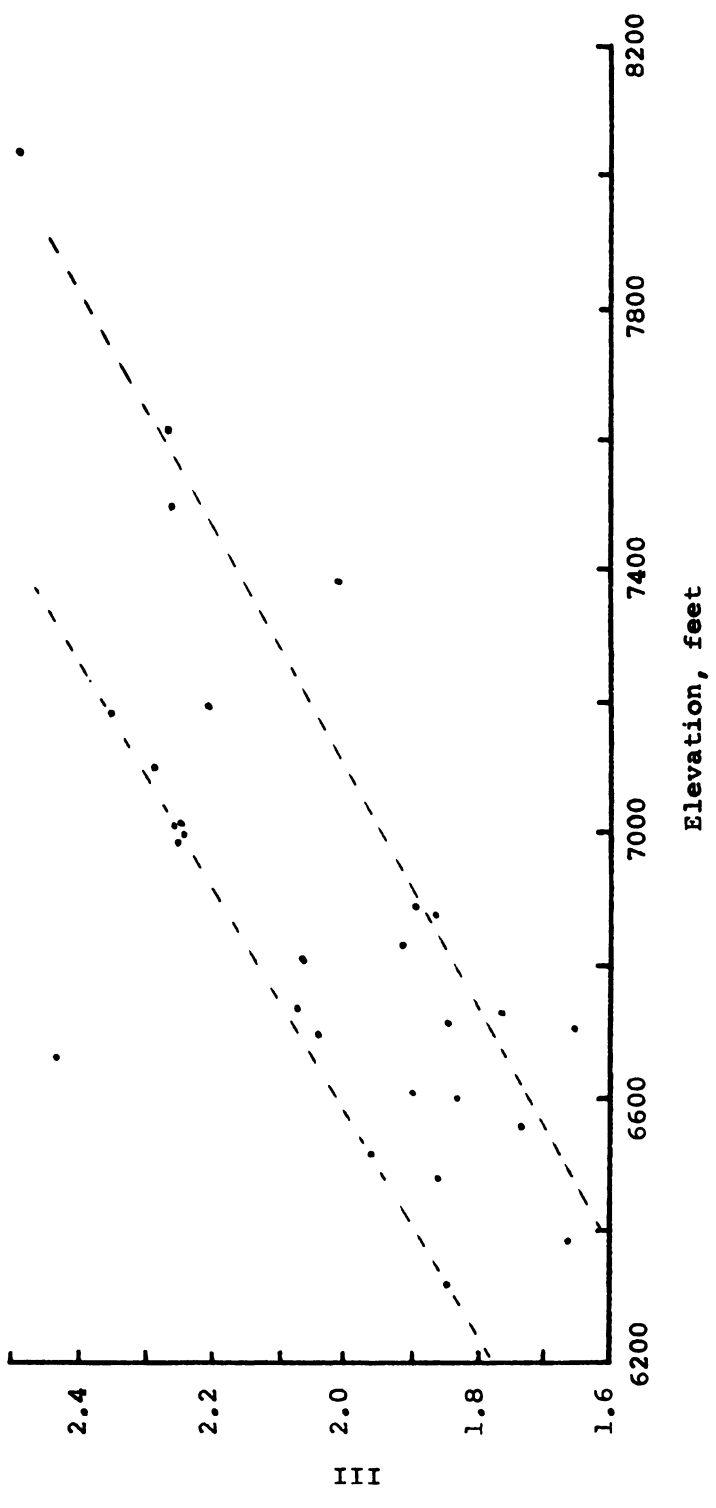
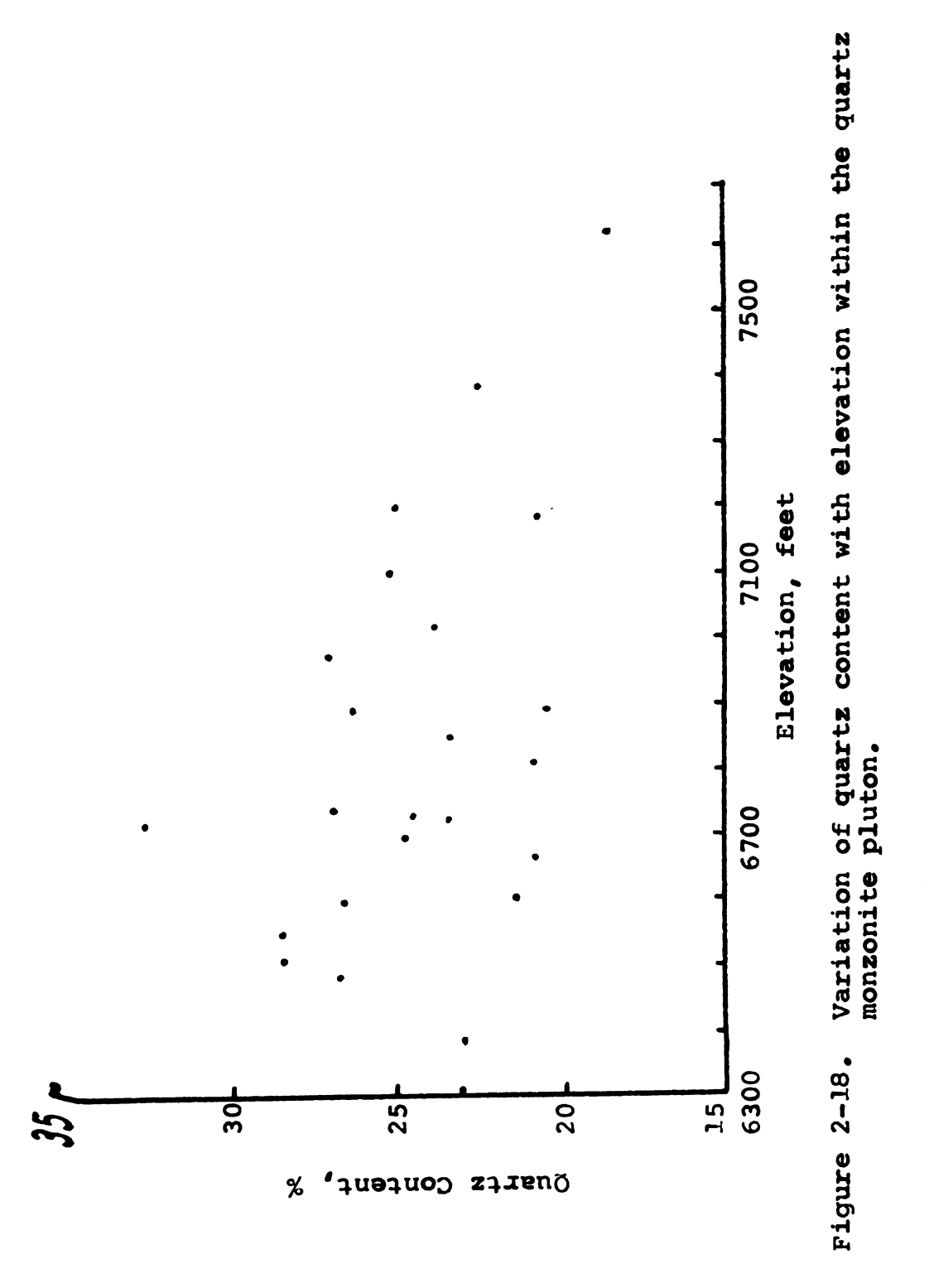


Figure 2-17. Variation of the interstitial-inclusion index with elevation within the quartz monzonie pluton.

Tion coefficients with elevation (Figure 2-24). This figure indicates that the III should take on lower values due to greater magnetite-hornblende associations. Either the assumption for this argument is incorrect or there is another factor predominating over the association affect on the III.

As a third possible origin, the trend of Figure 2-17 may reflect a viscosity variation within the cooling magma. In the early stages of crystallization (high in the chamber) the magma may be less viscous due to a slightly lower silica content and the resulting more mobile melt would permit the magnetite grains to be pushed to interstitial Positions. In the later cooling history, deep within the magma chamber, the viscosity would be greater and the magnetite grains would be less easily moved aside and more likely to be included. This idea is supported by the general increase in quartz content with lower elevations as shown in Figure 2-18. It is assumed that an increase in Silica content is reflected in the quartz content, an index of the relative viscosity of the magma. Of the three explanations considered for the change in the amount of included magnetite, the viscosity factor fits the observed data best and is thus favored. However, this may be a simplistic solution to a rather complex problem.

The monzonite histogram (Figure 2-15a) is shifted slightly to the left of the quartz monzonite histogram



The smaller grain size distribution of the magnetite within the monzonite (see Figures 2-4 and 2-5 and Table 2-2).

Furthermore, the results presented in Table 2-4 indicate that a significant amount of magnetite was formed by alteration and peritectic reactions, processes that will tend to decrease the III. Therefore, both the mode of formation and the grain size distribution may be the cause of the slight downward displacement of the peaks of the monzonite histogram. However, it is thought that the (quartz-poor) monzonite pluton, would have a lower viscosity than the quartz monzonite, thus suggesting that the III should be higher in the monzonite than the quartz monzonite. If this is true, then the above two effects more than offset the viscosity factor.

Figure 2-19 shows the relationship of the III values

With elevation within the monzonite pluton. There is no

direct relationship of the parameters as evidenced in the

Quartz monzonite. It does appear, however, that there is

a concave upward trend of the data. If viscosity was a

Controlling factor in the quartz monzonite pluton, then

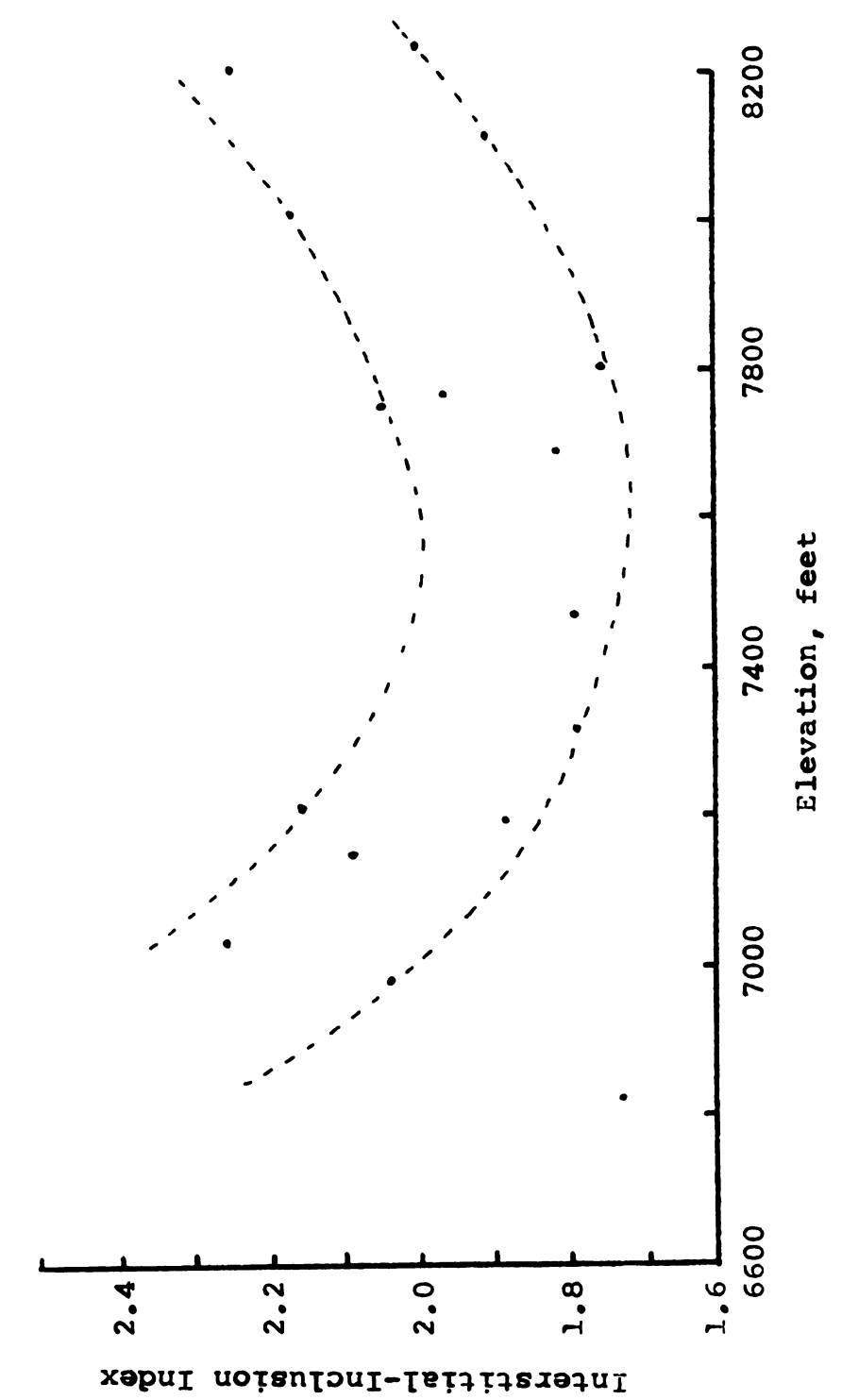
it should also apply to the monzonite pluton. The viscosity as shown above reflects the depth and in turn, something

of the geometry of the magma chamber. The high elevations

in the quartz monzonite pluton indicate an ascent towards

the roof or a margin of the intrusive. Similarly this can

be postulated for the monzonite pluton. The lower portion



Variation of the interstitial-inclusion index with elevation within the monzonite pluton. Figure 2-19.

sent, by analogy, an area of the monzonite where the quartz content is higher (the magnetite is preferentially inclued). The highest and lowest elevations in the monzonite show the magnetite to be interstitial reflecting a lower quartz content.

It is speculated that the monzonite pluton is a lenlike mass upon the quartz monzonite. The margins of the
monzonite pluton are thought to be those sites which form
the low grouping of the data in Figure 2-20. These are
the sites having a low quartz content and are thought to
have crystallized first. The upper group of data are
believed to represent the interior of the monzonite pluton
where the quartz content is higher. Figure 2-21 is the
Proposed model of the monzonite pluton.

It is conjectured that the monzonite pluton was emplaced before the quartz monzonite pluton. The margins of the monzonite pluton may have a lower quartz content than the center portion due to the normal enrichment of quartz as crystallization proceeds and perhaps due to delicification of the magma by the host rock. The loss of quartz due to desilicification is probably not an important factor because there is only minor calc-silicate contact metamorphism and silicification of the host rock. The monzonite pluton was not completely crystallized at the time of the quartz monzonite emplaced considering the gradational contact of the two plutons. The quartz

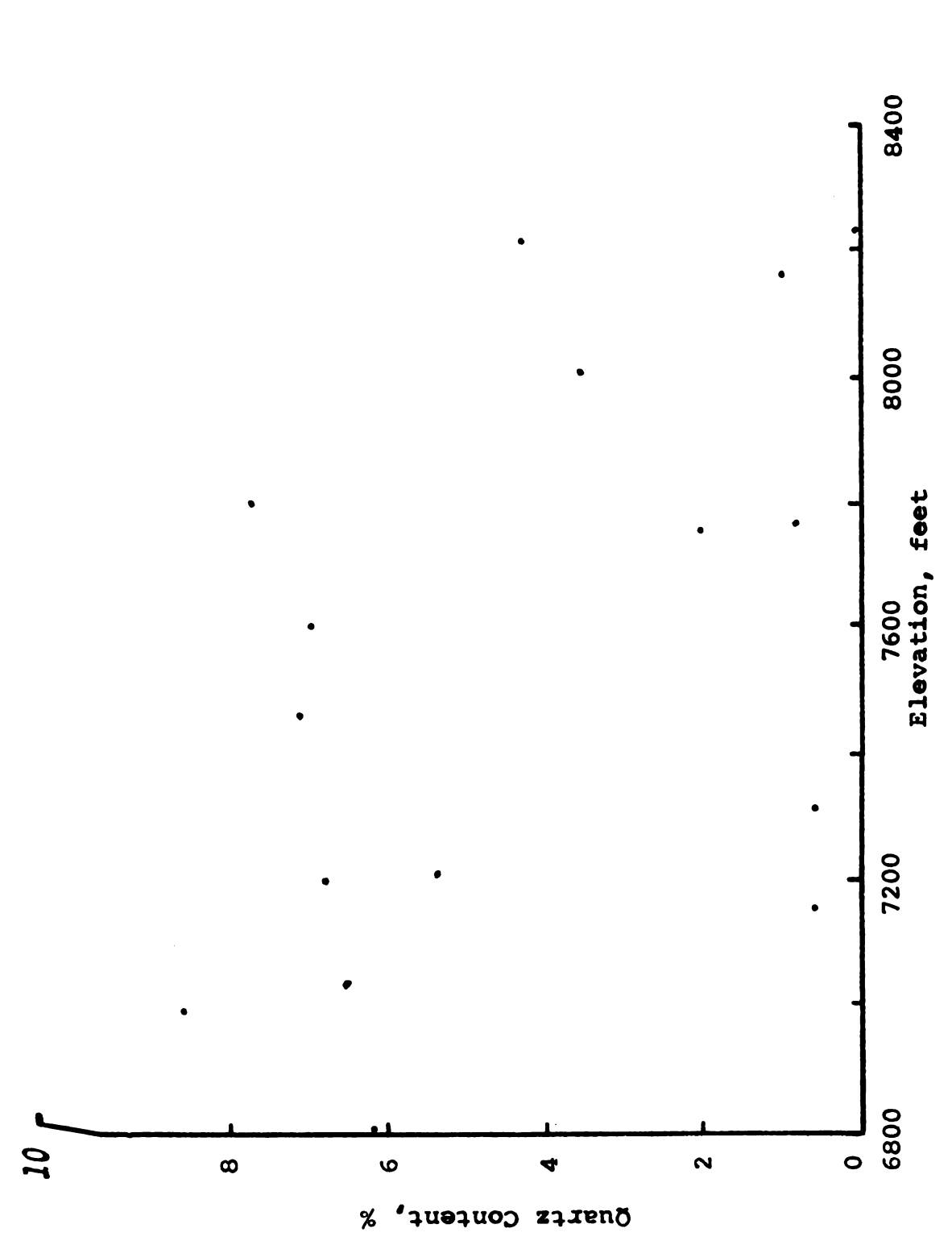
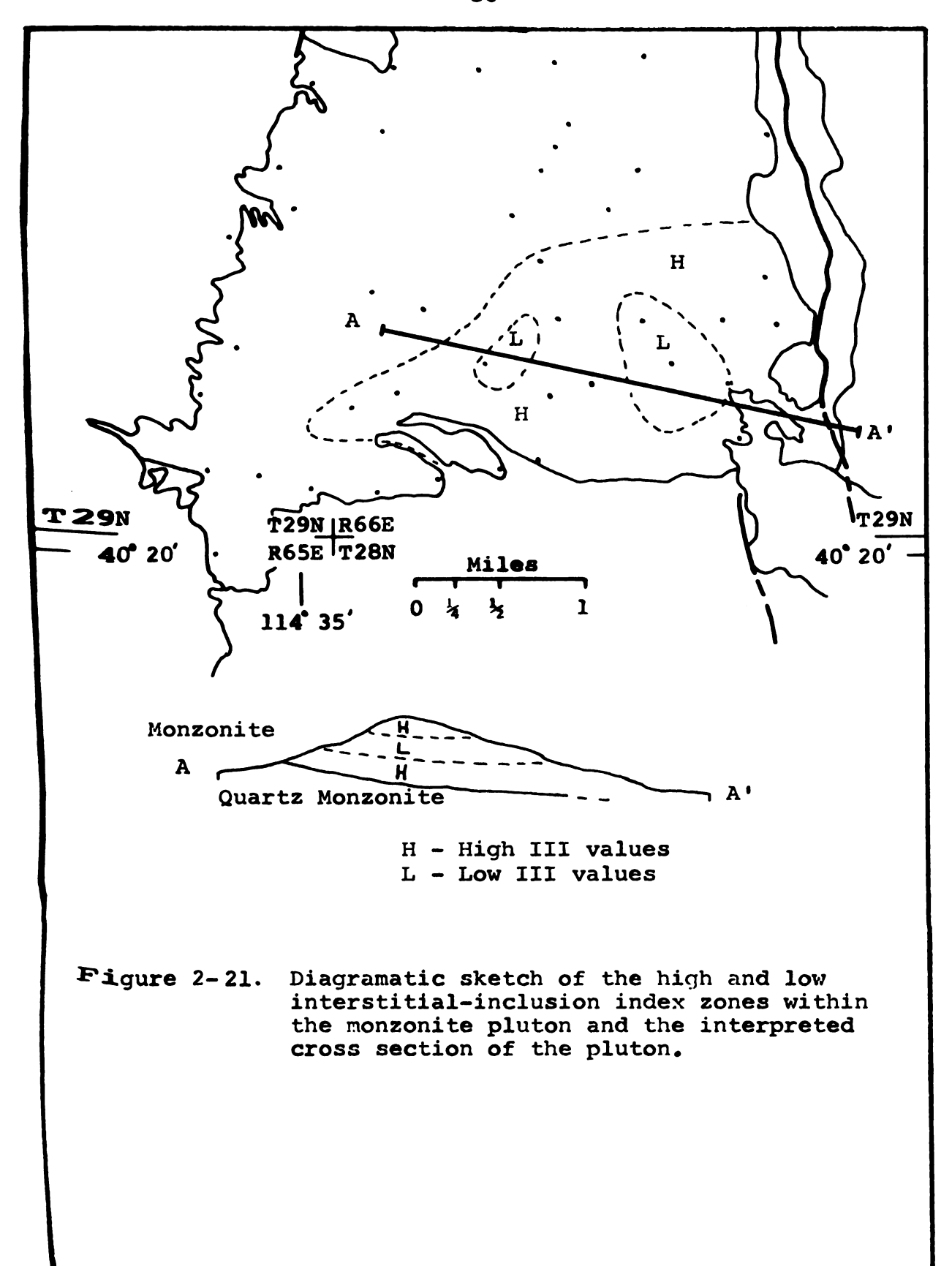


Figure 2-20. Variation of quartz content with elevation within the monzonite pluton.

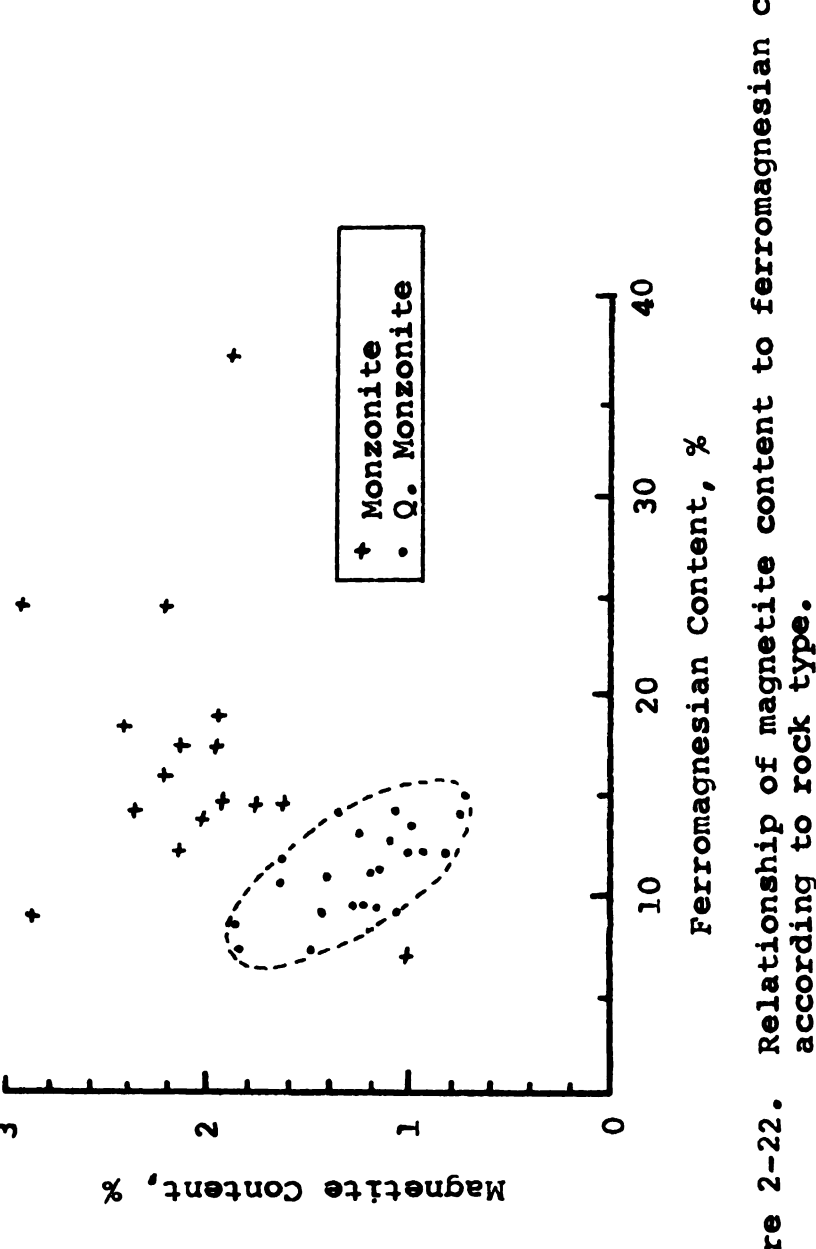


monzonite pluton was emplaced below and to the marginal side of the monzonite pluton.

2.6 Magnetite and the Ferromagnesian Minerals

The study of the association of magnetite with the other minerals has shown preferential association to the ferromagnesian minerals and furthermore, this association is more common in the quartz monzonite than the monzonite. A closer examination of the relationship of the ferromagnesian and magnetite contents may shed further light on the cooling history.

In Figure 2-22 the relationship of the total ferromagnesian content to the magnetite content is shown with respect to rock type. No particular pattern seems apparent for the monzonite, but the quartz monzonite, on the other hand, has a general inverse relationship of the two quantities. A decrease in magnetite content is accompanied by an increase in the ferromagnesians. This suggests conditions existed which favored greater amounts of iron in the oxide structure in some cases and greater amounts in the silicate structure for other cases. The atmosphere of the magma chamber, as determined primarily by the partial pressure of oxygen (pO2), controls the structure in which iron will ultimately reside. An oxidizing atmosphere in the magma chamber would create magnetite and therefore less iron would be available for the ferromagnesians. In a reducing environment the iron would find its way into



Relationship of magnetite content to ferromagnesian content according to rock type. Figure 2-22.

the silicates.

If the initial po₂ was high, then the magnetite should have little association with the ferromagnesians, but if the po₂ increased later in the cooling history, then we might expect a high magnetite-iron silicate association. A graph of the association values of the hornblende within the quartz monzonite with the ferromagnesian content can help to clarify this speculation (Figure 2-23). Disregarding the data that are high due to hydrothermal alteration, the remaining data exhibit an inverse relationship. As a result, it is believed that the magnetite-ferromagnesian inverse association arises from a loss of iron in the breakdown of the ferromagnesian minerals. The oxidation reaction which yields magnetite gives a high association of magnetite to hornblende at the expense of the iron silicate content.

The variation of the hornblende association coefficient with elevation suggests that more magnetite formed by an oxidation reaction at higher elevations (Figure 2-24). Thus, it is concluded that the upper part of the magma chamber represents a more oxidizing condition than the more deep-seated interior throughout much of the crystallization history. The concentration and migration of the volatile phase upwards during crystallization and assimilation of host rock could create the proposed oxidizing environment.

Figure 2-25 shows a breakdown of the ferromagnesians

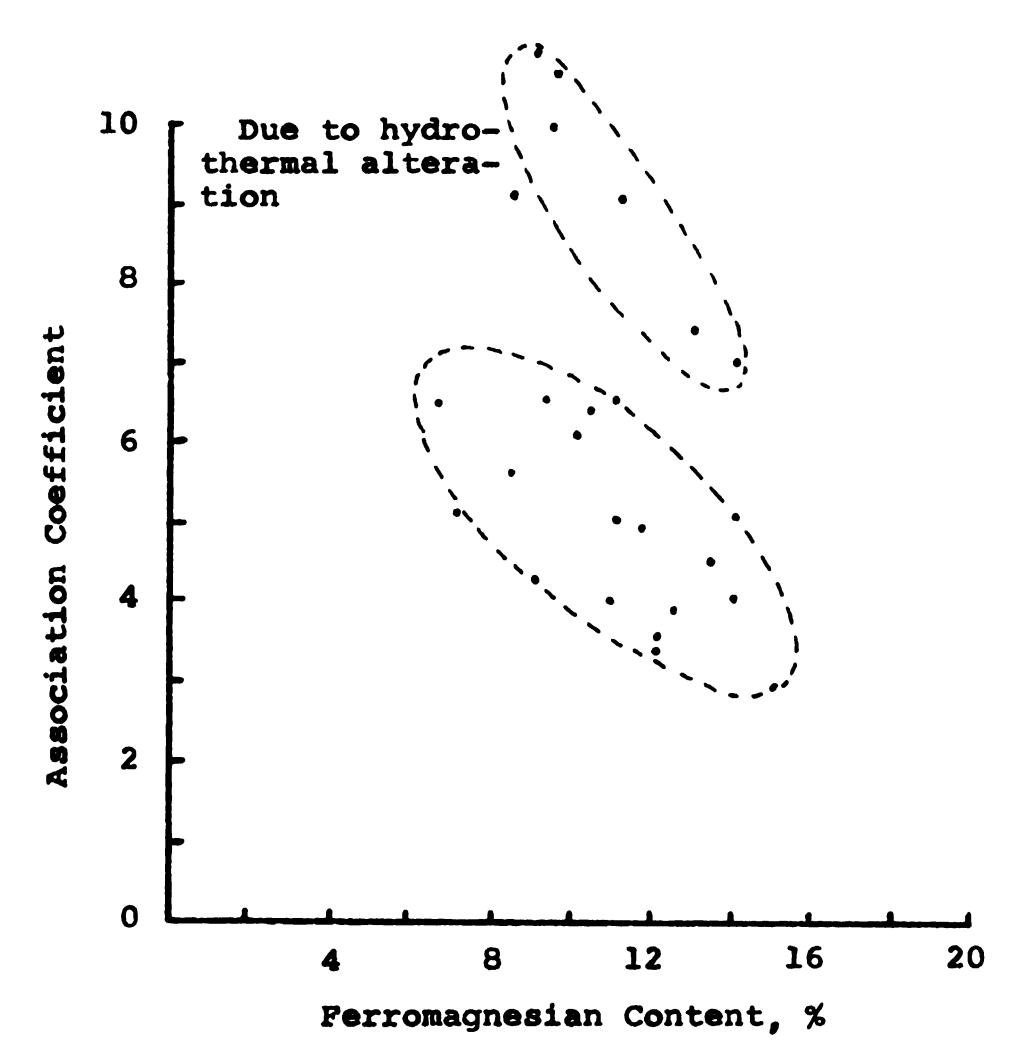


Figure 2-23. Variation of the hornblende association coefficient with ferromagnesian content within the quartz monzonite pluton.

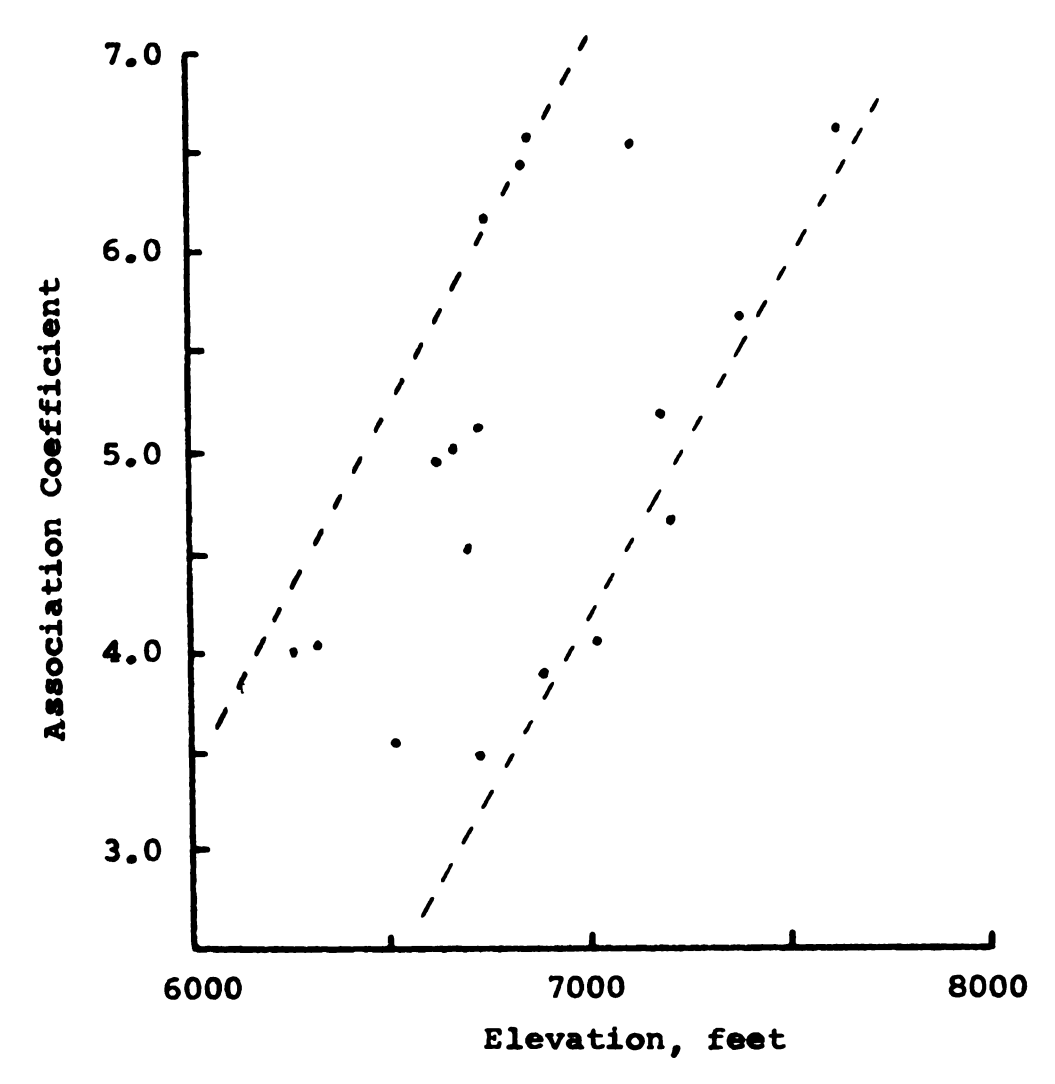
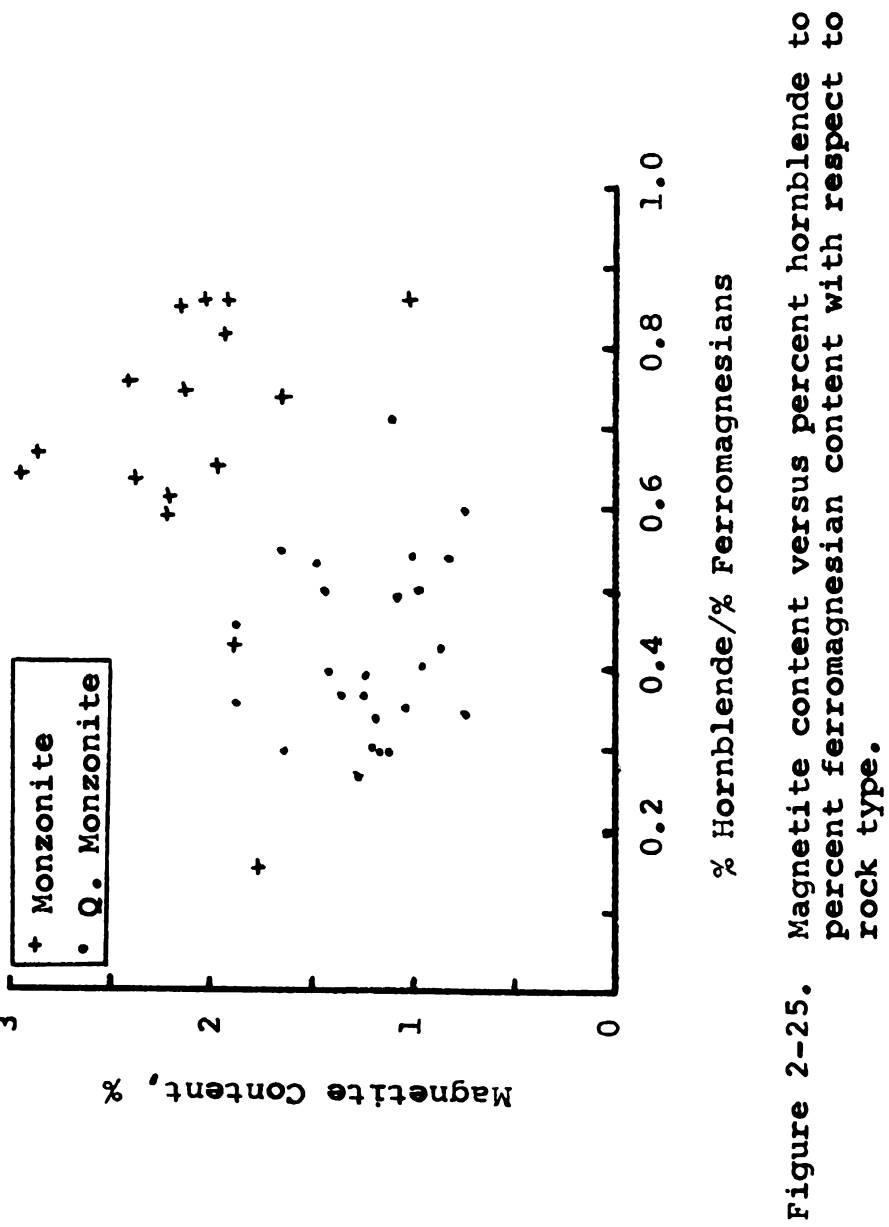


Figure 2-24. The relationship of the hornblende association coefficient with elevation within the quartz monzonite pluton. Excludes data of sites showing appreciable hydrothermal alteration of the ferromagnesian minerals.



as a normalized ratio of hornblende to total iron silicate content plotted against magnetite content. The ratio of the hornblende to the total ferromagnesian content is greater in the monzonite than in the quartz monzonite. This variation probably represents a higher calcium content in the monzonite due to either an initially more calcic magma or a greater amount of assimilation of carbonate sediments. Hornblende and augite are able to accommodate more Ca than biotite in their structures and are probably more likely to form as a result of the dissociations of limestone. This is substantiated by the observations made of a thin section of a xenolith (originally limestone?) adjacent the limestone contact (Site 11). The hornblende content in the xenolith is more than three times that of the surrounding host rock. The magnetic susceptibility of the xenoliths is from 50-100 percent greater than the host rock. In addition, a thin section from Site 18, previously not mentioned, which is a diorite-dike material intruded into the limestone near the contact with the monzonite, shows 60 percent plagioclase, 30 percent hornblende, 8 percent K-feldspar and the remaining as accessories. Clearly this has been modified by the surrounding limestone.

A check of the sites at which xenoliths were noted reveals that 14 of 16 were in the quartz monzonite. Even taking into account the greater number of quartz monzonite sites than monzonite sites, a disproportionately large

number of xenoliths occur in the former lithology. It is suggested that the more basic monzonite pluton was able to more completely assimilate the xenoliths than the more siliceous pluton.

The evidence presented in this section indicates that the magmas were modified to some extent by the surrounding host rock. This may account for some of the higher magnetite content in the monzonite in contrast to the quartz monzonite. Chemical analyses are necessary to determine the extent to which assimilation may have modified the magma and provide information on the iron content and its distribution between the oxide and silicate phases.

CHAPTER III

MAGNETIC SUSCEPTIBILITY

3.1 Introduction

3.1.1 Purpose

Variations in magnetic susceptibility among geologic bodies permits this physical property to be the basis for the magnetic geophysical method. The expression of the magnetic susceptibility through the magnetic mineral is a Sensitive indicator of past events. Then it follows that the examination of the magnetism of a geologic body, the determination of the association coefficients and interstitial-inclusion indices, and the investigation of the Petrologic properties of the magnetic minerals can reveal information leading to a more complete knowledge of geologic bodies. The magnetic susceptibility of the Melrose Stock has been investigated in order to determine its de-Pendence on lithology, and the intrusive's geometry, its expected and actual variations, and the manner in which it Can be analyzed to obtain a representative susceptibility. The magnetic susceptibility was investigated by measurements in situ and on cores.

3.1.2 Sources of Variation

The measurements of magnetic susceptibility are subject to both random and systematic variations. A basic assumption is that the magnetic susceptibility of a rock unit is deterministic.

Variations in susceptibility are due to the primary distribution of the magnetic minerals in the rock. The susceptibility will be the summation of the discrete susceptibilities of each magnetic constituent (assuming negligible magnetic interaction for magnetite contents of a few percent or less). The measured variation or dispersion in the susceptibility is a function of the size and number of samples and their homogeneity. If a sufficient number of data are available, then it should be possible to determine whether the susceptibility displays a normal or Gaussian distribution or a logrithmic distribution in addition to a mean value. It has been found that a logrithmic distribution best fits the scattered data common to rock magnetism (Runcorn, 1967).

The primary distribution of magnetic minerals can be subsequently changed by secondary chemical and physical processes. Mechanical weathering, such as the breakdown of rock by frost action, probably does not directly affect the magnetic properties, but it does help to promote more rapid chemical weathering. Weathering reduces the susceptibility as a result of the relatively nonmagnetic oxides forming at the expense of the magnetite. Deuteric

and hydrothermal alteration can also change the primary susceptibility. Hematization of pre-existing magnetite lowers the susceptibility, whereas breakdown of the ferromagnesian minerals can increase the susceptibility with formation of additional magnetite.

3.1.3 Measurement Variations

Scatter in data can result from instrumentation, the number and size of the samples, and their manner of selection. The dispersion introduced into the data from the repeatibility of the susceptibility bridges is less than one percent standard deviation. The least weathered portions of the outcrop surface were selected for in situ measurements and coring. This would obviously eliminate some dispersion. The collection of several measurements at each site makes recognition of anomalous data easier than when only few data are available. In addition, unusually low in situ readings were rejected in the field. Six to eight in situ measurements and four to fifteen core specimen susceptibilities were obtained for each site.

Systematic susceptibility due to calibration errors in the instruments used for the in situ and core measurements was eliminated by measuring approximately 100 uncut field cores (3 inches length) with the internal coil system of each bridge. The mean of the differences for each specimen was used to determine a correction factor. The core specimens measurement were reduced by 5 percent.

The dispersion of magnetic minerals in a rock poses the problem of determining a representative value of magnetic susceptibility. It would be expected that one measurement of susceptibility on a rock unit would not suffice, unless the measured volume was very large. Since a sample volume is limited, the number of measurements must necessarily increase. The two methods employed in this study will help to establish necessary guide lines for determination of magnetic susceptibility.

The measurement of susceptibility was performed on two different size volumes, 0.70 cubic inches, the core specimens and 57 cubic inches, the effective hemispherical volume measured by the in situ coil. The ratio of these volumes to each other is approximately 80 to 1.

The large difference in the volumes measured by each technique allows the evaluation of the heterogeneity of the rock units within the scale of the specimens. If homogeneity of the rock unit exists at the 0.70 cubic inch volume, then the dispersion in the data between the two techniques should be approximately the same. If the in situ volume is nearer the level of magnetic homogeneity, these data will show less dispersion than the core specimen data. And lastly, if both methods give wide dispersion, it can be inferred that the rock unit is heterogeneous on a scale greater than the in situ volume.

The effective depth of measurement for the core and in situ methods is 3 inches. The in situ technique does

penetrate deeper than 3 inches, but the contribution is not appreciable. The specimens permit observations of the susceptibility with depth from the outcrop surface, however, no systematic increase of susceptibility with depth was noted within three inches of the outcrop surface. This observation does not lead to an insight into the amount of dispersion attributable to weathering.

3.2 Discussion of Results

3.2.1 Normal versus Logrithmic Distribution

The individual in situ data were qualitatively analyzed to determine the type of distribution of the measurements. In the following sections, the analyses of the data assume a normal distribution of the data and that assumption is verified.

The wide scatter of values of magnetic data in many cases best fits a lognormal distribution rather than a normal distribution, this scatter ranging as much as several magnitudes (Irving and others, 1966; Runcorn, 1967). However, the data of this study does not show a wide scatter and hence suggests that the distribution may be normal or Gaussian.

The plotting of frequency distribution of lognormal data on a linear scale gives a graph which is skewed towards increasing values of the abscissa. The same data plotted as the logrithim of the data will display a bell-shaped curve. On the other hand, plotting data possessing a

normal distribution on a logrithmic scale yields a curve which is skewed towards decreasing values of the data and, once again, plotting it on a linear scale yields the bell-shaped curve.

All of the individual in situ measurements collected are plotted, according to rock type, on both linear and logrithmic abscissa histograms as shown in Figures 3-1 and 3-2. The data from the monzonite pluton (Figure 3-1) appears to be skewed slightly to the left on the lognormal plot and symmetrical on the linear or normal plot. The same respective shapes are noted for the data from the quartz monzonite pluton, although it is less marked than in Figure 3-1.

The results shown in these histograms supports the contention that the distribution of the susceptibilities is normal. This places greater confidence in the meaningfulness of the arithmetic mean and subsequent analysis of the magnetic susceptibility.

3.2.2 Inter-site Variations

This section is concerned with the analysis of the data, determining which are reliable, which should be discarded and how many data are necessary to establish a representative susceptibility. To this end, the six to eight magnetic susceptibility means at each site were averaged and the extreme values, the lowest and highest, are plotted against the site mean as in Figure 3-3. Thus,

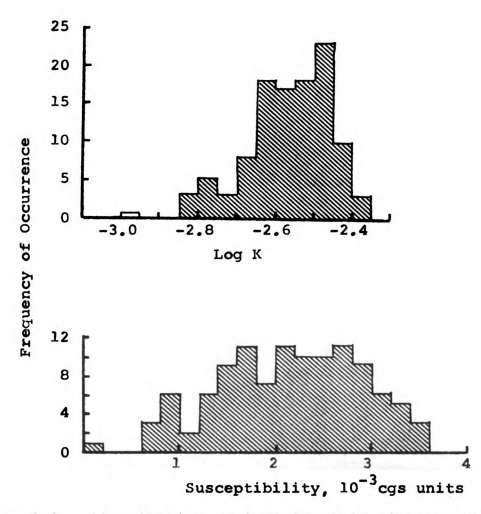
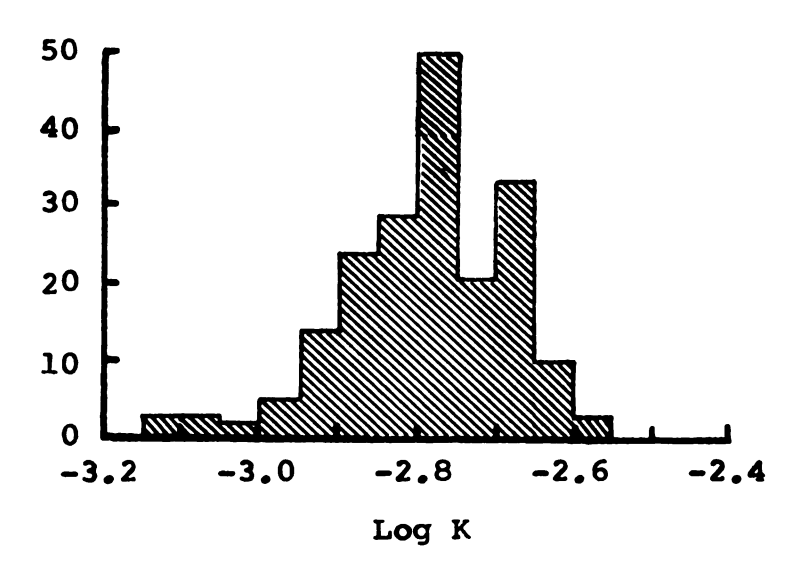


Figure 3-1. Distribution of individual in situ magnetic susceptibility measurements in the monzonite pluton on linear and logrithmic scales.



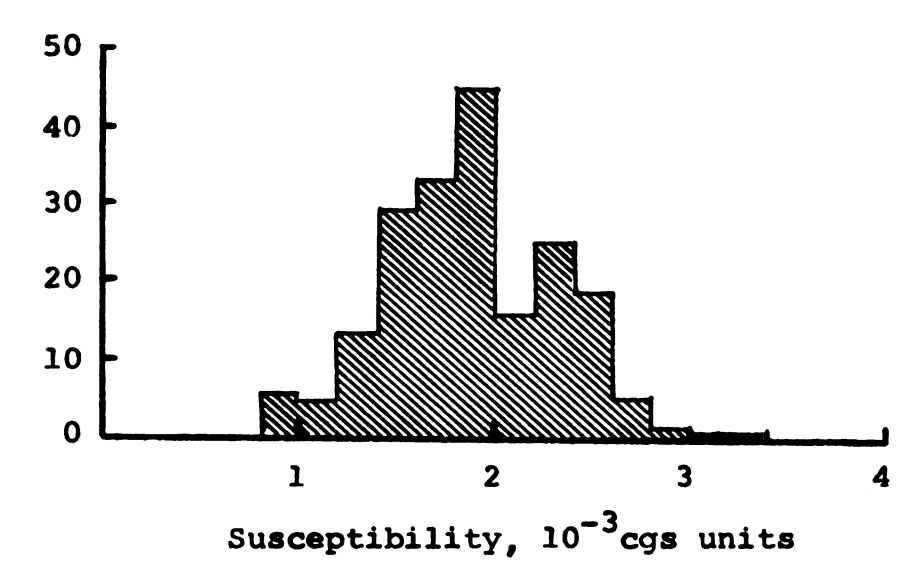


Figure 3-2. Distribution of individual in situ magnetic susceptibility measurements in the quartz monzonite pluton on linear and logrithmic scales.

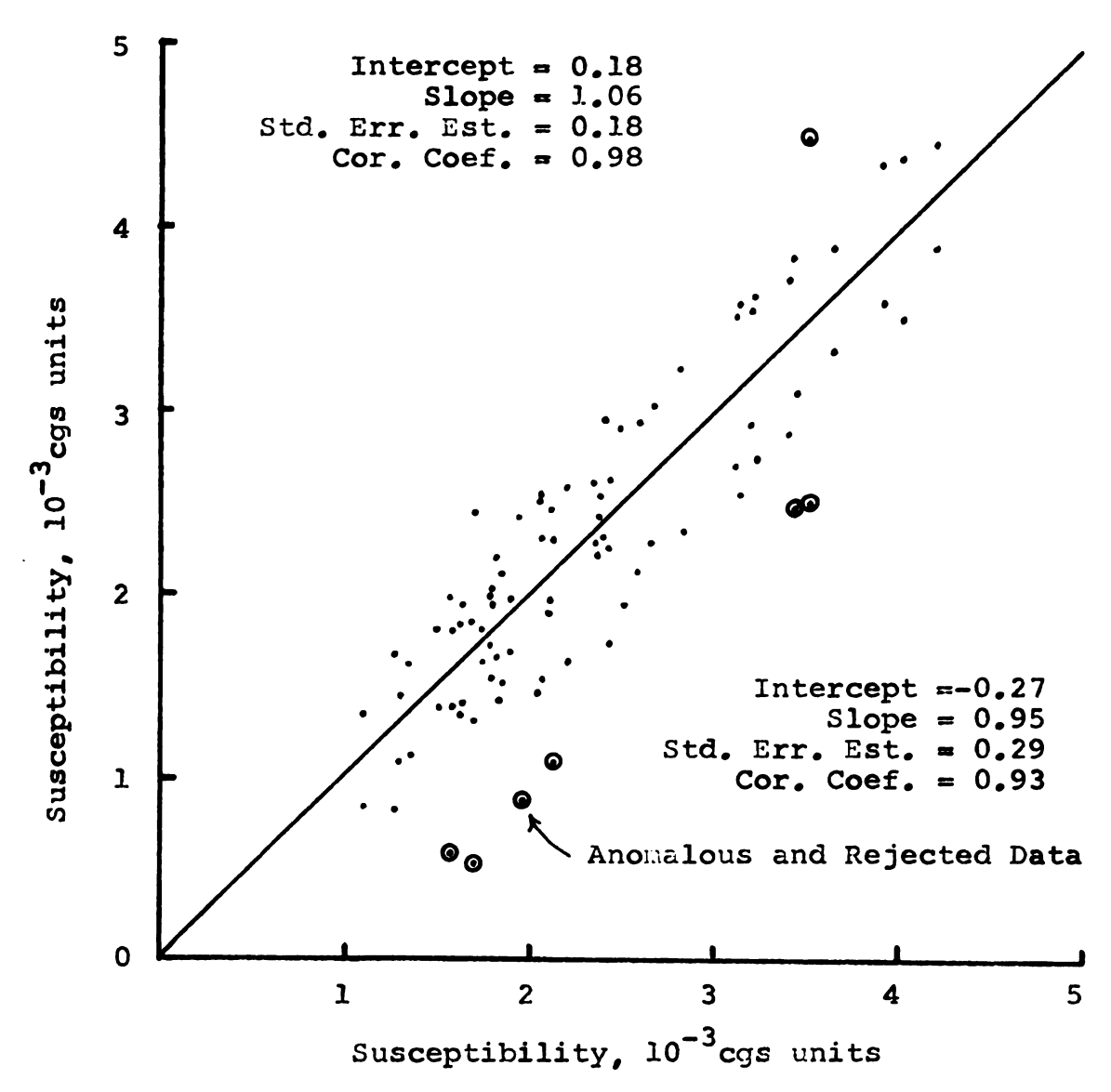


Figure 3-3. Site susceptibility extremes versus site means of in situ measurements. Unity slope line separates maximum and minimum values. Included are the intercept, slope, standard error of the estimate, and correlation coefficient for each of the two data groups.

each site is represented by two points, one each above and below the line of unity slope at the value of the site mean. If the data are evenly distributed about the mean, the distance of the two extreme points off the unity line will be the same. In this manner the dispersion can be generalized and the sites which obviously have anomalous data are easily recognized.

To delineate data which fall noticably outside of the two linear groupings paralleling the unity slope line, linear regression lines were computed for each of the two data groups. Data falling outside of two standard error of the estimates (S.E.E.) from the upper data group were rejected. The pertinent parameters of zero intercept, slope, S.E.E. and correlation coefficient are given adjacent to each data grouping as in Figure 3-3. The S.E.E., which is analogous to the standard deviation, allows a comparison of the scatter of the two data groups.

3.2.3 In Situ

The S.E.E. of the upper in situ data group (Figure 3-3) was chosen as a reference for eliminating poor quality or erroneous data because of its smaller dispersion than the lower group. With a 95 percent certainty that the data points rejected are not representative of the sampled population, points falling greater than two S.E.E. (0.36 \times 10⁻³ cgs units) from the least square lines were rejected (See Figure 3-3). Seven data points representing

6 sites fall outside of the acceptance limits. The site means were recalculated after discarding the anomalous data and the results are shown in Figure 3-4. The S.E.E.'s have been greatly reduced, especially for the lower group, and the two values do not differ appreciably from each other. It is concluded that the data at this stage reasonably represents a normal distribution with a mean being representative of the surface rock at the sites.

A calculation based on the least squares lines from Figure 3-4 indicates that the percent difference between the extreme points near $4,000 \times 10^{-6}$ cgs units is only one-half (20 percent) of the value calculated at 1,000 $\times 10^{-6}$ cgs units (40 percent). This indicates that the rocks of lower susceptibility show greater heterogeneity either due to primary origin or secondary alteration.

Interestingly, there is a distinct change in the distribution of points on either side of a site mean of 2400 \times 10^{-6} cgs units. Below this value the data cluster near the unity slope line as contrasted to above where they are regularly farther away from the line. This value roughly coincides with the values separating the magnetic susceptibility of the two major rock units. The majority of the monzonite sites have a mean susceptibility of greater than 2400×10^{-6} cgs units while the quartz monzonite means are generally less than this value. The origin of the variations in the extreme values may be either original homogeneity or subsequent alteration.

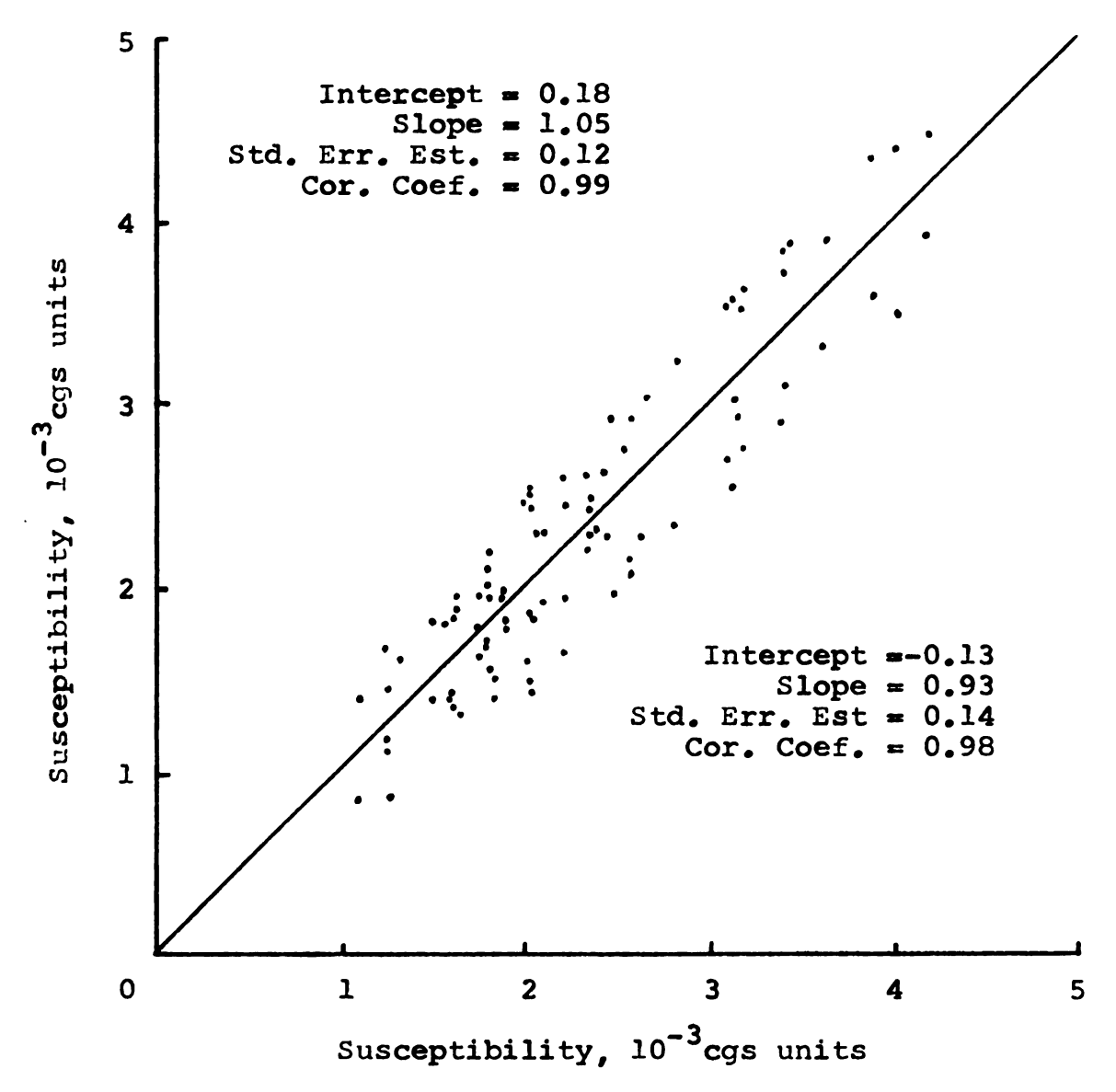


Figure 3-4. Site susceptibility extremes versus site means of in situ measurements after rejection of anomalous data. Unity slope line separates maximum and minimum values. Included are the intercept, slope, standard error of the estimate, and correlation coefficient for each of the two data groups.

A number of the quartz monzonite sites show little alteration, hence less dispersion, and would represent the data falling near the unity line. Some of the quartz monzonite sites are finer grained and therefore may show greater homogeneity and less dispersion.

3.2.4 Cores

The susceptibility measurements of the core specimens were subjected to a similar analysis. The original data, Figure 3-5, show a much greater scatter than the data in Figure 3-3 as shown by a comparison of the S.E.E.. The same criterion was used to eliminate anomalous as in the in situ analysis. The recalculated data are presented in Figure 3-6.

Even after rejection of more data than in the in situ method, the S.E.E. values of the core specimens are larger than those of the in situ method. This difference is a result of the two different volumes sampled by the in situ coil and core measurements. Twenty-nine percent of the core sites required removal of poor data as contrasted to only 14 percent with the in situ sites. It is believed that greater inhomogeneities exist on the level of the core volume than on the in situ volume, which has led to greater dispersion in the data of the former. The in situ method apparently is able to "average out" many of the inhomogeneities which are observed by the smaller volume measurements. The small sample volume

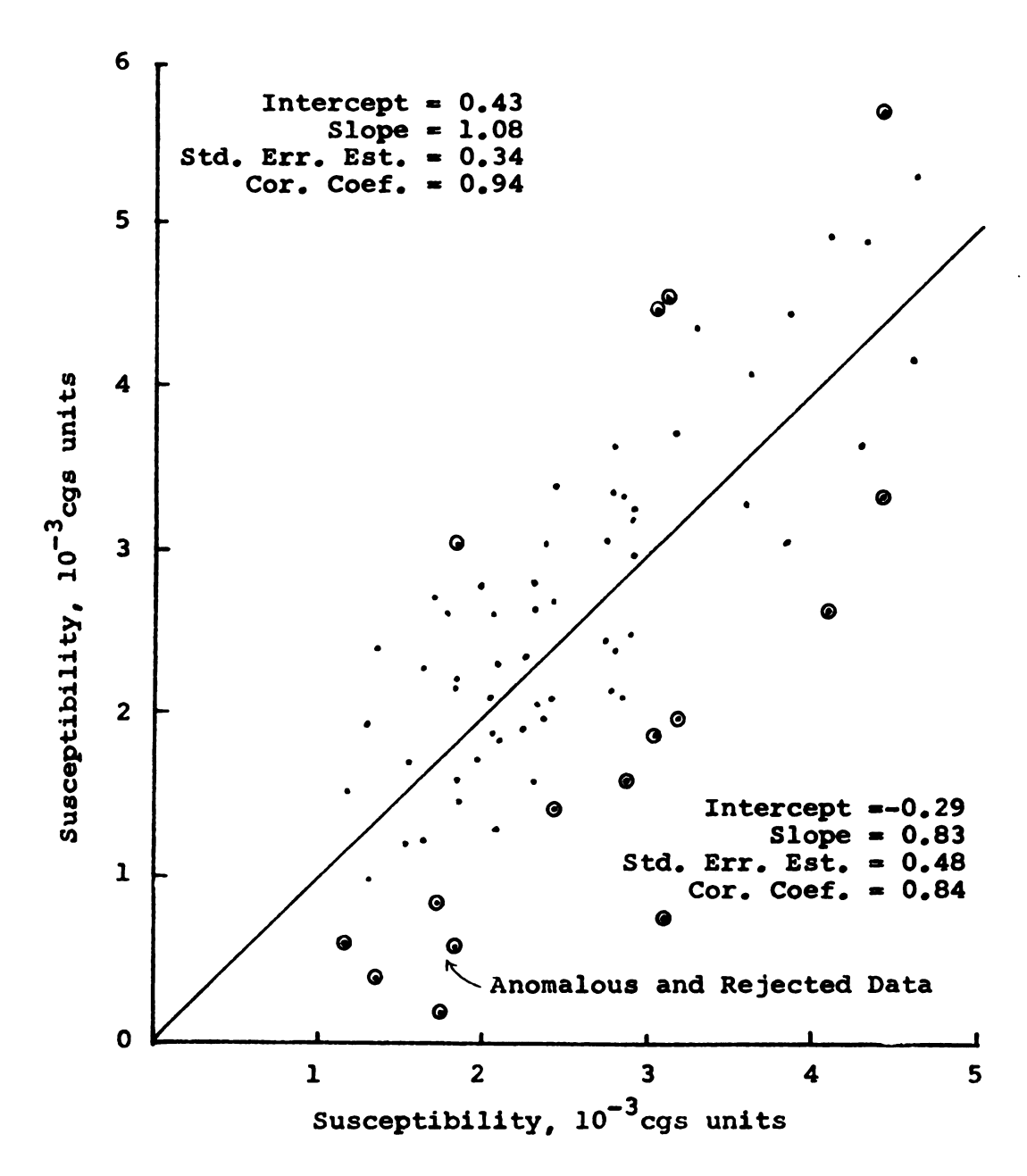


Figure 3-5. Site susceptibility extremes versus site means of core specimen measurements. Unity slope line separates maximum and minimum values. Included are the intercept, slope, standard error of the estimate, and correlation coefficient for each of the two data groups.

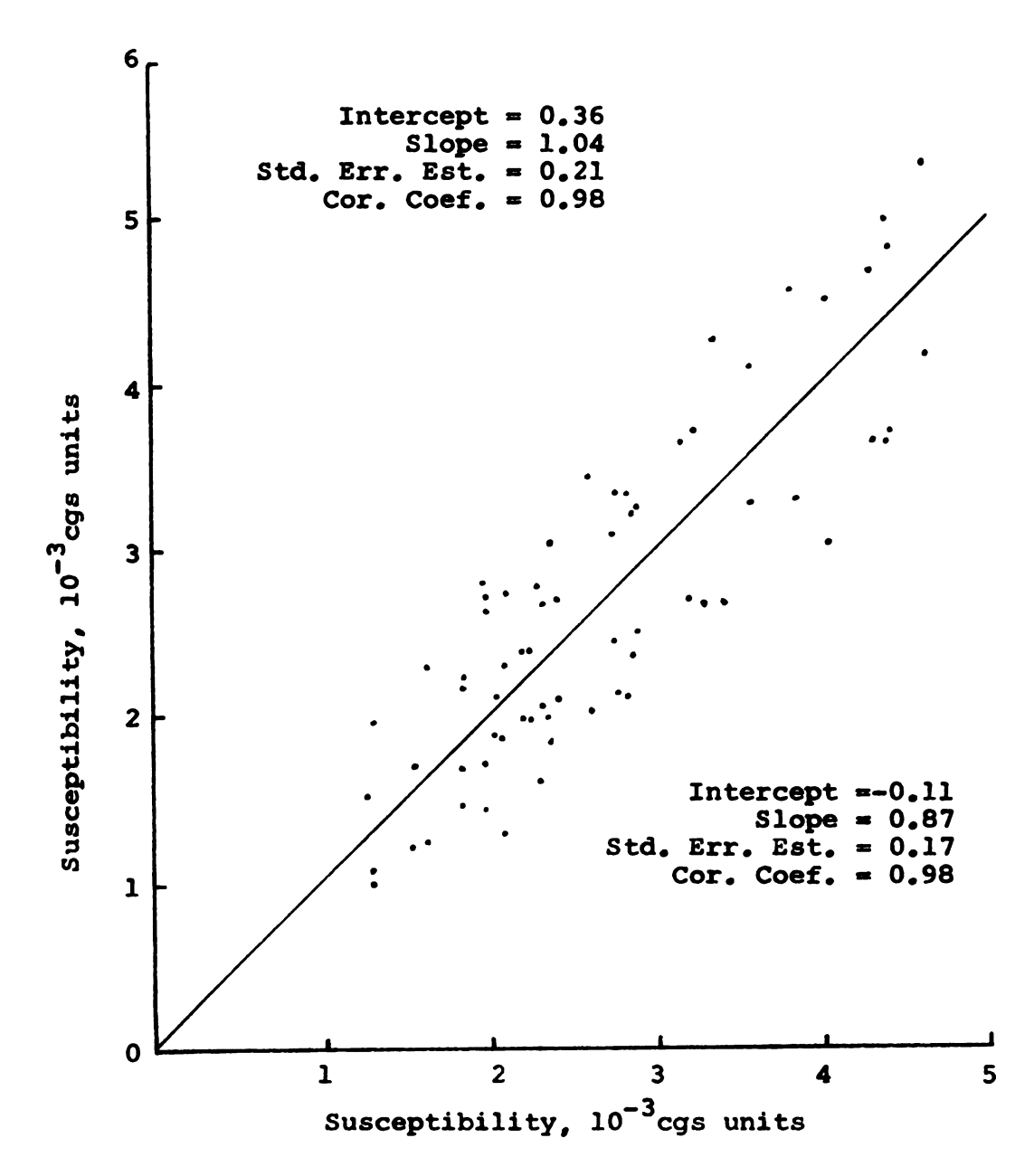


Figure 3-6. Site susceptibility extremes versus site means of core specimen measurements after rejection of anomalous data. Unity slope line separates maximum and minimum values. Included are the intercept, slope, standard error of the estimate, and correlation coefficient for each of the two data groups.

shows about 50 percent more dispersion than the large volume. This is based upon the separation of the linear regression lines of Figures 3-4 and 3-6 in the middle of the mean susceptibility range.

The analysis clearly demonstrates that the core data is subject to notably more dispersion than the in situ data, which necessitates a closer inspection of the data, preferably analytically. The results of the foregoing analysis indicate the "poor" data were almost always low values which are thought to be the effects of weathering. Weathering destroys the magnetite and consequently lowers the susceptibility of the rock.

The in situ data do not appear to need as careful scrutiny as the core data. If volumes greater than the 57 cubic inches were measured, the amount of dispersion and anomalous data would be expected to decrease. The chances of collecting anomalous susceptibility data are inversely proportional to the sample volume.

A test of the effectiveness of removing anomalous data comes from a comparison of the results of the two methods. The susceptibility values should display a normal distribution and the means of the two methods should be equal.

Figure 3-7 shows the resulting means of Figures 3-4 and 3-6 separated according to rock type. The range and overlap of the rock types for each method of measurement are nearly identical with less than 10 percent separating

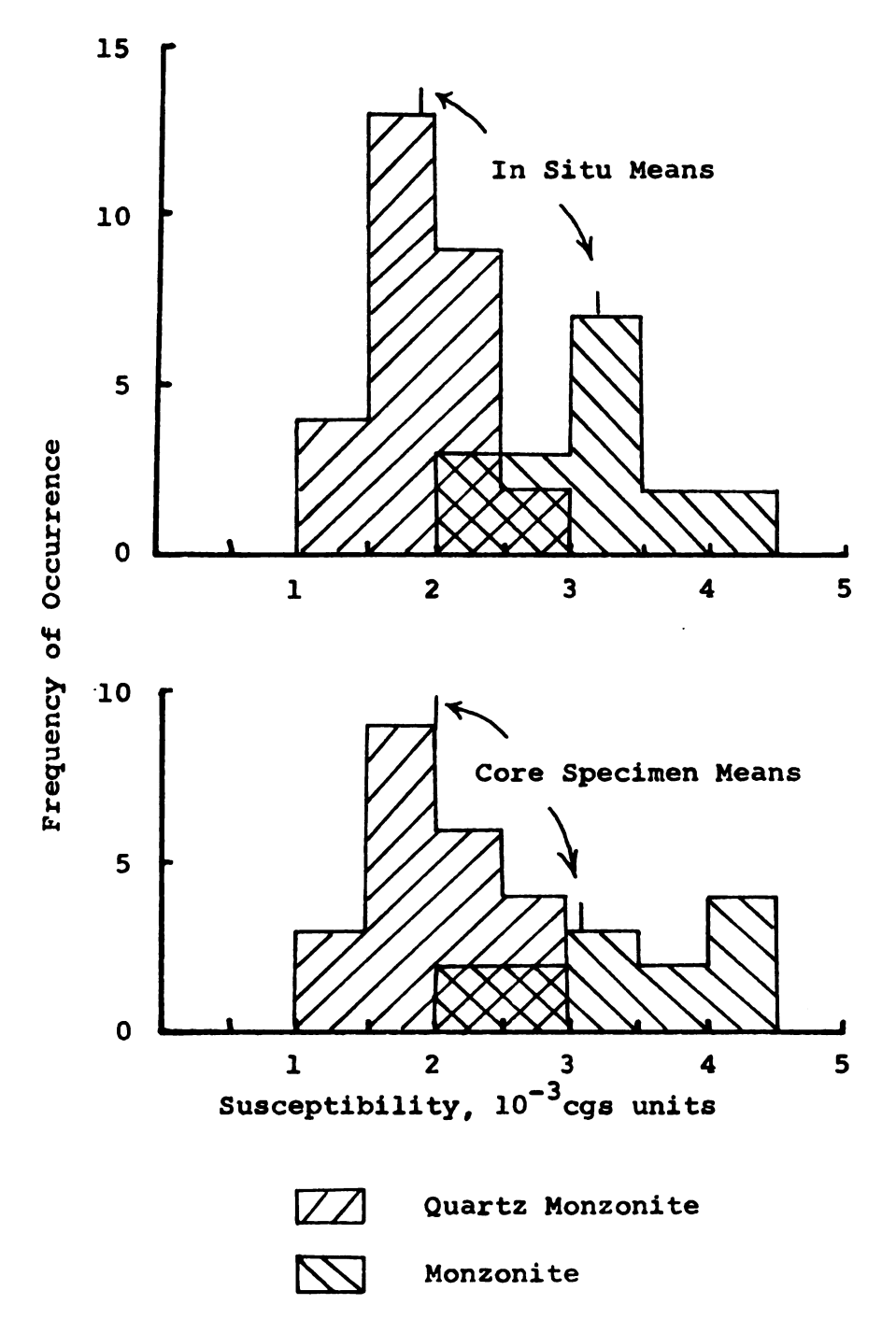


Figure 3-7. Magnetic susceptibility distributions of in situ and core specimen measurements by rock type.

the respective means. The in situ histograms (Figure 3-7) show an approximate, normal distribution with a distinct separation between rock types. The core samples show less distinction between rock types, although the mean values agree reasonably well with the in situ method. This lack of a strong separation may, in part, reflect the smaller sample population of the core measurements as opposed to the in situ measurements. The in situ means and standard deviations are $(1880 \pm 400) \times 10^{-6}$ and $(3130 \pm 640) \times 10^{-6}$ egs units for the quartz monzonite and monzonite respectively. The core specimen means and standard deviations are $(2030 \pm 460) \times 10^{-6}$ and $(3400 \pm 700) \times 10^{-6}$ egs units. A student t test shows the difference between the susceptibility means of the rock types to be highly significant for both methods of measurement.

There is concern as to the amount of weathering the outcrop surfaces have undergone. The field generated by the in situ coil does penetrate the outcrop surface more than the effective hemispherical radius of the coil (3 inches). If the field does couple with fresh rock, then the in situ means would be expected to be slightly higher than the core sample mean. This difference is not observed. Also, specimens from a given field core do not show a consistent increase of susceptibility with depth. These observations suggest that no weathering has occurred in the top few inches of the outcrop surface or that there is uniform weathering of the top several inches.

In situ measurements were made on a few boulders which had apparently broken by rolling downhill. The values obtained at a distance of about one foot from the surface of the boulders were approximately 30 percent greater than the surface in situ values of the boulder. This suggests that there may be a uniformly weathered zone, perhaps a foot deep on the outcrop surface. However, lack of detailed evidence on the boulder measurements precludes any definitive statement. Cores of several feet in length would provide the necessary information to resolve the problem.

The following conclusions can be stated from the foregoing discussion.

- 1) Larger sample volumes lead to appreciably less dispersion in the original data.
- 2) Larger sample volumes are less subject to anomalous data.
- 3) The delineation of magnetic rock units is noticably better with larger sample volumes than small volumes.
- 4) The approach of plotting site means and extremes provides a way of recognizing poor quality data.
- Two magnetically distinct units were delineated in the Melrose Stock. These are correlative to the lith-ologic units. The quartz monzonite has a mean magnetic susceptibility of 2000×10^{-6} cgs units, the monzonite, 3200×10^{-6} cgs units.

3.3 Sampling

A fundamental problem in determining the susceptibility of a rock unit is knowing the number of samples and sites that are necessary for a representative value of the unit (e.g., Case, 1966). Sufficient data are available from this study to suggest guidelines for sampling of intrusives similar to the Melrose Stock.

To aid in the evaluation of the sampling procedure, matrices were constructed with the number of sites sampled as rows and the number of measurements per site as columns. The in situ data of 29 quartz monzonite sites were used to generate one matrix and 17 monzonite sites were used for another. The entries in a sampling matrix are susceptibility means based upon the number of sites and samples per site. All of the means in a matrix will approach the grand mean, the average of all the sites and samples. Tables 3-1 and 3-2 are sampling matrices which, instead of giving the various means, give the percentage deviation of the various means from the grand mean. The grand mean is considered a representative value of the rock unit. In this manner, the number of samples and sites can be determined which bring a particular matrix entry or mean to within a certain percentage of the grand mean.

The entries of Tables 3-1 and 3-2 were derived in the following manner. Numbers for each quartz monzonite site were put into a box, shaken, and then drawn out randomly to obtain the necessary data for Table 3-1. This gave a

Magnetic susceptibility sampling matrix in percent deviation from the grand mean of the quartz monzonite pluton. Table 3-1.

Number of Sites
3 5 7 10 15 +9 +7 +2 +2 +4 +9 +9 +2 +2 +3
3 5 7 10 15 +9 +7 +2 +2 +4
3 5 7 10 15

Table 3-2. Magnetic susceptibility sampling matrix in percent deviation from the grand mean of monzonite pluton.

		Number of Sites							
		2	3	5	7	10	15	17	
Specimens	1	-10	- 5	+6	-3	+1	+1	+3	
	2	-10	- 6	+3	- 5	+2	0	+4	
	3	- 8	-4	+4	-4	+1	-1	+2	
	4	-8	- 6	+2	- 6	-1	-2	+1	
	5	- 6	- 5	+2	- 6	-2	- 3	0	
	6	-13	- 5	+3	- 5	-2	- 3	0	

random selection order of sites in the quartz monzonite and the sequence of data at each site were taken as recorded in the field notes. Originally the sites were selected to give a relatively uniform sample pattern over the intrusive.

To arrive at the upper left entry in the Table 3-1, the first in situ readings at the first two randomly chosen sites were averaged, subtracted from the grand mean, and then calculated in terms of percent from the grand mean. The algebraic sign indicates whether the array entry was greater or less than the grand mean. As a further example, the entry for 7 sites and 5 in situ readings per site is determined by taking the average of the first 5 readings from the first 7 randomly selected sites. This mean is 6 percent less than the grand mean (Table 3-2).

The results of the quartz monzonite measurements in Table 3-1 show a decrease in the deviation with increasing number of sites, but no trend is apparent from the number of samples per site. Similar results are shown for the monzonite (Table 3-2). These data indicate little advantage is gained by increasing the number of measurements taken at a site. Thus, greater variation exists among the sites than within the sites. In the quartz monzonite the deviation is reduced to less than 10 percent of the grand mean with 7 sites in the rock unit, but in the monzonite only 3 sites are necessary to bring the mean within 10 percent. Part of the difference in the indicated number of sites can be attributed to the size

difference of the two plutons. The monzonite has an exposure of approximately 3 square miles and with 3 sites necessary to bring the mean within 10 percent of the grand mean, at least one site for each square mile of surface exposure is needed. The quartz monzonite has an areal extent of nearly 9 square miles, so the necessity of 7 sites suggest a collection density of just slightly less than one site per square mile. The two values agree rather closely with each other.

The results suggest that the number of sites to be sampled in order to obtain representative magnetic susceptibility values is in proportion to the size of the pluton, roughly one site to each square mile. The stated site density would also permit the distinction of major magnetic units within an intrusive which might be overlooked with just a few sites within the intrusive. Obviously, the greater the number of sites, the greater the probability of approaching the representative susceptibility of the unit. This study indicates little advantage is gained by several measurements per site, although it should be remembered that in the preceding section several measurements per site permitted easier removal of anomalous data. There is little extra time required to take a few additional data at a site. More time is consumed establishing additional sites.

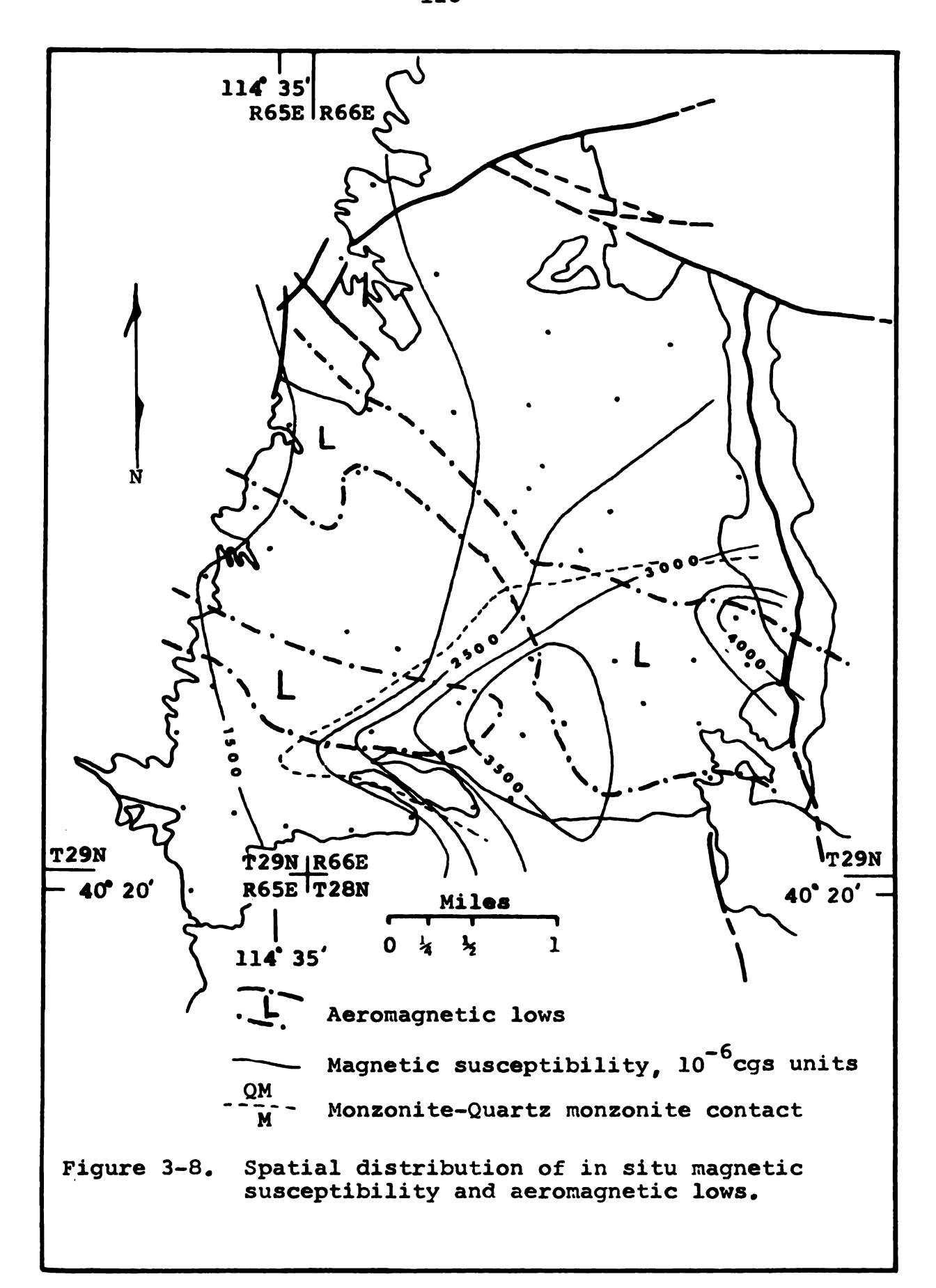
The quartz monzonite showed less dispersion than the monzonite (See 3.2.3) which suggests the need for a greater

sample density within the monzonite pluton. However, on a relative basis the dispersion (reflected by the standard deviation) of the two rock units is nearly identical. Hence, the guidelines as outlined above are consistent with the difference in dispersion.

3.4 Susceptibility and the Geometry of the Intrusive

The presentation of the magnetic susceptibility data with respect to the geometry of intrusives has been limited to profiles (May, 1967; Pothacamury, 1970). Sufficient data are available from this investigation to study the areal distribution of the magnetic susceptibility.

The magnetic susceptibility of the Melrose Stock is contoured in Figure 3-8 irrespective of rock type. The dashed lines delineate the areas of relative aeromagnetic highs and lows. The area of highest susceptibility, of course, falls over the monzonite pluton. Within the monzonite zone, no real distinction or trends exist. In the quartz monzonite there is a general increase of susceptibility to the east. The lack of apparent correlation or response of the contours to the known contacts suggest little relation between the two quantities. This observation is corroborated by Figure 3-9 which indicates no systematic trend in the susceptibility with respect to the contact distance for either rock type. Either there is no magnetic zoning related to the geometry of the intrusive or the observed contact is not a good representation



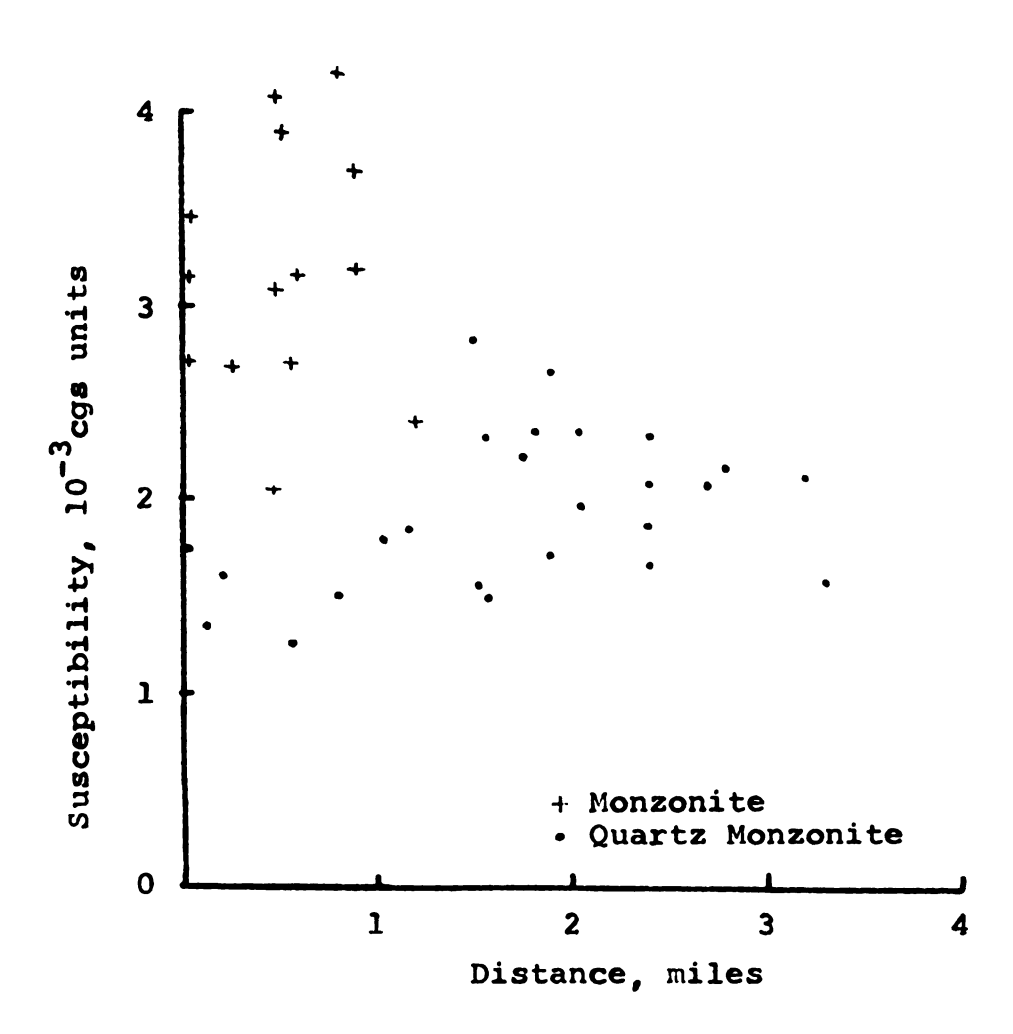


Figure 3-9. In situ magnetic susceptibility versus distance from the south contact of the Melrose Stock.

of the body's geometry. An interesting feature on the map is the transcurrent nature of the large magnetic lows to the susceptibility contours. The southern of the two magnetic lows may be due to topographic effects of a large ridge. The other magnetic low seems to be independent of topography and consequently, it must be attributed to magnetization variations within the intrusive. The surface susceptibility pattern bears no correspondence with the aeromagnetic pattern. This infers that the susceptibility of the subsurface is not the same as that on the surface. In the areas of aeromagnetic lows the susceptibility in the subsurface is less than what is expressed at the surface, assuming the effects of remanent magnetization to be uniform throughout the intrusive.

Figures 3-10 and 3-11 were constructed in order to determine the relationship of the susceptibility to vertical position in the intrusive. The monzonite (Figure 3-10) shows no apparent relation of susceptibility with elevation. On the other hand, the quartz monzonite (Figure 3-11) displays an increase in susceptibility with elevation at a rate of about 450 x 10⁻⁶ cgs units per 1,000 feet. This change can be attributed to either primary or secondary causes. The decrease in susceptibility at lower elevations could be due to alteration of the magnetite increasing downward and, hence, cause a general lowering of the susceptibility. The evidence for this suggestion is not strong for most sites at lower elevations do not

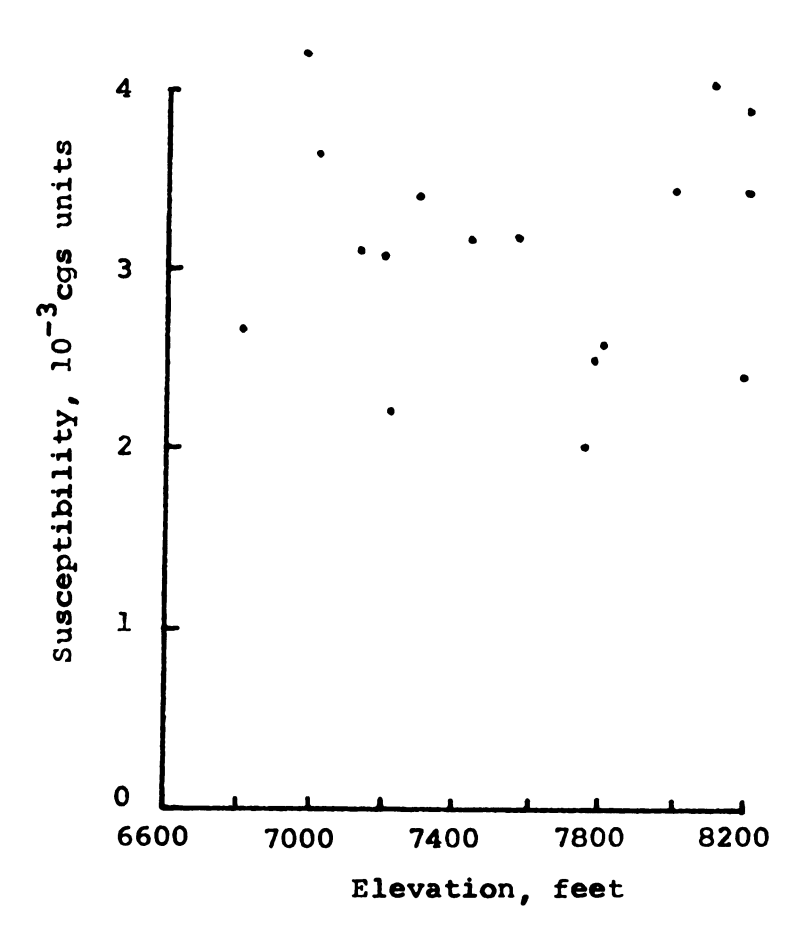


Figure 3-10. Variation of in situ magnetic susceptibility with elevation within the monzonite pluton.

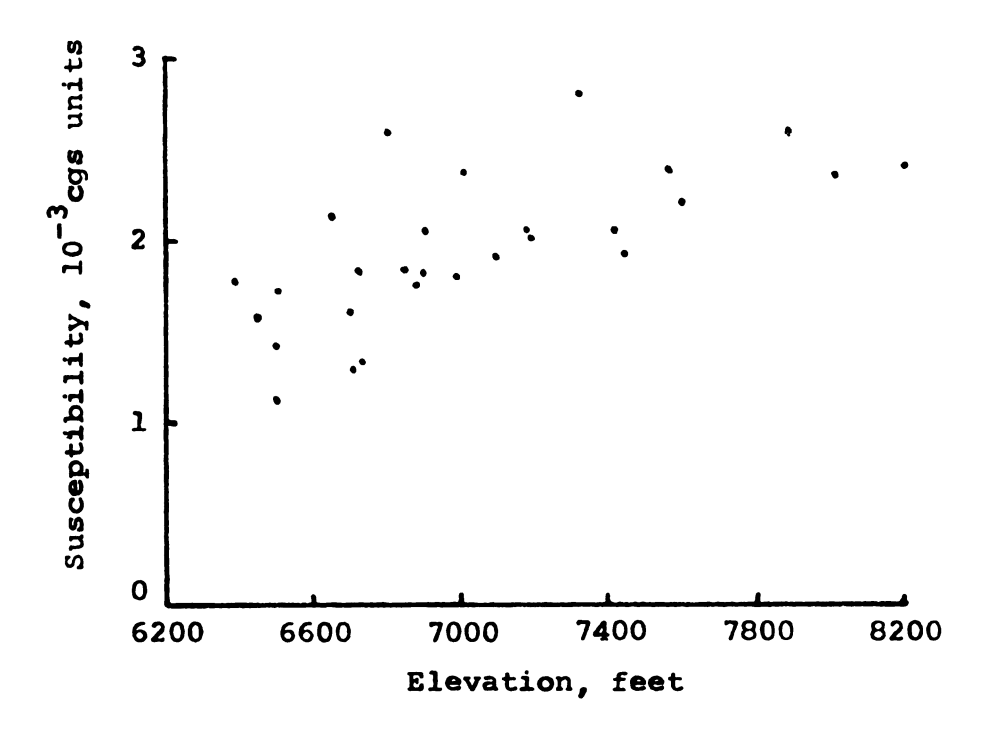


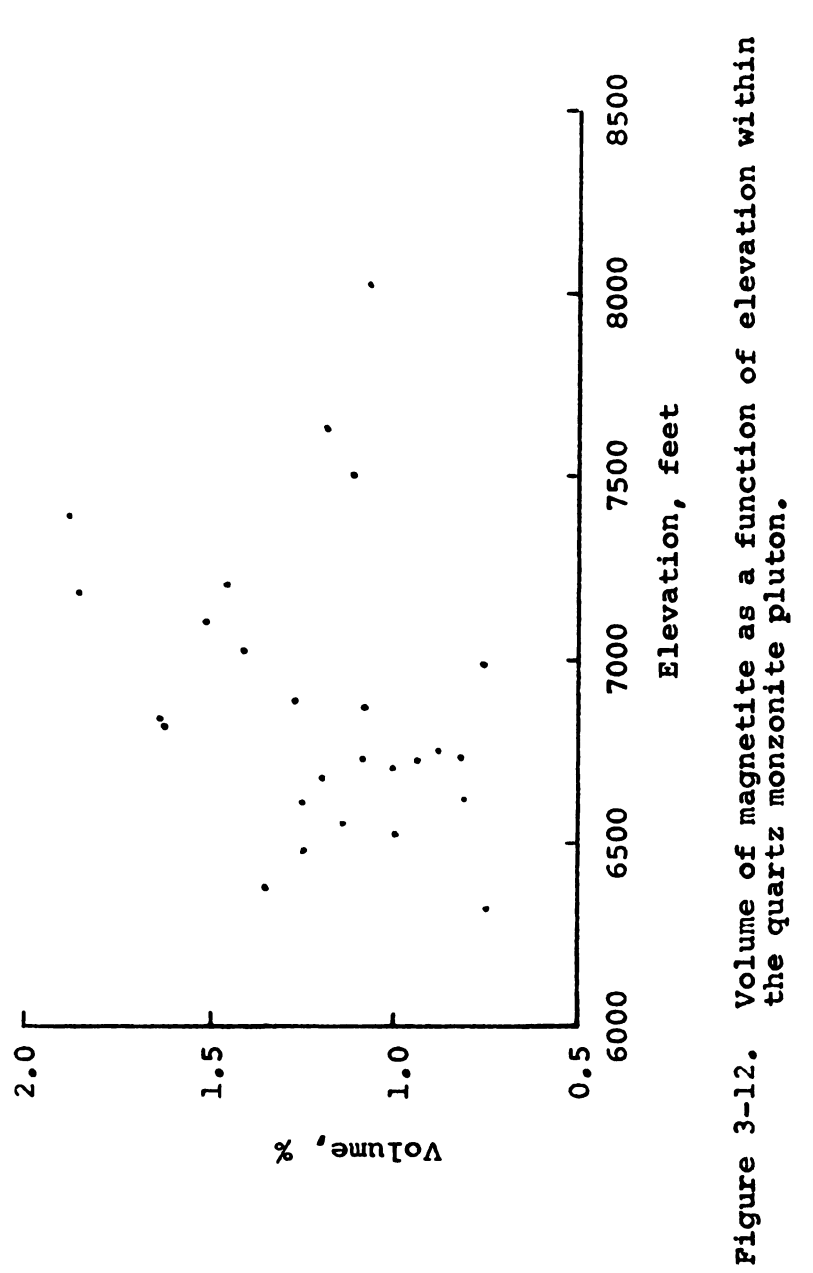
Figure 3-11. Variation of in situ magnetic susceptibility with elevation within the quartz monzonite pluton.

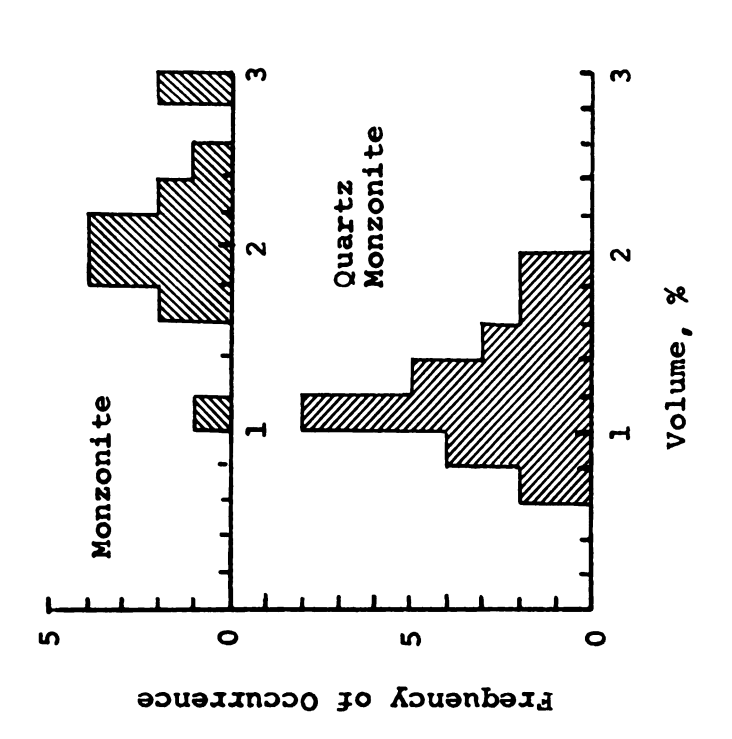
show significant amounts of hematite, an indication of alteration. A primary increase of magnetite upwards, is another possibility. The magnetite content does increase with elevation, but only in a very general way as shown in Figure 3-12. The change of susceptibility with elevation is too great to be attributable to a variation in grain size. It is likely that the susceptibility increase with elevation is not simply a function of one variable, but rather due to several factors.

3.5 Susceptibility and Magnetite Content

The magnetic susceptibility of the monzonite and quartz monzonite has been shown to average 3200 x 10⁻⁶ and 2000 x 10⁻⁶ cgs units respectively. Therefore, as expected the magnetite content which was determined during the modal analysis study also shows a difference between the monzonite and quartz monzonite. A normal shaped distribution is shown in Figure 3-13 for the frequency of occurrence of the opaque content in the two rock types. Averages for the monzonite and quartz monzonite are respectively 2.1 and 1.2 percent and a correction for the 10 percent of the opaques which is ilmenite reduces these values to 1.9 and 1.1 percent for the magnetite content.

A plot of the average in situ susceptibility as a function of opaque content is shown in Figure 3-14. The opaque content data are in most cases limited to a value from one thin section whereas the susceptibility is the





Distribution of magnetite content by site with respect to rock type. Figure 3-13.

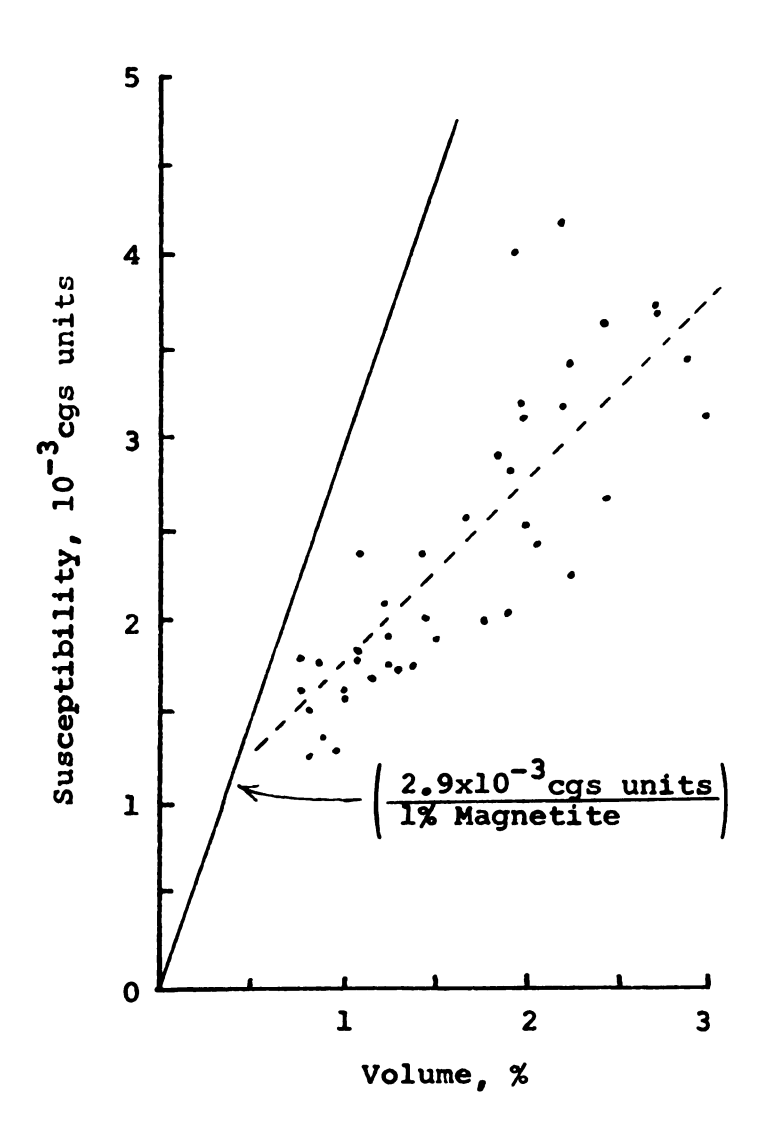


Figure 3-14. Magnetic susceptibility versus magnetite content. The expected susceptibility- magnetite relationship (Mooney and Bleifuss, 1953) is indicated by the solid line. The best fit line through the data is indicated by the dashed line.

site mean based on several readings. Greater scatter is shown on a graph of the specimen susceptibility and opaque content of a given field core than is displayed in Figure 3-14. The use of means tends to eliminate scatter in the data by means averaging out the scatter shown in individual data. A direct relationship of the two is readily apparent. However, a least squares line through the points does not intersect the origin.

A number of linear approximations of susceptibility versus magnetite content have been derived for small modal volumes of magnetite (<3 percent), (e.g., Schlicter, 1929; Mooney and Bleifuss, 1953). The best fit line of Mooney and Bleifuss (1953) is shown in Figure 3-13.

The fact that the observed data does not correlate well with the expected is considered to be significant.

A number of plausible explanations do exist, however, many of them can be dismissed in regards to this study. Errors in measurements, systematic or random, do not explain the gentler slope of the observed regression line in contrast to the expected and the non-zero intercept. The ilmenite content and magnetite composition are not pertinent in explaining the observed results. A minor contribution to the non-zero intercept can be due to the differential grain size distribution of the two rock types. The smaller grain size distribution in the monzonite than in the quartz monzonite will give the monzonite a slightly smaller susceptibility per unit volume of magnetite.

The effects of weathering resulting in the formation of the hydrous iron oxides are thought to be an important factor in modifying the magnetic mineral suite which is expressed in the susceptibility. The effects of a uniform weathering to all sites will decrease the slope of the best fit line, but it should pass through the origin. If there is a nonuniform weathering in the specimens as a function of magnetite content then samples of high magnetite content are weathered to a greater amount. Since the monzonite has a greater magnetite content than the quartz monzonite this suggests that the monzonite has undergone more surface alteration or perhaps hydrothermal alteration than the quartz monzonite. If the general weathering character of the bulk rock can be used as a guide to magnetite weathering, then the monzonite should have a greater amount of magnetite altered to goethite. The monzonite would be expected to be more sensitive to surface alteration than the quartz monzonite because it is a more mafic rock. This would allow the magnetite in the monzonite to be exposed to surface fluids. A minor contribution to the weathering might be made by the slightly smaller grain size of the monzonite which increases the surface area of the magnetite susceptibile to chemical reactions.

Weathering appears to be the best explaination for the expected and observed results of Figure 3-14. If this is true, the susceptibility has been appreciably reduced by surface weathering by perhaps as much as 50 percent. As noted previously, a few measurements on broken boulders lend support to substantial surface alteration.

CHAPTER IV

REMANENT MAGNETIZATION

4.1 Introduction

Remanent magnetism was measured on 4 to 15 specimens per site at 34 sites and 6 additional sites of unoriented specimens. One-half of the 34 oriented core sites were collected in the summer of 1968 and the remaining 17 in the summer of 1970. There is no bias in rock type with time of collection. The measurements on the earlier collected samples were carried out at least 18 months after they had been collected, whereas the 1970 samples were measured within the month following collection. The delay in measurement of the 1968 specimens was caused by instrumentation problems.

The data from the remanent measurements were reduced on a CDC 3600 computer with a program provided by the U.S. Geological Survey. Programs were written to statistically analyze the data (Fisher, 1953) according to formulae given by Irving (1964) and to plot the remanent directions on generated equal area projections.

The standard deviation is normally used as a measure of the spread of data, however, in spherical distributions

a circle of confidence is used which gives the radius of the cone in which the true mean is expected to lie. In this study the confidence level of the circles are at 95 percent, the value most commonly used for paleomagnetic results.

Another statistical measure of the spread or dispersion in the data is the precision parameter, K. For a random distribution the parameter 0.0 and for a tight cluster of data about a given direction the parameter becomes large (e.g., > 100).

4.2 NRM Results

4.2.1 NRM Data Evaluation

The results of the NRM measurements including number of specimens, mean site direction and intensity, and circles of confidence are found in Appendix C. The circles of confidence of the 34 sites span a large range, 11.9° to 127.5°. In most published results the values are typically from a few degrees to approximately 15°.

Since changes in magnetization could be detected during measurement, it is suspected that the specimens have a component of secondary magnetization which is soft. A compilation of the site circles of confidence according to when the specimens were collected is displayed in Figure 4-1. Circles of confidence from the 1968 sites range to over 120° as contrasted to the 1970 sites which have circles less than 80°. Just three 1968 sites have circles of

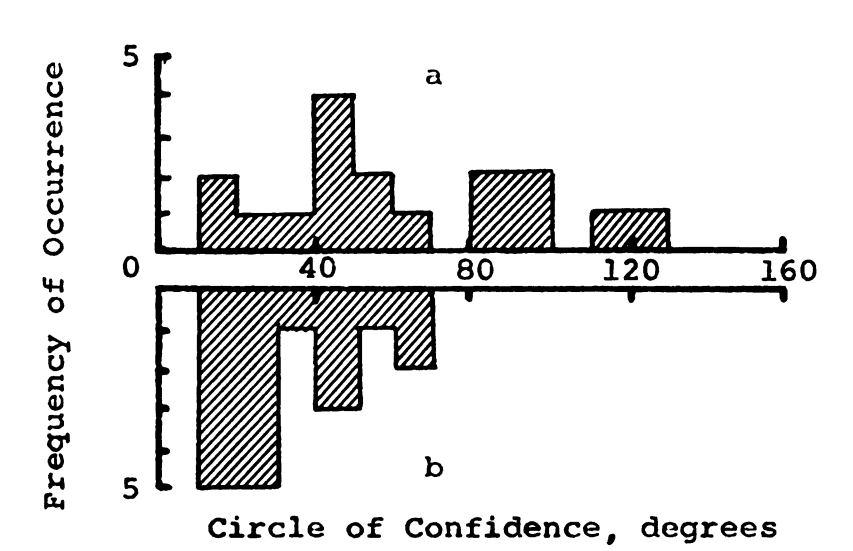
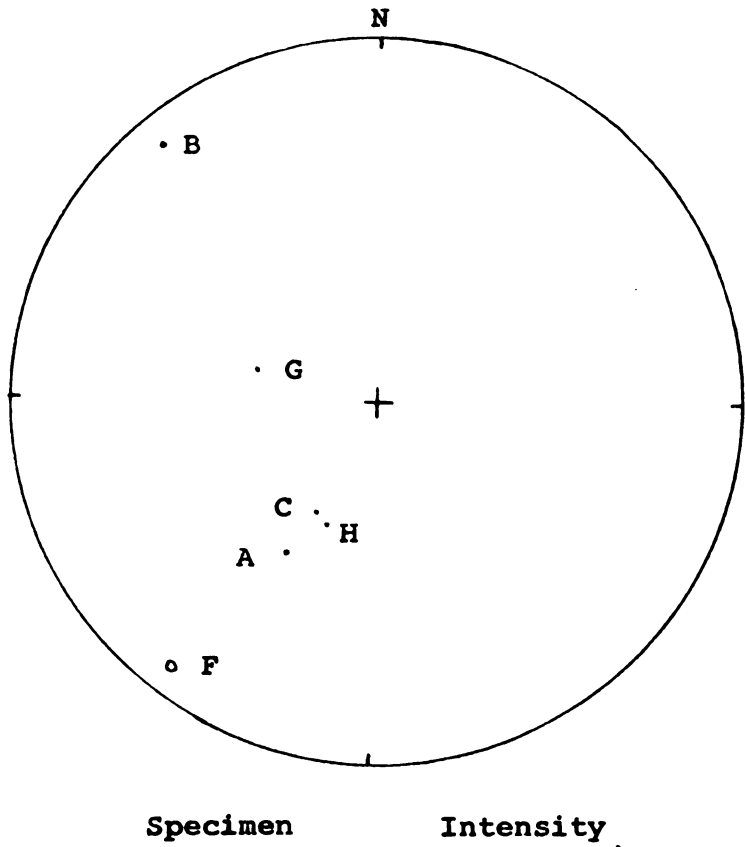


Figure 4-1. NRM site circles of confidence according to time of collection.
a) 1968 specimens, 18 months of storage; b) 1970 specimens, 1 month of storage.

confidence under 30°. This comparison strongly suggests that the 1968 specimens have acquired significant secondary components while in storage.

The intensity and direction of magnetization in coarse grained igneous rock is rather sensitive to magnetic modifications from the time of formation to measurement. Therefore, anomalous NRM data are anticipated and must be eliminated. Anomalous data are illustrated from two typical sites in Figures 4-2a and b. Anomalous results have a remanent intensity several times greater than the grouping of the other specimens of the sites and in many cases their direction will also be scattered from the others. In Site 10, specimen B and in Site 21, specimens F-1, F-2, and F-3 were eliminated from further analysis. All site stereograms and intensities were inspected in a similar manner. Revised Fisher statistics were calculated after rejection of anomalous data.

A histogram, Figure 4-3, shows a comparison of the circles of confidence of the sites before and after removal of the anomalous data. Not surprisingly, there is a noticable shift of the circles of confidence to lower values. However, there are still a large number of sites with results that could not be expected to yield reliable remanent directions. Suitable remanent directions might be obtained upon demagnetization of sites having circles of confidence less than 30°. Only three of the sixteen sites having circles of confidence of confidence of less than 30° are from 1968.



Specimen	Inte	nsity	
VN-10A	1.09	x10-	4 emu/cc
VN-10B	26.60	11	•
VN-10C	5.13	33	
VN-10F	1.74	***	
VN-10G	5.50	11	
VN-10H	0.90	11	

Figure 4-2a. NRM of Site 10, directions and intensities. Equal area projection.

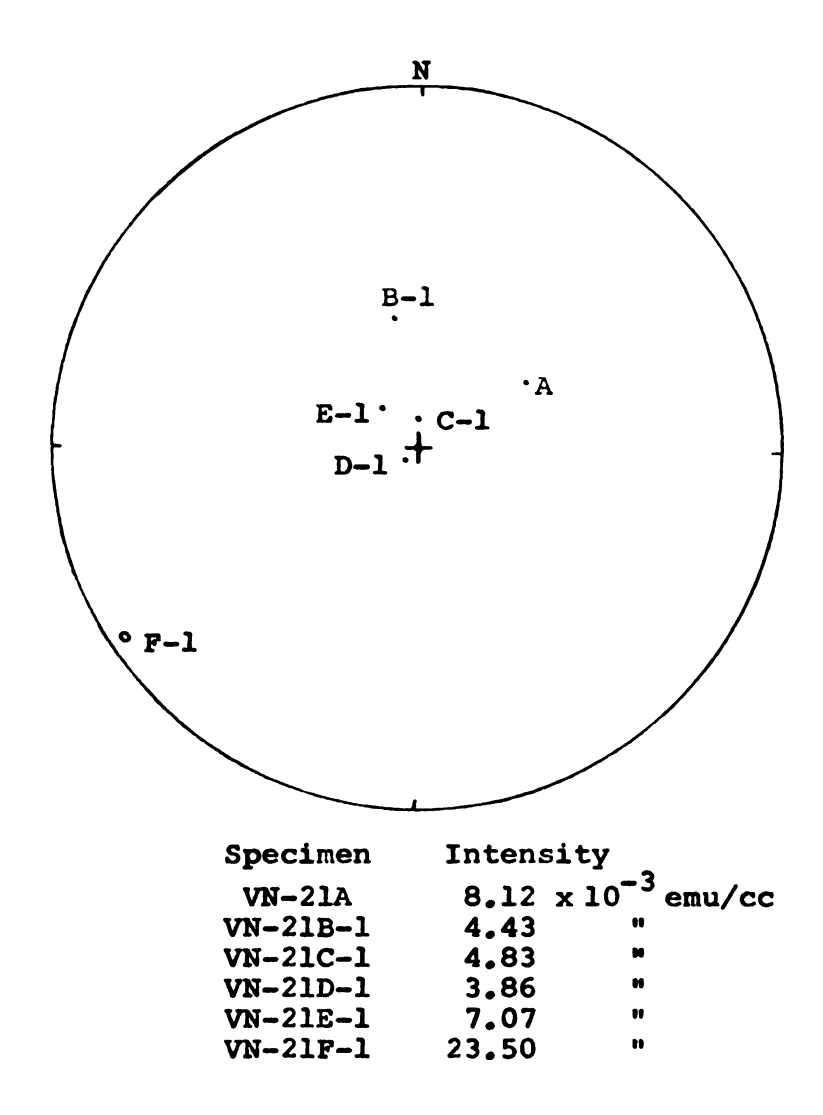
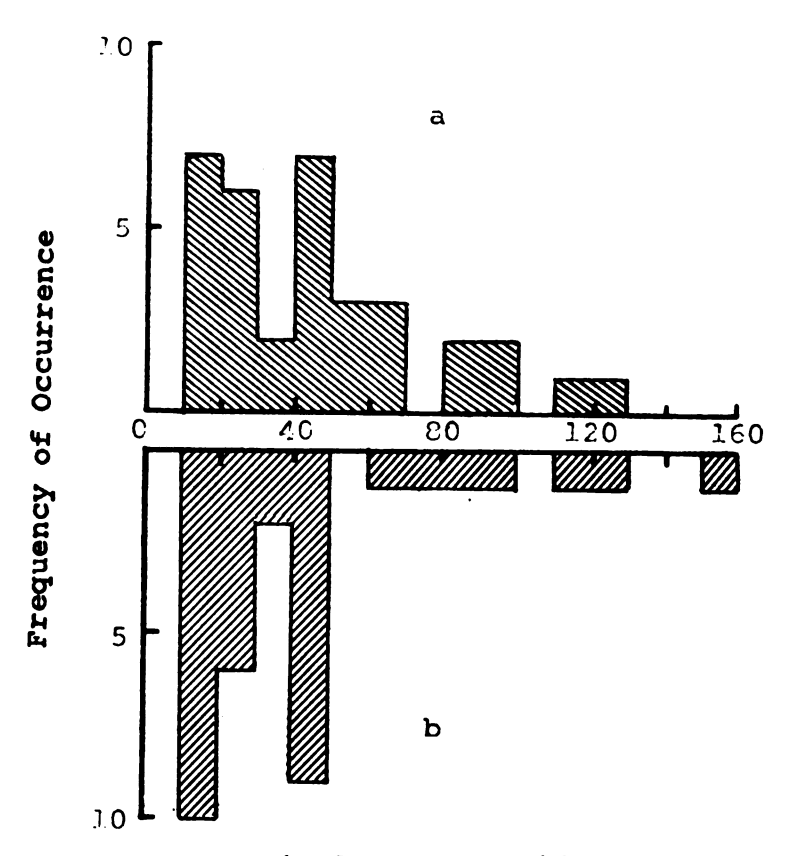


Figure 4-2b. NRM of Site 21, directions and intensities. Equal area projection.



Circles of Confidence, degrees

Figure 4-3. NRM site circles of confidence before (a) and after (b) rejection of anomalous data.

Chi-square test shows there is a less than one percent probability of this being due to chance. This observation supports the view of dispersion being a direct function of storage time. A check of the number of monzonite and quartz-monzonite sites in the group of 16 sites shows no preference of dispersion to rock type.

made on the samples of Sites 32 which were drilled from a rock pile adjacent to an old prospect pit. The seven specimens from this site were each given the same arbitrary orientation which resulted in a site circle of confidence of 46, a value less than many sites given their correct field orientation. This prompted consideration of the other sites using the laboratory orientation in calculating their mean directions and dispersion.

All of the specimens from Sites 1-17 (1968) were grouped together and their mean direction and dispersion calculated suing both their field and laboratory orientations. The laboratory orientation is the same for each specimen while the field orientation varies from sample to sample. The results are shown in Table 4-1.

The directions resulting from the two sets of orientation seemingly differ greatly in declination, but in reality only 18 of great circle distance separate the two directions. If there was little modification during storage then the laboratory orientation should have given wide dispersion because it represents a reduction of each

Comparison of NRM data of Sites 1-17 with reduction to field and laboratory orientations. Table 4-1.

Orientation	Dec.	Inc.	Cir. Con.	Pre. Par.
Field	17	80	13	2.2
Laboratory	191	82	12	2.6

specimen to an orientation different from that of the collection. The circles of confidence and precision parameter are very much the same, indicating with little doubt that storage in the laboratory has significantly modified the remanent magnetism of the 1968 samples in particular.

4.2.2 NRM Directions

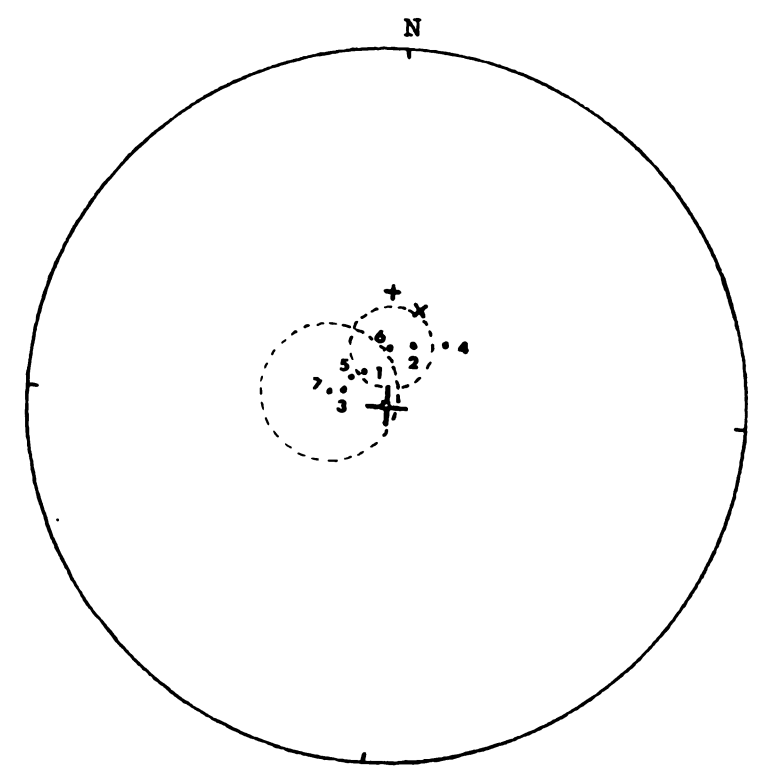
The mean NRM directions and corresponding dispersion statistics of specimens from 29 sites are compiled in Table 4-2. Five sites with high scatter of remanent directions and intensities were eliminated from the study due to the poor quality of the data. The data were grouped according to collection date and lithology and analyzed in various ways. The only appreciable difference in the 1968 and 1970 samples is in declination. The declination is shifted towards the north for the sites sampled in 1970. In all comparisons the monzonite shows less dispersion than the quartz monzonite.

The location of 7 of the directions given in Table
4-2 are graphically presented in Figure 4-4. Point 1
in the figure is the mean direction of all 29 sites and
it is midway between the monzonite and quartz monzonite
directions, points 2 and 3, respectively. Although not
plotted, the circles of confidence of these two groups
overlap with only one degree of closure and represent nearly significantly different directions. An interesting

NRM results of 29 sites grouped in various combinations. Table 4-2.

*	Sites	Number	Dec.	•ouI	Cir. Con.	Pre. Par.
1	All	29	325.3	80.8	8.2	11.6
	1968	12	358.9	6*61	12.7	12.6
	1970	17	303.0	79.4	11,3	10.9
2	Monz.	10	19.5	74.9	7.5	42.6
м	Q. Monz.	19	288.6	78.4	11.4	7.6
4	'68 Monz.	Ŋ	33,8	71.3	11.8	42.7
2	'68 Q. Monz	7	305.1	80.0	19.9	10.1
9	'70 Monz.	ß	358,9	17.1	10.5	54.3
7	'70 Q. Monz	12	281.1	77.0	15.5	8*8

* Designation used in Figure 4-4.



- × Present field
- + Axial dipole field

Figure 4-4. NRM directions of 29 sites grouped in various combinations. Circles of confidence shown for the 1970 monzonite sites and the 1970 quartz monzonite sites.

Equal area projection.

feature of the sterogram is the positions of the monzonite (points 4 and 6) and quartz monzonite (points 5 and 7)
site means of 1968 and 1970. In both cases the points of
1968 are in approximately the same relative direction away
from the 1970 points and with about the same angular distance (6° for quartz monzonite, 10° for monzonite).

The coincidence of the relative difference in direction of the two 1968 means from the 1970 means suggests that length of storage or magnetic field of the storage facility influenced the shift. In view of this, the best direction for the NRM should be shown by the 1970 samples. Drawn about the mean directions of the two rock types collected in 1970 are the respective circles of confidence. The circles show that there could be a difference in the mean directions, though it is not a significant difference at the 95 percent confidence limit.

If the two plutons have the same mean direction, then the monzonite pluton has had its NRM changed through geologic time in the direction of the earth's field. The results illustrated in Figure 4-4 suggest that the monzonite unit has a larger and more unstable VRM component. Demagnetization and a storage test may provide further information on whether the NRM directions are the same as the TRM direction, the directions assumed to be representative of the paleomagnetic direction. If the two directions are different upon demagnetization, then there may be support to the idea that the two directions are different

paleo-pole positions.

4.3 Alternating Field Demagnetization

4.3.1 Preliminary Demagnetization

Twenty-nine of the 34 sites with oriented specimens were chosen for demagnetization. Samples from all sites established in 1970 were demagnetized. The measurements from sites sampled in 1968 with the largest circles of confidence were all eliminated except one, the highest. This extreme was included as a check of the dispersion reduction upon demagnetization. One specimen from each core was selected for the demagnetization study.

Af demagnetization was used to isolate the TRM acquired at the time of the intrusive's consolidation. Characteristically, coarse grained igneous rocks contain components of VRM and other stray components. The level at which the demagnetization removes unwanted components varies, but in general the best level of demagnetizing for coarse grained intrusive rocks falls below an alternating field of 300 oersted peak strength (As and Zijderveld, 1958).

Initially a group of nine sites from the 29 sites were randomly chosen for demagnetization at five levels, 50, 100, 150, 200 and 300 oersteds. The technique employed by Gromme and others (1967) for determining the level of demagnetization which gives minimum dispersion stabilization of the remanent magnetization was followed in this study.

The major criterion for choosing the optimum level of demagnetization is the circle of confidence which should be a minimum. At minimum dispersion the direction of magnetization should be stablized. Inclination, declination, intensity and circle of confidence are shown as functions of the level of magnetic cleaning in Figures 4-5a to i.

Seven of the nine sites yield a minimum dispersion at 50 oersteds while the remaining two sites show least dispersion for the NRM. It could be argued that Sites 4, 10, 19 and 25 have the best level of demagnetization at 100 oersteds, in view of the leveling of the intensity and only minor increase in the circles of confidence between 50 and 100 oersteds demagnetization.

In comparison to the results of Gromme and others (1967), the data presented here is much more variable and of poorer quality. There is greater change in the inclination and declination values with demagnetization. The amount of reduction in the remanent intensity by demagnetizing fields as low as 100 oersteds is rarely exceeded by other published results. These soft and relatively large moments of magnetization are characteristic of secondary VRM.

Figures 4-6 and 4-7 are equal area projections showing the paths of the mean site directions with increasing demagnetization intensity for specimens collected in 1968 and 1970 respectively. It is apparent that the

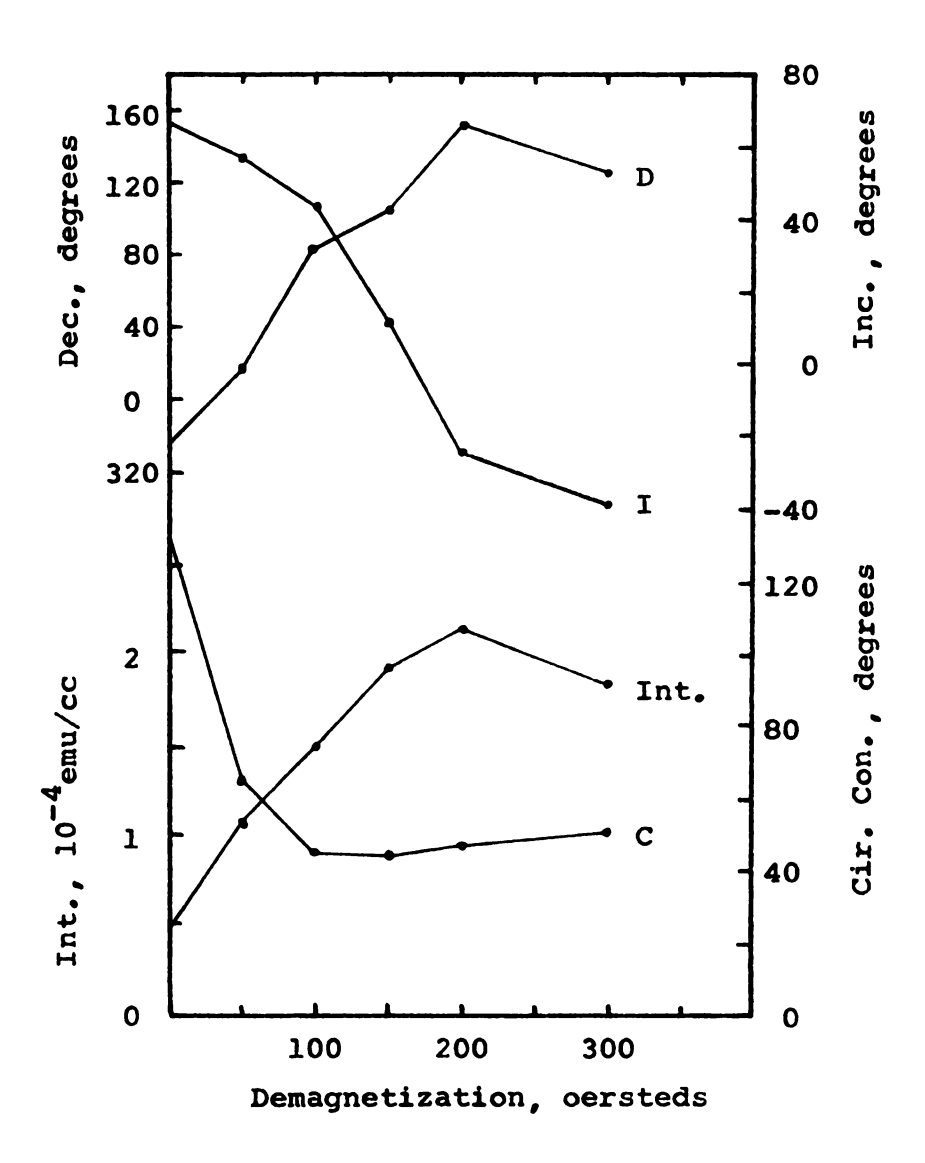


Figure 4-5a. A.f. demagnetization results of Site VN-4.

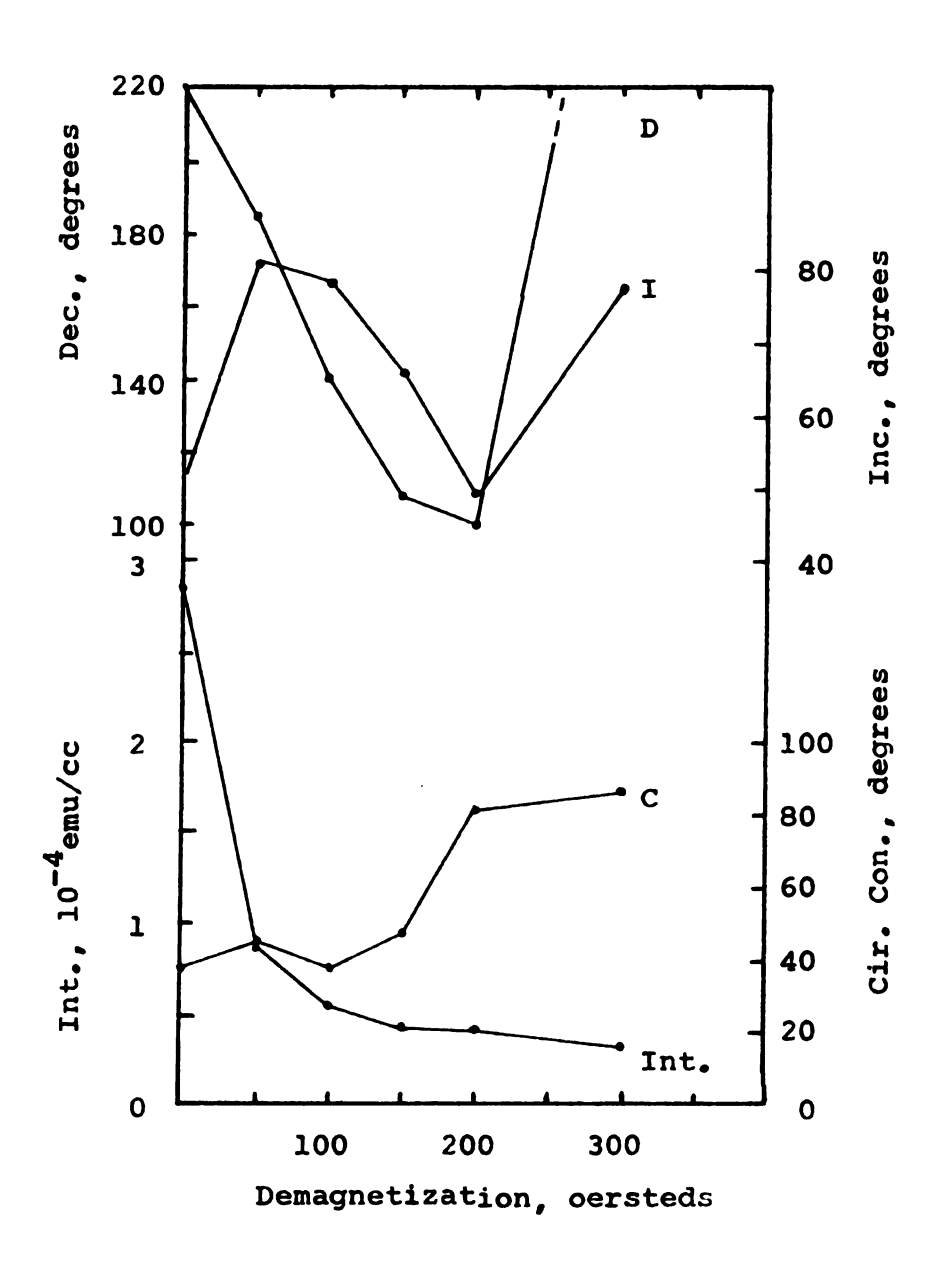


Figure 4-5b. A.f. demagnetization results of Site VN-10.

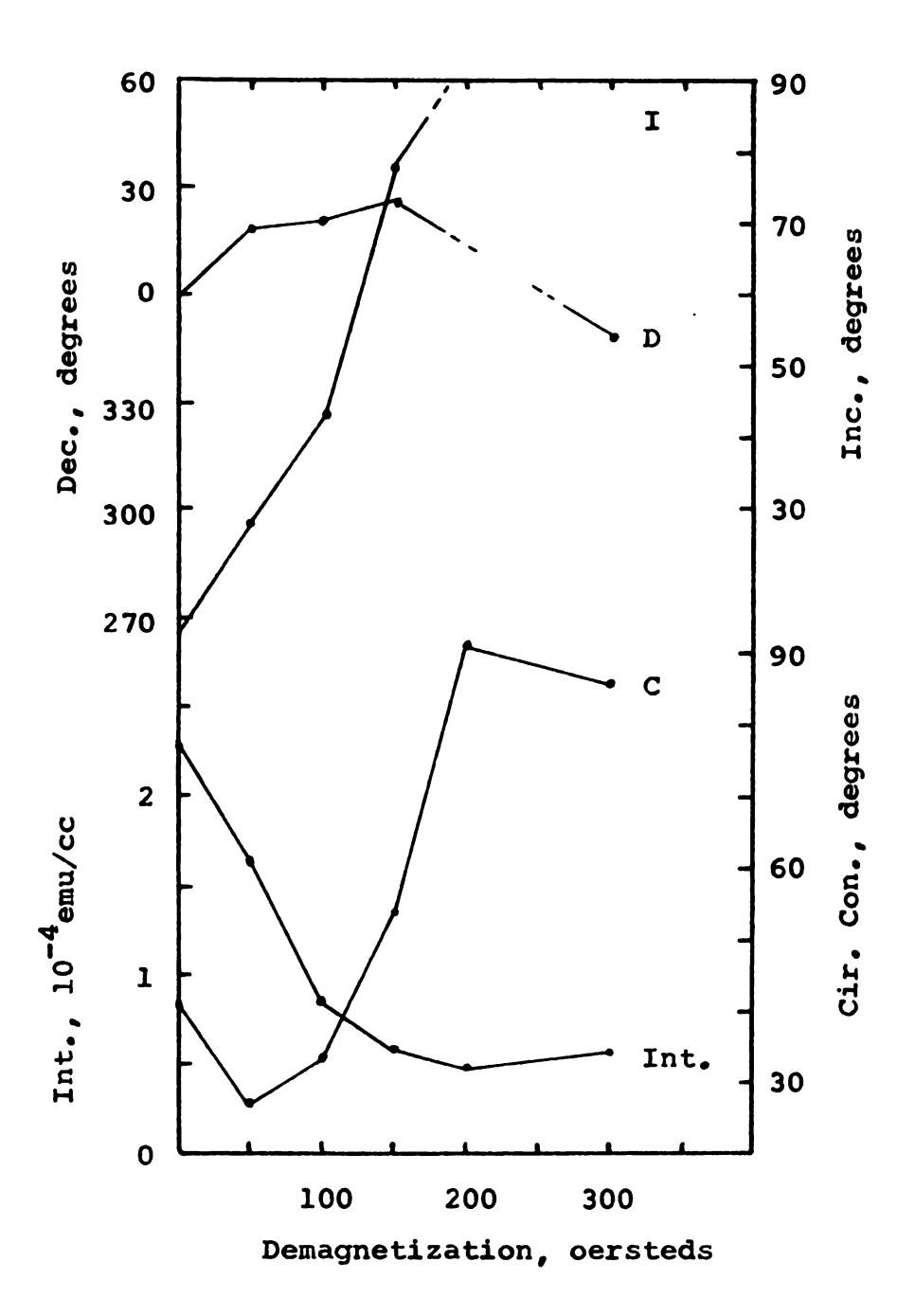


Figure 4-5c. A.f. demagnetization results of Site VN-13.

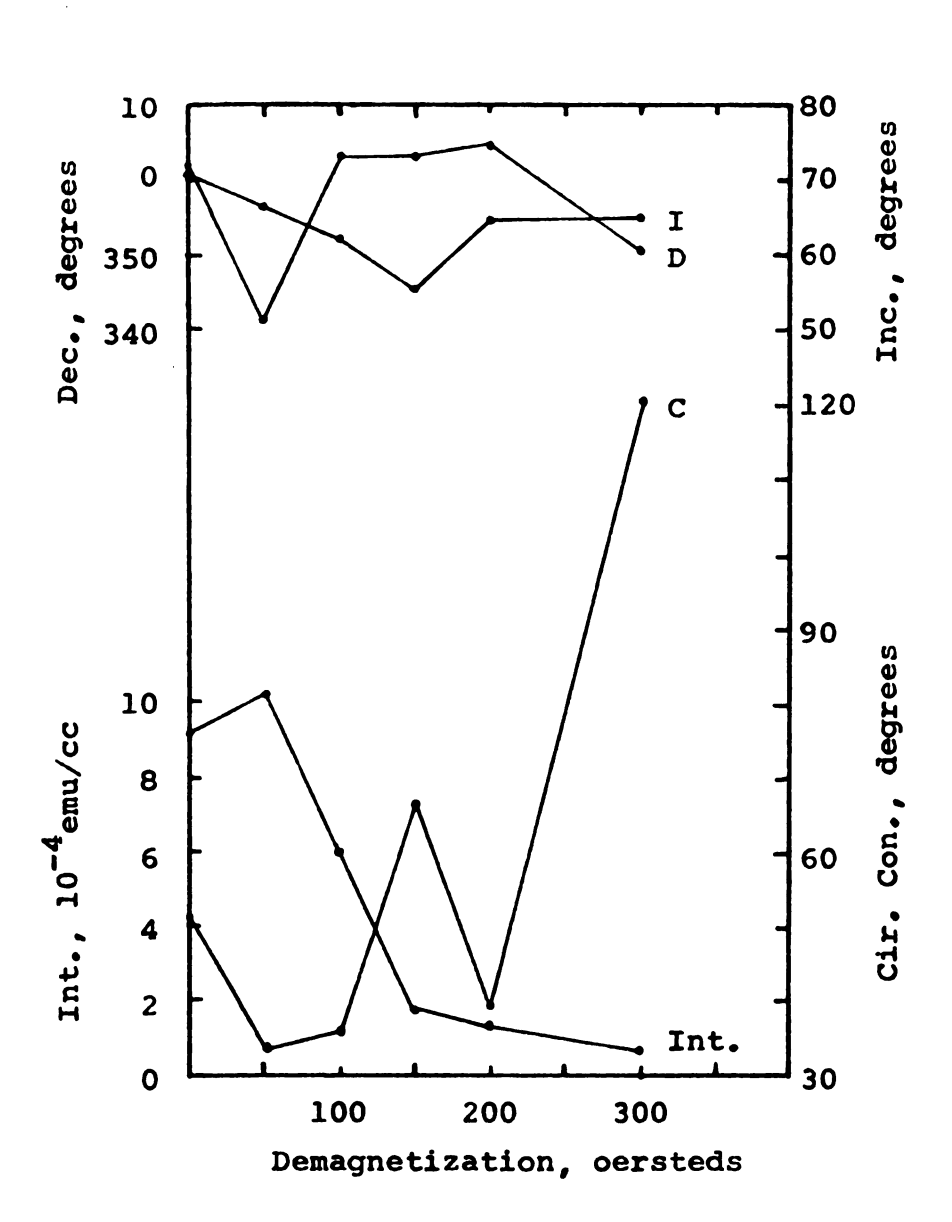


Figure 4-5d. A.f. demagnetization results of Site VN-19.

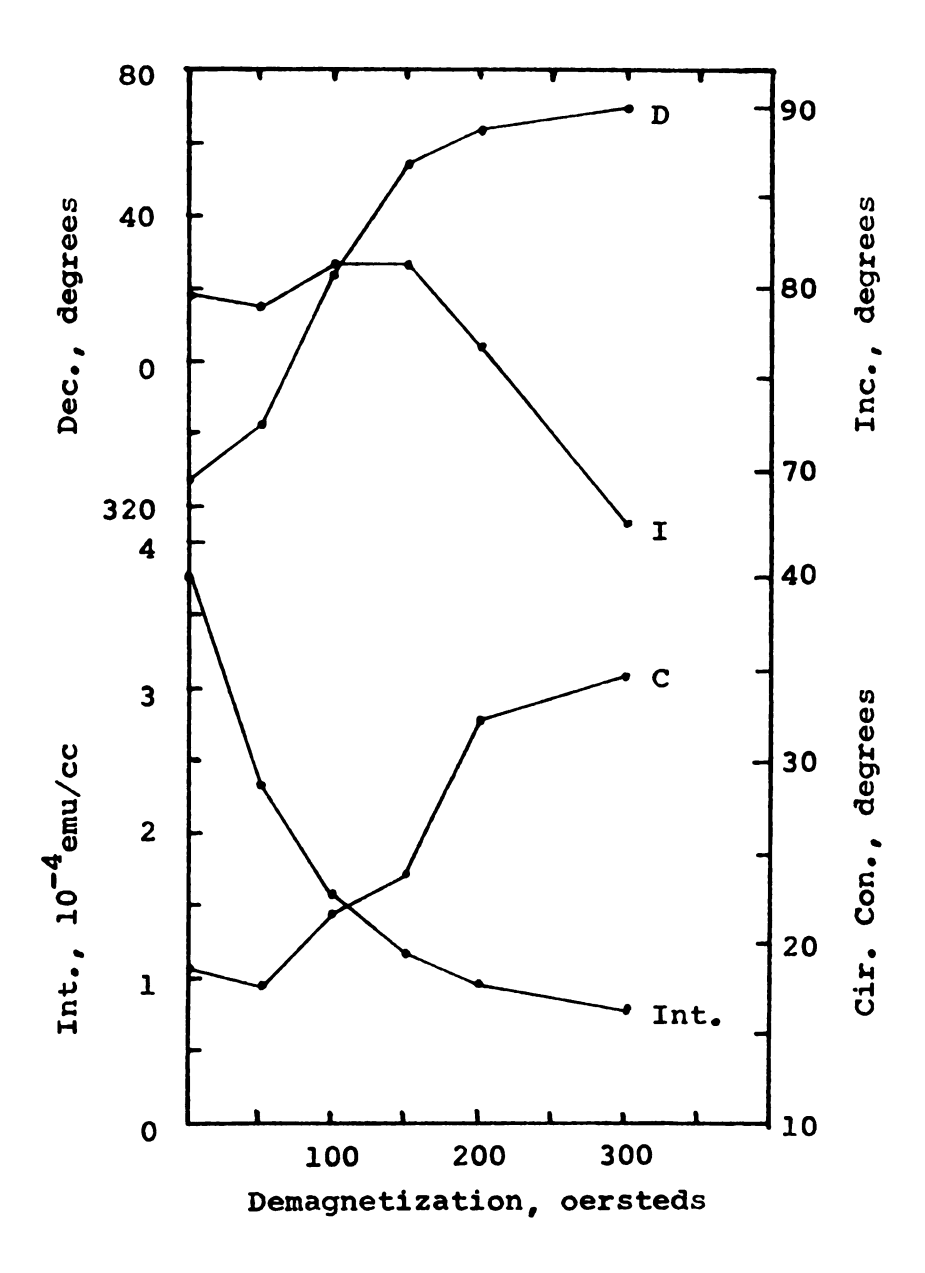


Figure 4-5e. A.f. demagnetization results of Site VN-20.

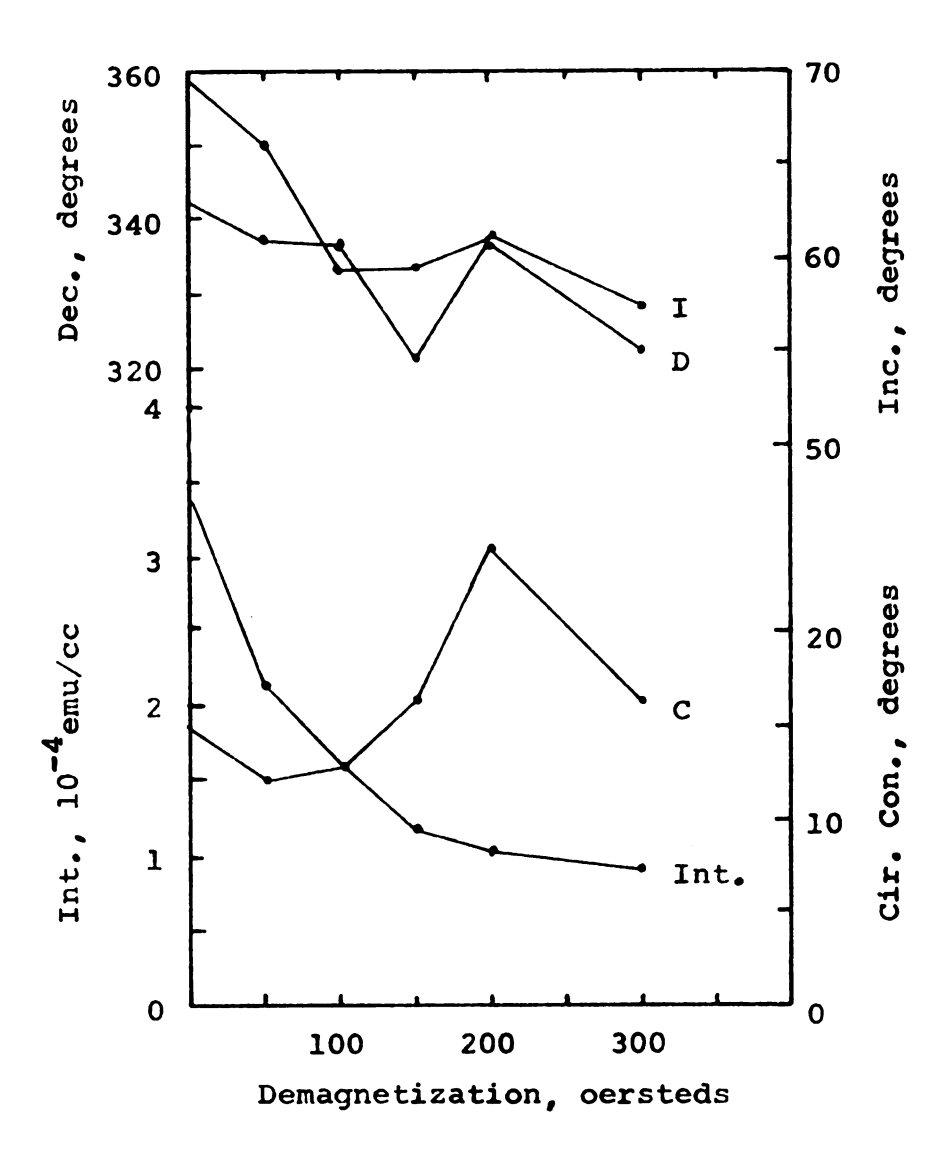


Figure 4-5f. A.f. demagnetization results of Site VN-22.

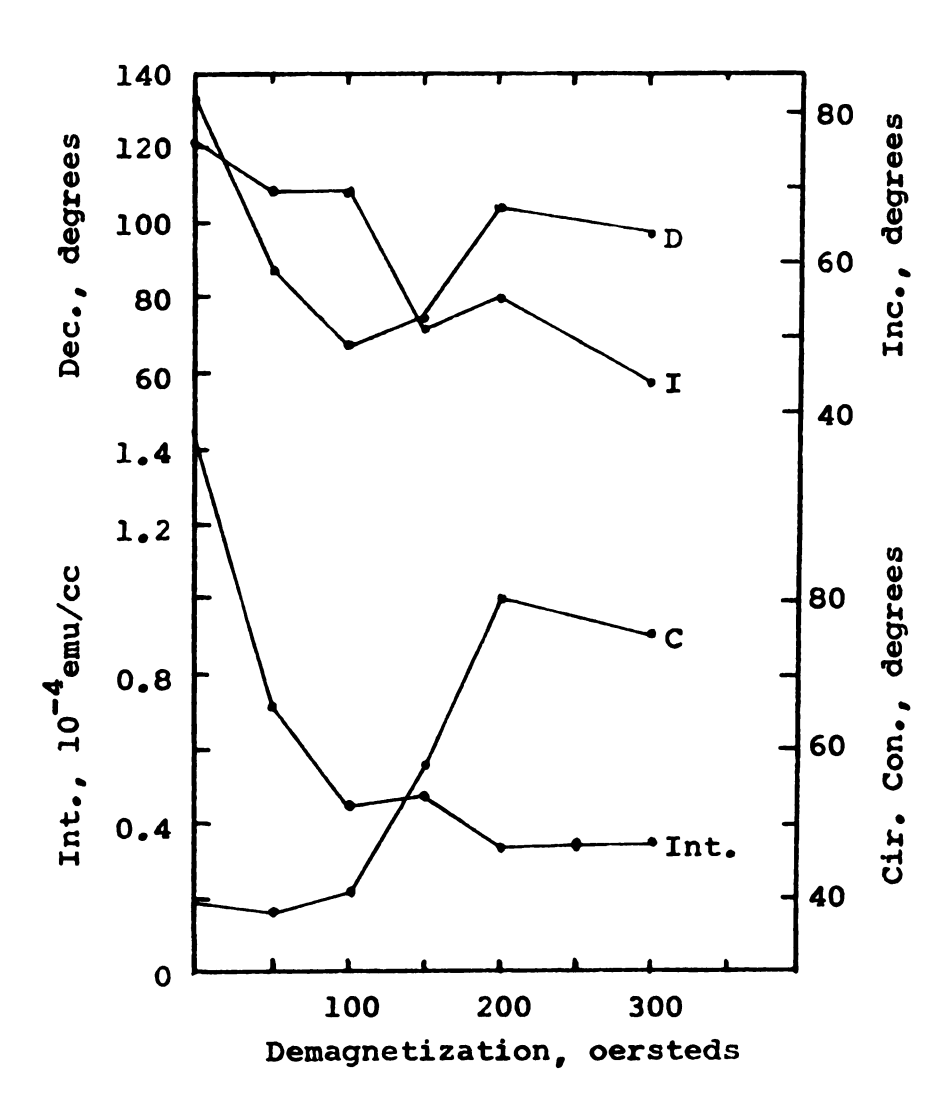


Figure 4-5g. A.f. demagnetization results of Site VN-25.

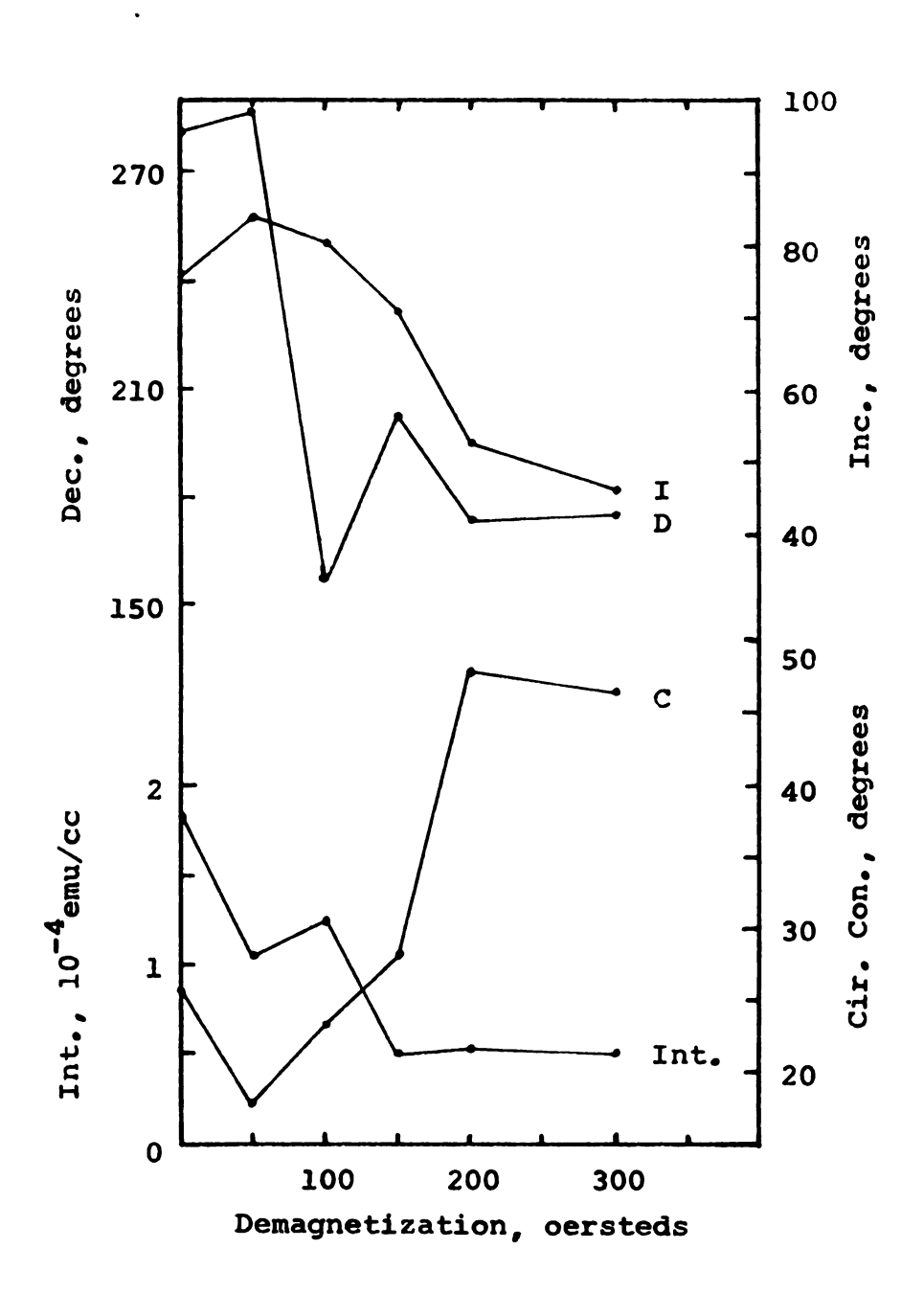


Figure 4-5h. A.f. demagnetization results of Site VN-30.

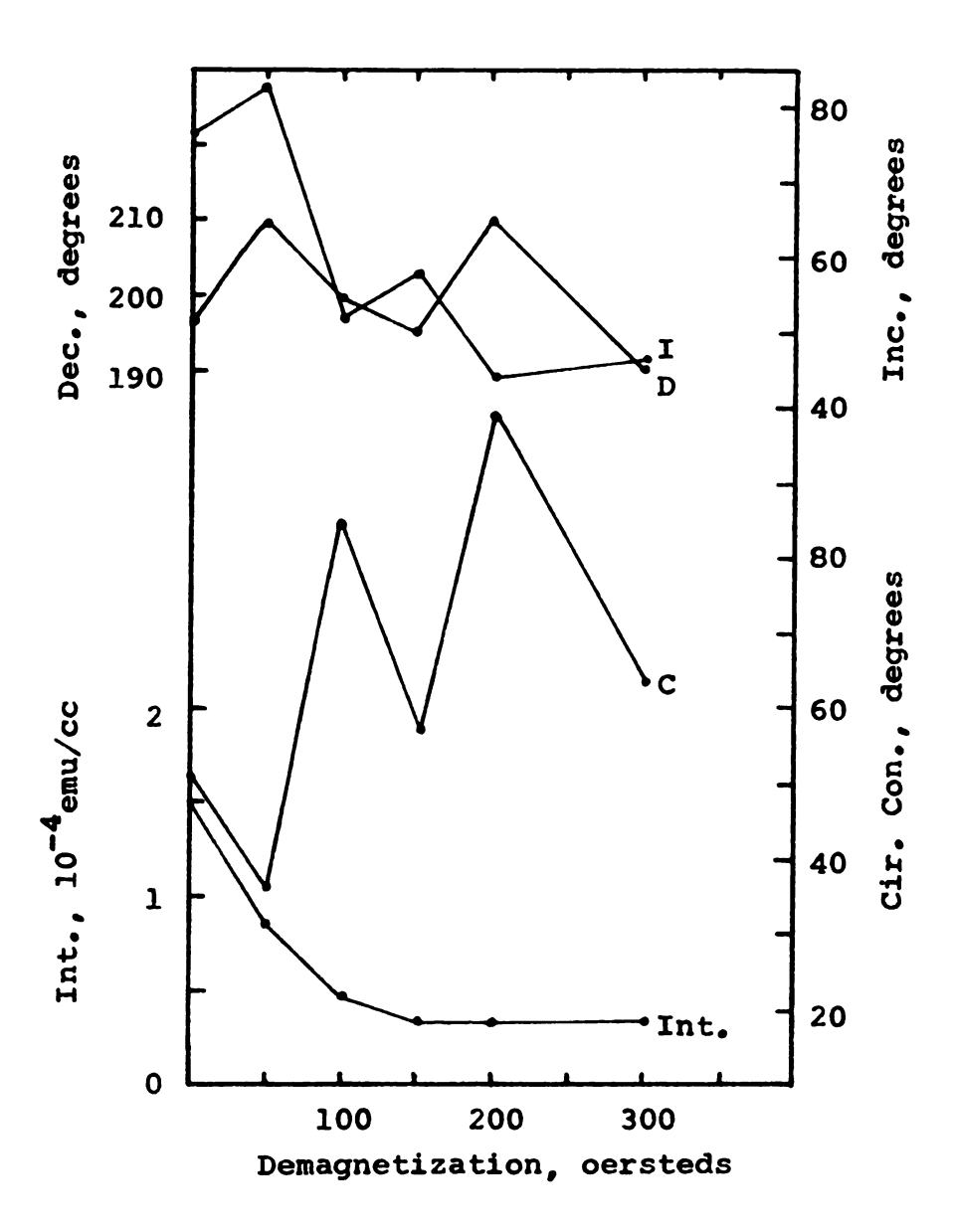
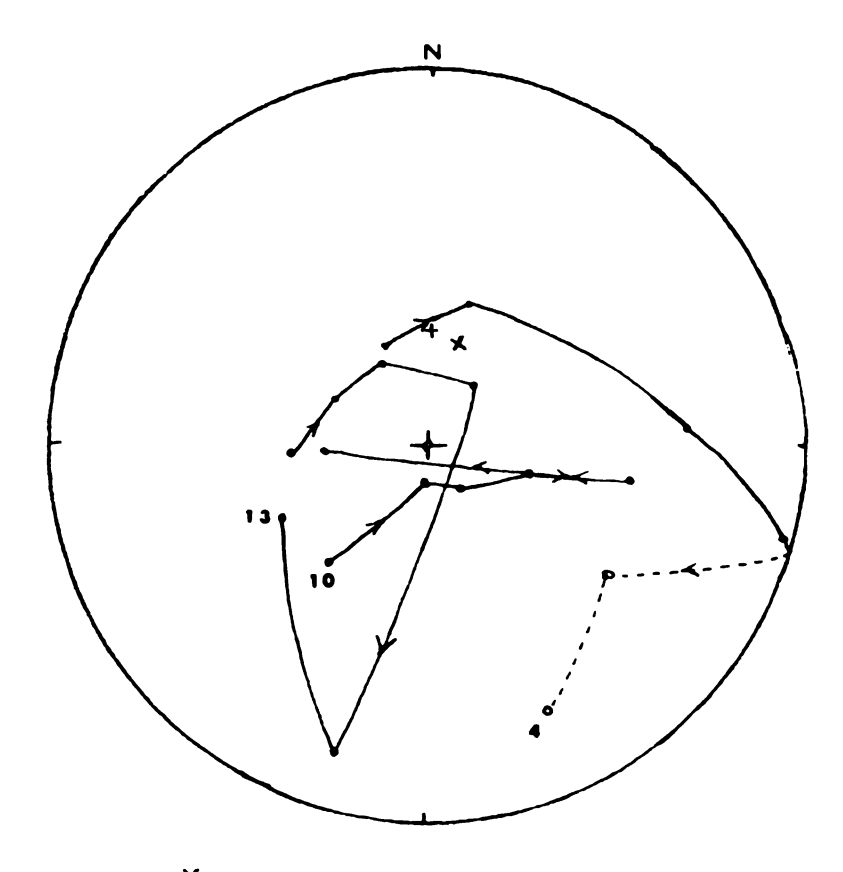
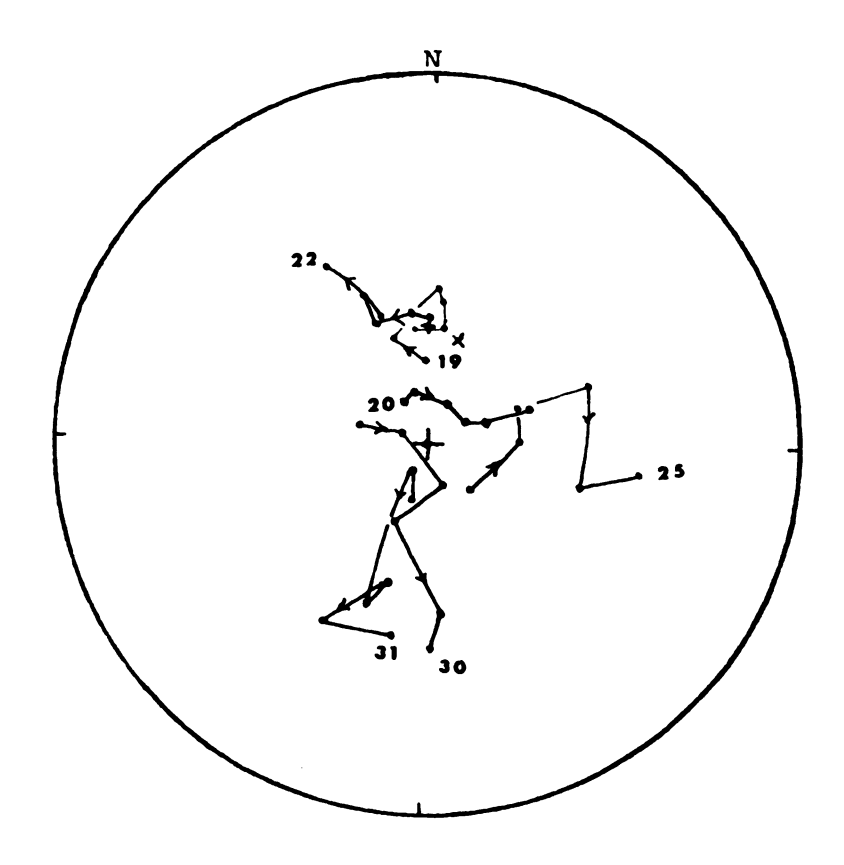


Figure 4-5i. A.f. demagnetization results of Site VN-31.



- X Present field
- + Axial dipole field

Figure 4-6. Mean site directions for NRM, 50, 100, 150, 200, and 300 oersteds demagnetization of Sites 4, 10, and 13, those collected in 1968. Equal area projection.



- × Present field
- + Axial dipole field

Figure 4-7. Mean site directions for NRM, 50, 100, 150, 200, and 300 oersteds demagnetization of Sites 19, 20, 22, 25, 30, and 31, those collected in 1970. Equal area projection.

direction of the remanent magnetization of the three sites collected in 1968 show considerable movement upon demagnetization. The 1968 and 1970 sites show respectively 170° and 54° average great circle movement from the NRM to 300 oersteds demagnetization levels. Obviously, storage time has had considerable effect on the earlier collected samples.

The acquisition of VRM will in general skew a distribution of points from the primary magnetization direction towards the direction of the ambient field along the great circle including the two directions. Inspection of the paths in Figure 4-6 and 4-7 does not indicate consistent movement along great circles from the NRM to the 300 oersted positions. A reasonable explanation of the complex pattern of paths is that the samples have a soft TRM of significant proportions coupled with a more stable VRM acquired through "long storage" in the field. The TRM also is probably soft and is being removed at low demagnetizing fields. If there were no VRM acquired during laboratory storage then the demagnetization paths should have moved along great circles away from the direction of the earth's magnetic field to the TRM direction.

4.3.2 Demagnetization at Optimum Levels

The 20 remaining sites were demagnetized at both 50 and 100 oersteds in order to be reasonably certain that the best level was being attained, yet of course, certainty

of this does not exist unless the sites are demagnetized at many levels.

The remanent magnetization of the specimens after demagnetization is tabulated in Tables 4-3 and 4-4 in the same format as Table 4-2. In all but one of the listings, the NRM shows higher quality data than either the 50 or 100 oersted demagnetization results. The added dispersion was not expected and this undoubtedly reflects the "soft" nature of the remanence to the demagnetization apparatus.

To aid in the evaluation of the magnetic stability and the storage, the directions listed in Tables 4-2, 4-3 and 4-4 for both lithologies and years are plotted in Figure 4-8. The remanent directions of the 1968 specimens show greater migration than the 1970 samples upon demagnetization, averaging 17 and 7 of great circle movement respectively. Only a few degrees of angular distance separate the NRM and 100 oersted directions of both the 1970 monzonite and quartz monzonite specimens. This indicates that the remanence removed during demagnetization lies nearly parallel to the NRM direction because the directions remained very close while the intensity decreased from the NRM value by over 50 percent.

The path of the 1968 quartz monzonite specimens upon magnetic cleaning is on a great circle towards the direction of the earth's magnetic field in the field area.

This is unusual behavior for the residual remanent vector,

50 oersted demagnetization results of 29 sites grouped in various combinations. Table 4-3.

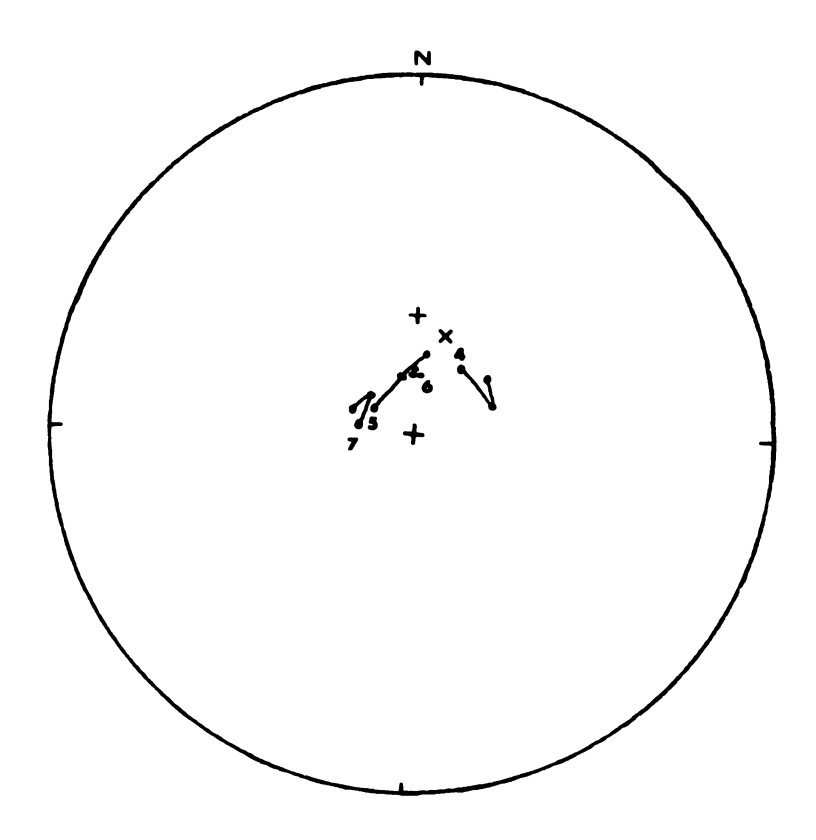
*	Sites	Number	Dec.	Inc.	Cir. Con.	Pre. Par.
-	All	52	349.6	80.2	10.2	7.1
	1968	12	25.2	78.2	20.2	5.6
	1970	19	325.1	79.1	12.9	8.6
7	Monz.	10	33.4	77.3	23.5	5.2
ю	Q. Monz.	19	326.6	79.0	12,1	8.7
4	'68 Monz.	ហ	69.2	6.69	57.5	2.7
လ	'68 Q. Monz		349.6	77.4	14.7	17.8
9	'70 Monz.	ĸ	353,3	77.0	14.3	29.4
7	'79 Q. Monz	12	309.8	79.0	18.4	6.5

* Designation used in Figure 4-8.

100 oersted demagnetization results of 28 sites grouped in various combinations. Table 4-4.

*	Sites	Number	Dec.	Inc.	Cir. Con.	Pre. Par.
Н	A11	28	352,3	78.3	10.9	7.3
	1968	11	24.7	71.1	13.4	12.6
	1970	17	312.6	78.9	15.7	6.1
7	Monz.	0	26.9	73.4	13.8	14.9
က	Q. Monz.	19	327.2	78.3	15.0	0•9
4	'68 Monz.	4	51.2	9*99	24.6	15.0
2	168 Q. Monz	7	5.7	71.5	18.0	12,1
9	'70 Monz.	Ŋ	356.0	75.3	18.4	18,3
7	170 Q. Monz	12	288.9	7.77	22.1	4.8

* Designation used in Figure 4-8.



- × Present field
- + Axial dipole field

Figure 4-8. NRM, 50, and 100 oersted demagnetization directions of the monzonite and quartz monzonite collected in 1968 and 1970. Numbers refer to Tables 4-2, 4-3, and 4-3 and are located at the NRM positions. Equal area projection.

as it is expected to move in the opposite sense upon demagnetization. Since it is the only group to show this movement, it is considered anomalous. This can be explained by a TRM coercivity spectrum which is lower than the VRM spectrum, however, this is unusual.

The monzonite shows less movement upon demagnetization to than the quartz monzonite. The demagnetization to 300 oersteds of three sites collected from each of the rock types shown in Figure 4-7 gives an average movement of the remanence of 38° for the monzonite and 71° for the quartz monzonite. The 1970 specimen results shown in Figure 4-8 reveal that the remanence of the monzonite sites moved 4° upon demagnetization as contrasted to 11° for the quartz monzonite. The greater stability of the monzonite is believed to be influenced by the difference in the magnetite size distribution as shown in Section 2.2.

The results of the demagnetization are not strongly convincing as would have been anticipated. The remanent results from the 1970 specimens are believed to be more representative of the remanent directions. No distinction can be made between the NRM and demagnetized directions of remanence because both are nearly parallel.

4.3.3 Remanent Intensities

A tabulation of the intensities of magnetization before and after demagnetization are presented in Table 4-5.

Remanent magnetization intensities (x10-4 emu/cc). Table 4-5.

		N	NRM	50 oer.	er.	100	100 oer.
•20	Mean	7.4	4	0*5	0	3,1	1
MOT	Extremes	2.7	2,7 18,6	1.3	15.6	8*6 6*0	8.6
zuo	Mean	3.7	7	2,3	3	1.2	2
M.Q	Extremes	1.5	6.3	7.0	6.4	0.4	4.0

Individual specimens have magnetizations which range from 1×10^{-2} emu/cc to 5×10^{-5} emu/cc. Most samples, however, are of the order of magnitude 10^{-4} emu/cc. The extremes for each entry in the table show a wide separation. The difference within a rock type (NRM, 50 oer., 100 oer.), and between rock types are not statistically significant. However, the means of the different entries appear to be consistent. The calculations are based upon specimens from the 29 demagnetized sites.

The range for each of the entries into Table 4-5 is about one magnitude, even after demagnetization. This suggests that the variation in the NRM is not from a range of intensities of superimposed secondary components on a uniform TRM. If this were true, the range or extremes for the two rock types should have decreased with each successive level of demagnetization. The variation is likely due to the normal distribution inherent to the lithologies. There is nearly a two to one relationship of the monzonite to quartz monzonite intensities at each of the three levels, which directly reflects the magnetite content.

Included in Table 4-6 are various ratios of remanent intensities. Each step of demagnetization removed approximately 40 percent of the remanence and at 100 oersteds, slightly over one-third of the remanence remains in each rock type. In contrast, basalts generally show only a few percent decrease in magnetization at 100 oersteds. The

Table 4-6. Remanent intensity ratios.

	(R ₅₀)	$\left(\frac{R_{100}}{NRM}\right)$	$\left(\frac{R_{100}}{R_{50}}\right)$
Monzonite	0.59	0.39	0.60
Q. Monzonite	0.62	0.36	0.60

he removal of the remanence is typical (Strangway, 970, p. 79) of that for granitic rocks in which the agnetite is coarse grained.

.4 Storage Tests

4.4.1 Storage Procedure

Nine specimens from four sites were selected for storage and subsequent demagnetization tests. The object of these tests was to determine the significance of the VRM contribution and how easily it could be removed.

Movements along great circles of as much as 50° due to VRM acquisition have been noted by Akimoto and Kushiro (1959) for a suite of dolerite specimens. Experimentally, Rimbert (1958) has shown that VRM is more stable to af demagnetization the longer the period over which it has been acquired. Extrapolating the results of Rimbert, in conjunction with the results of this study, should suggest whether the amount of VRM acquired during storage, both for the 1968 and 1970 specimens, has been removed by the af demagnetization.

The specimens used for this experiment were given arbitrary orientations because they were cored from unoriented hand samples. After the cores had been prepared and stored in the same position (ambient field of the laboratory) for several months, they were rotated 180° about an axis nearly at right angles (8° off) to the magnetic meridian. The proximity of the magnetic meridian to the plane

of rotation permits, as a reasonable approximation, one-half of the difference in the change of the three mutually orthogonal components as the means to calculate the amount of VRM acquired during storage. The experiment commenced with the rotation of the specimens and the subsequent determination of the resulting remanence from zero time to over 100 days later.

4.4.2 Results

The migration of the NRM direction for each of the 9 specimens is shown in Figure 4-9. The best fitting great circle was visually drawn through each set of points. These intersect about the direction of the ambient field in the laboratory. The NRM directions have been moved through 15° to 80° of great circle arc in three months. The magnitude of this movement indicates a large ratio of VRM to the magnetically stable components and shows that the original remanence can be significantly altered in a short period of time.

The magnitude of VRM attained as a function of the storage time was calculated and the results are shown in Figures 4-10 and 4-11. The VRM intensity shows an exponential growth with time and in just a few days an appreciable quantity of VRM is acquired.

The acquisition of VRM is a time dependent phenomenon thought to be due to thermal agitations allowing the magnetization to be "trapped" in the direction of the ambient

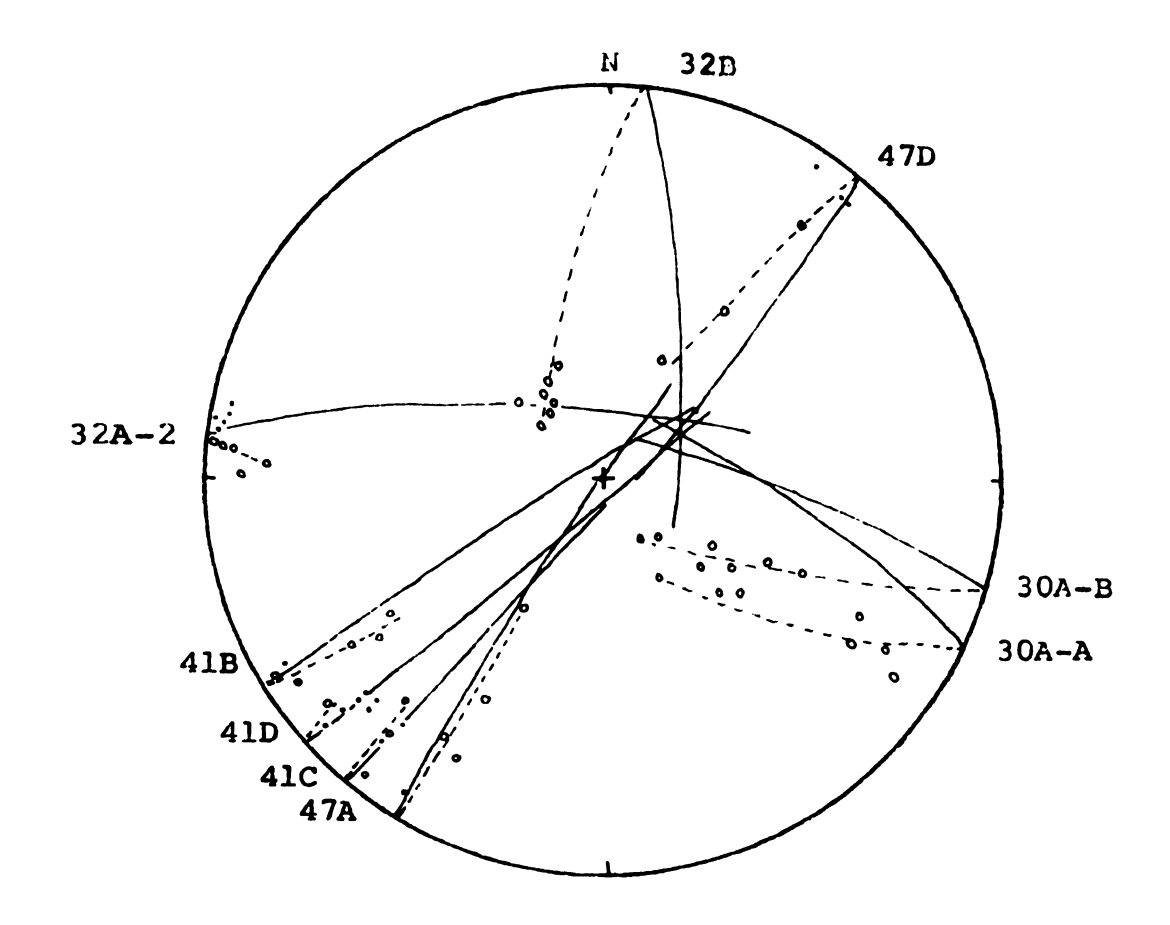


Figure 4-9. Migration of remanent magnetization upon storage in the laboratory.

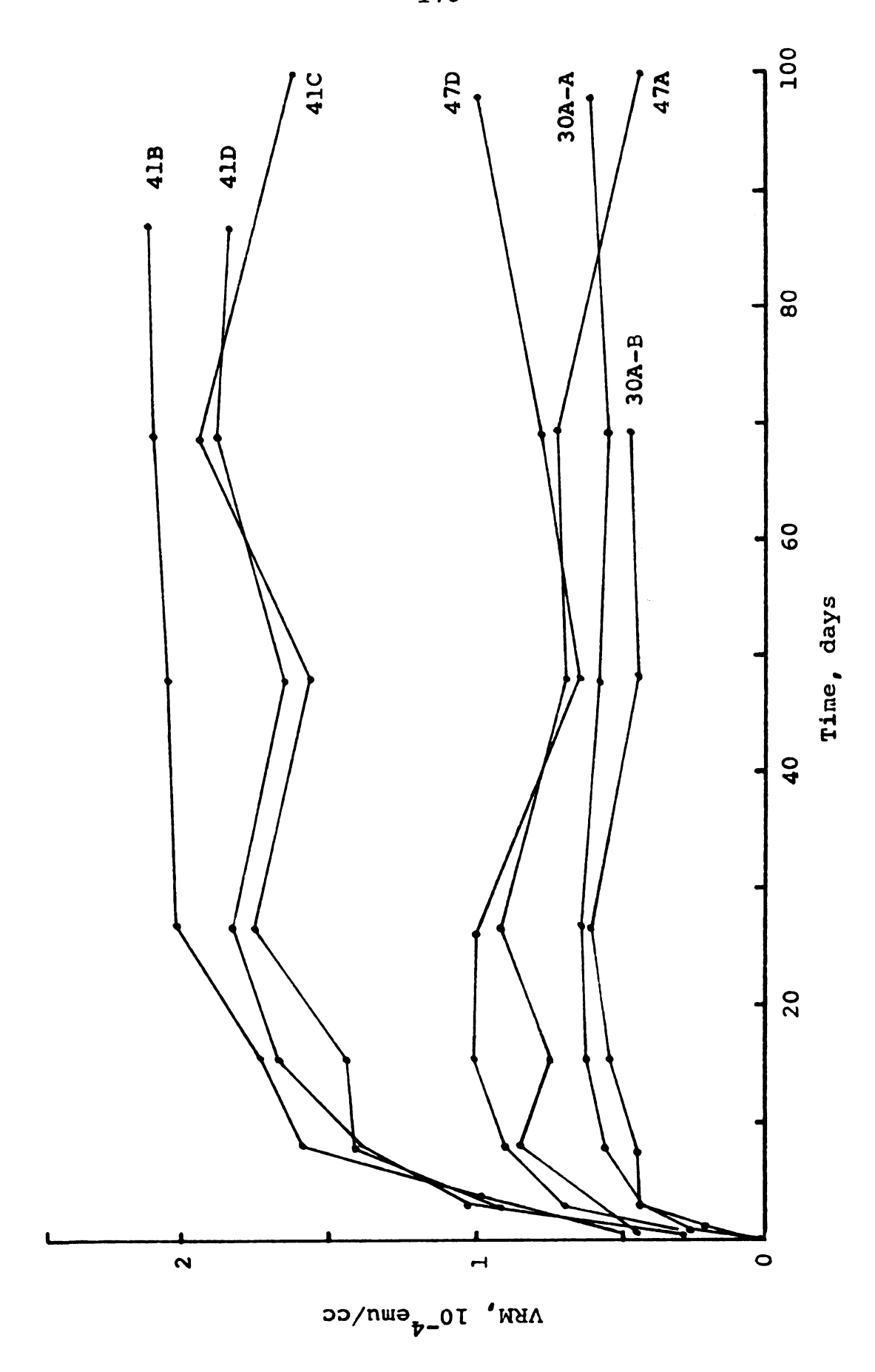
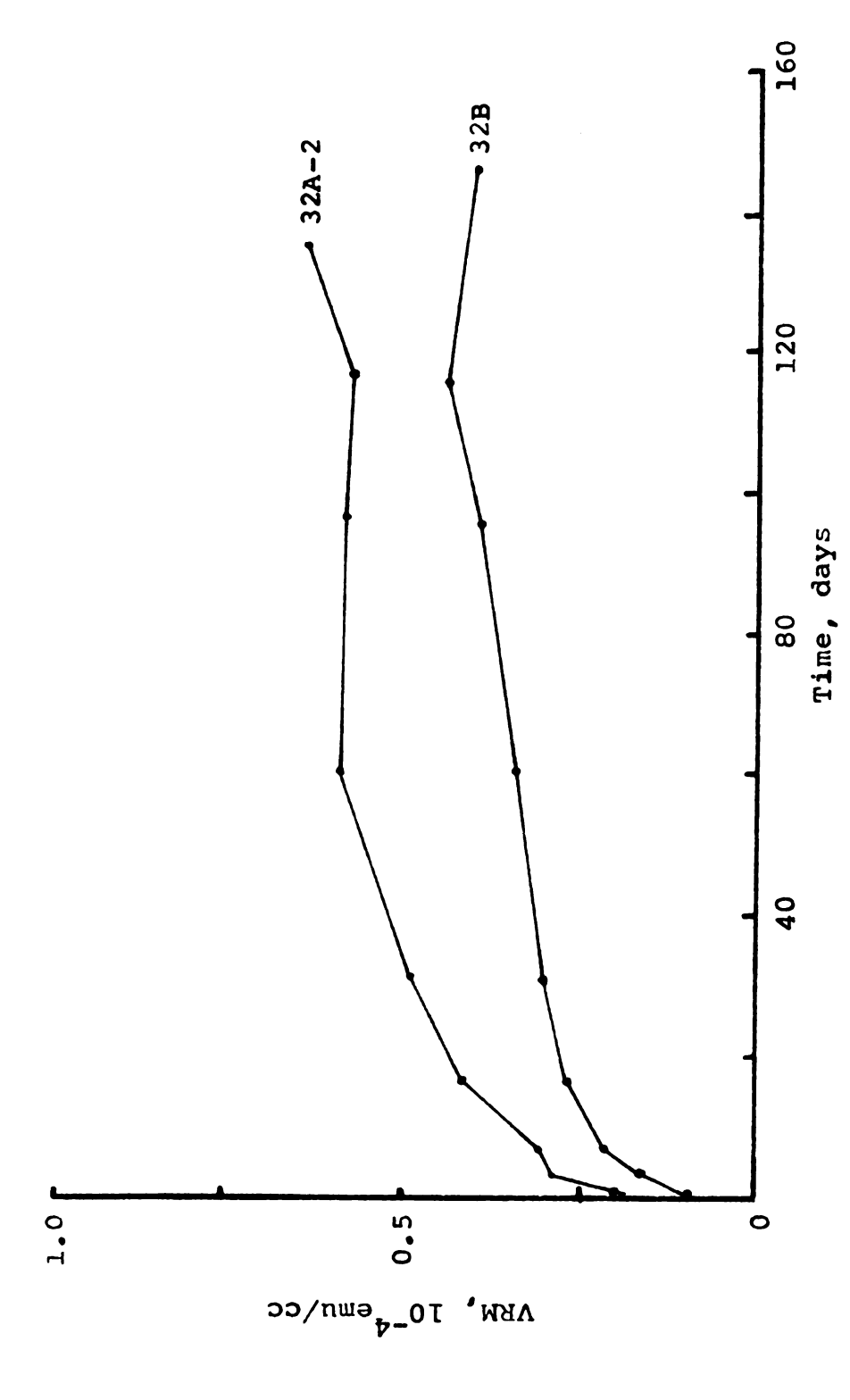


Figure 4-10. Intensity of VRM acquired during storage in the laboratory.



Intensity of VRM acquired for two specimens from Site 32 during storage in the laboratory. Figure 4-11.

field when it crosses over energy barriers. Mathematically the acquisition of VRM is expressed by the formula:

I = constant + $s \log t$

where I is the acquired remanence during time t and s is an index of magnetic viscosity.

The data of Figures 4-10 and 4-11 are plotted on a semilog plot as shown in Figure 4-12. The trends of the semilog plot can be projected in order to estimate the intensity of VRM acquired during long periods of storage. Equation 1 predicts that the growth of the VRM component is a straight line when plotted on a similog graph. Figure 4-12 shows data from Sites 30A and 32 are nearly linear whereas the data from Sites 41 and 47 are not linear. A simple calculation shows that in less than 1 million years, the samples from Site 41 would attain a VRM equal to their VRM. It is apparent that the equation 1 does not hold its semilog linearity for a great number of magnitudes. However, it does lend insight to the fact that the remanence of the rock at Site 41 must be largely VRM. Projecting the trends of the specimens from Sites 30A and 32 reveal that approximately three-fourths of the NRM can be attributed to VRM for a storage time of 125 m.y. from the time the rocks were formed (125 m.y.).

The ratio of the VRM acquired during storage to the NRM at the commencement of the test is compiled in Table 4-7 (data in the last column is referred to in the following section). No distinction can be made as to which rock

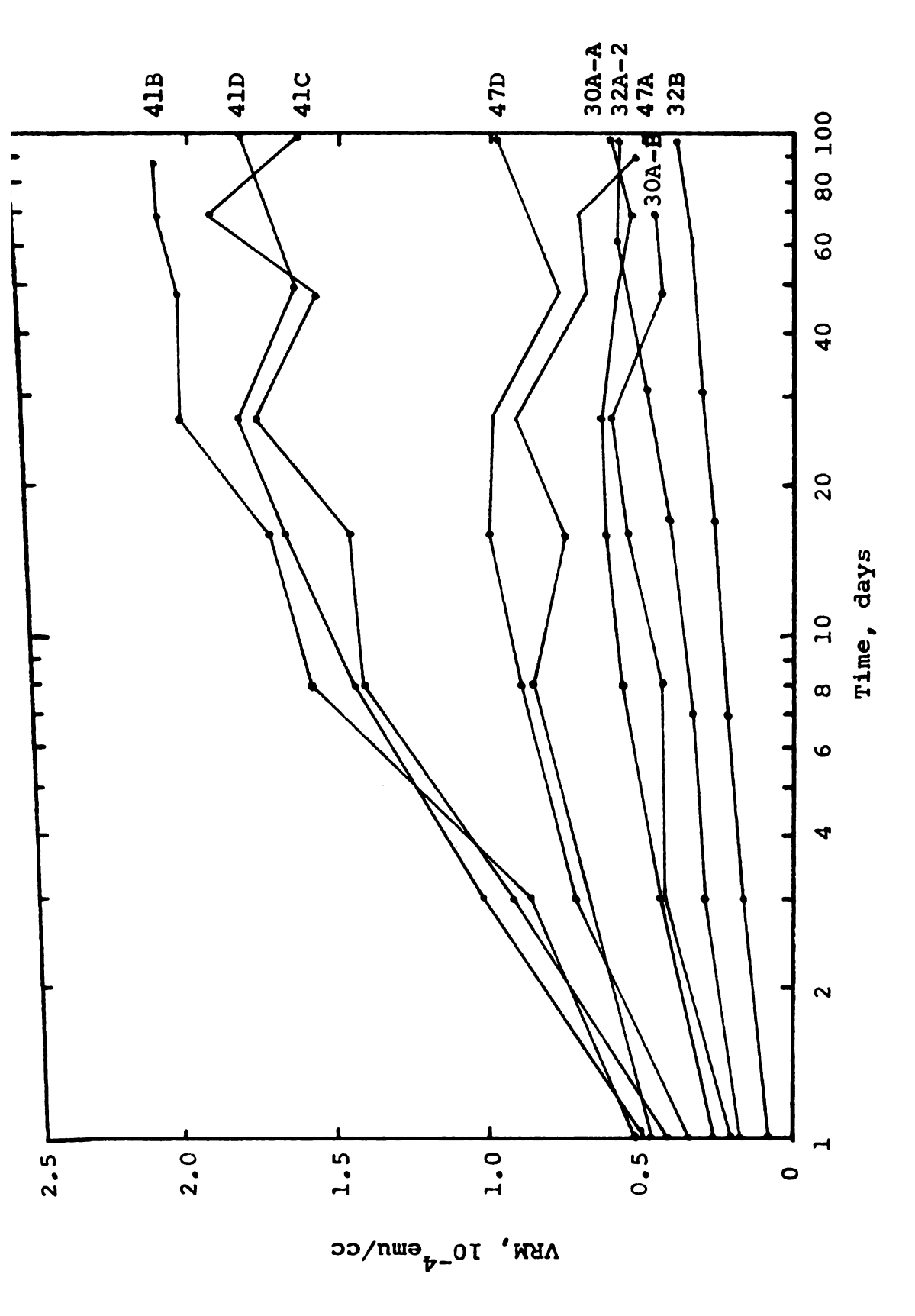


Figure 4-12. Semilogrithmic plot of VRM acquisition with respect to time.

Table 4-7. Results of storage test.

Smoothon	Storage	* VRM Added	** VRM Demag.
Specimen	(Days)	%	Field
VN-30A-A	98	40	25
VN-30A-B	69	30	-
VN-32A-2	135	15	20
VN-32B	117	25	20
VN- 4 1B	87	35	20
VN-41C	100	40	10
VN-41D	99	25	5
VN-47A	100	35	5
VN-47 D	100	50	20

^{*(} VRM at 100 days/ NRM at 0 days) \times 100

^{**} af demagnetization in oersteds necessary to remove VRM acquired during storage

type has larger amounts of VRM. It is clear, however, that the NRM can be significantly changed in a matter of a few months and has certainly been appreciably modified since the time of rock formation by VRM.

4.4.3 Demagnetization of Stored Samples

Eight of the samples were progressively af demagnetized in order to determine the level of demagnetization necessary to remove the VRM acquired during storage. The demagnetization results will indicate whether the VRM's of the 1970 specimens acquired during a month of storage were removed with the magnetic cleaning. With the aid of Rimbert's demagnetization results, a reasonable extrapolation can be made to determine whether the VRM was also removed from the 1968 specimens.

rigures 4-13a through h show the results of demagnetization of the stored sampled for five progressive steps of af demagnetization (20, 40, 60, 80 and 100 oersteds). The positions of the net component removed are connected by great circle segments. The direction of the component of the magnetization removed in each interval is shown by the isolated points. The first point of the net component and of the first interval are, of course, coincident. The zero time position, terminal storage direction and the direction of the total VRM acquired are also illustrated in the stereograms.

Figure 4-13a shows the first component of

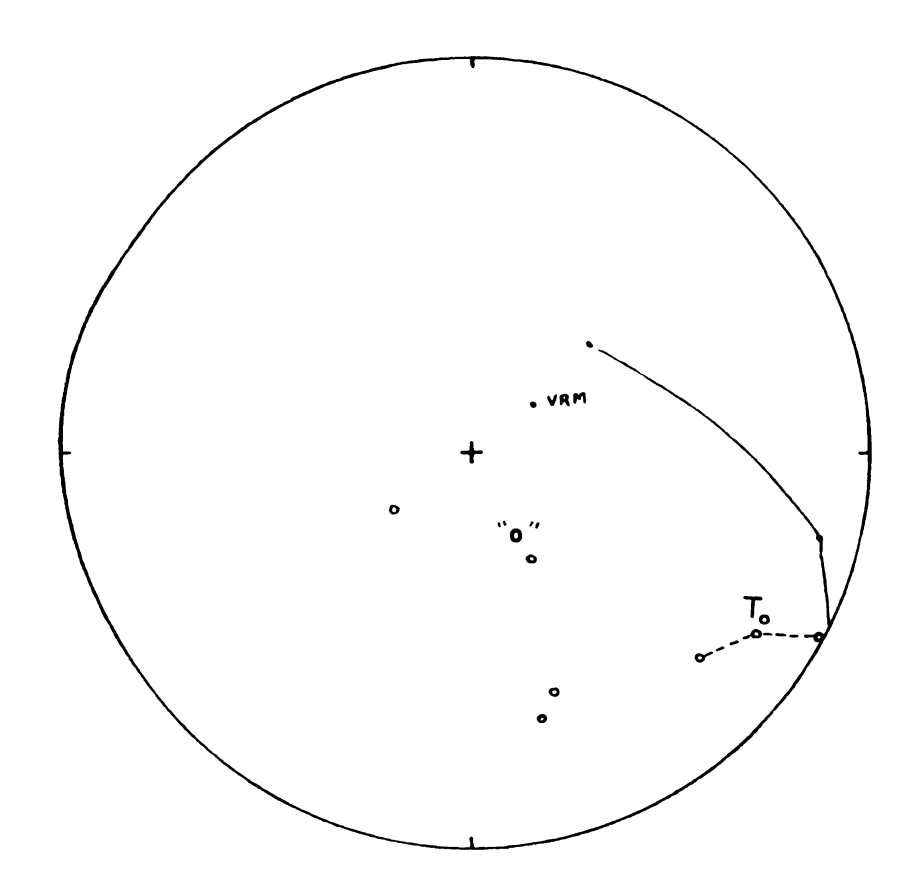


Figure 4-13a. Storage test and demagnetization of specimen VN-30A-A. Equal area projection.

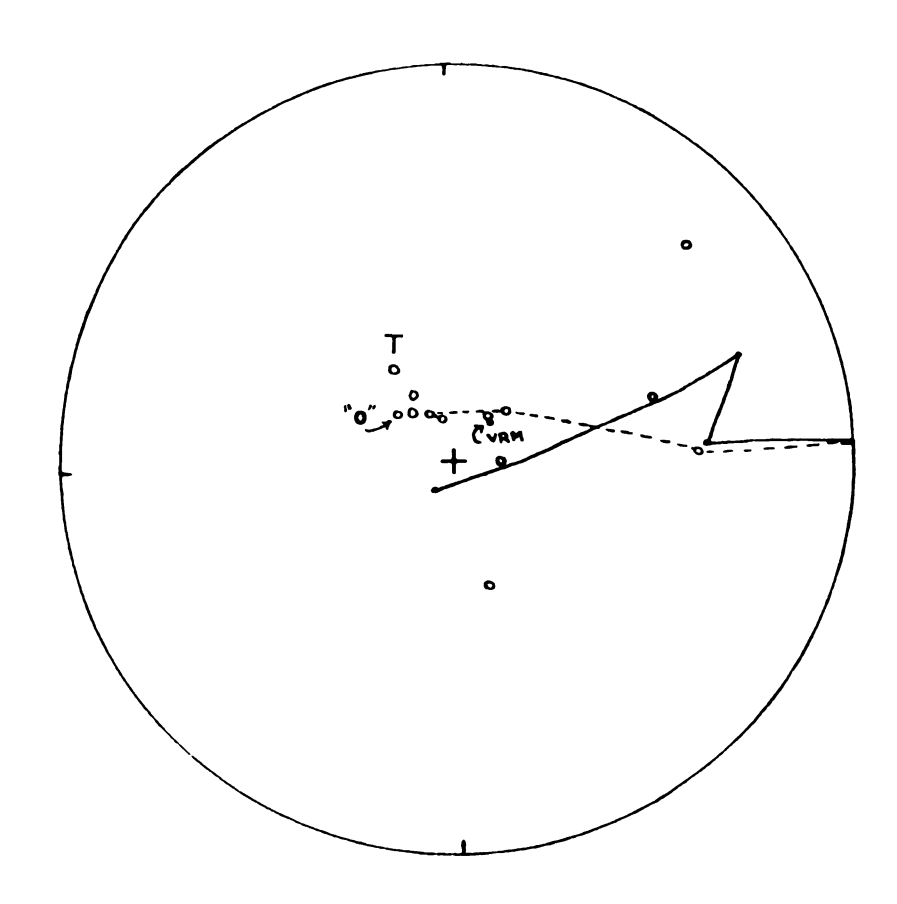


Figure 4-13b. Storage test and demagnetization of specimen VN-32A-2. Equal area projection.

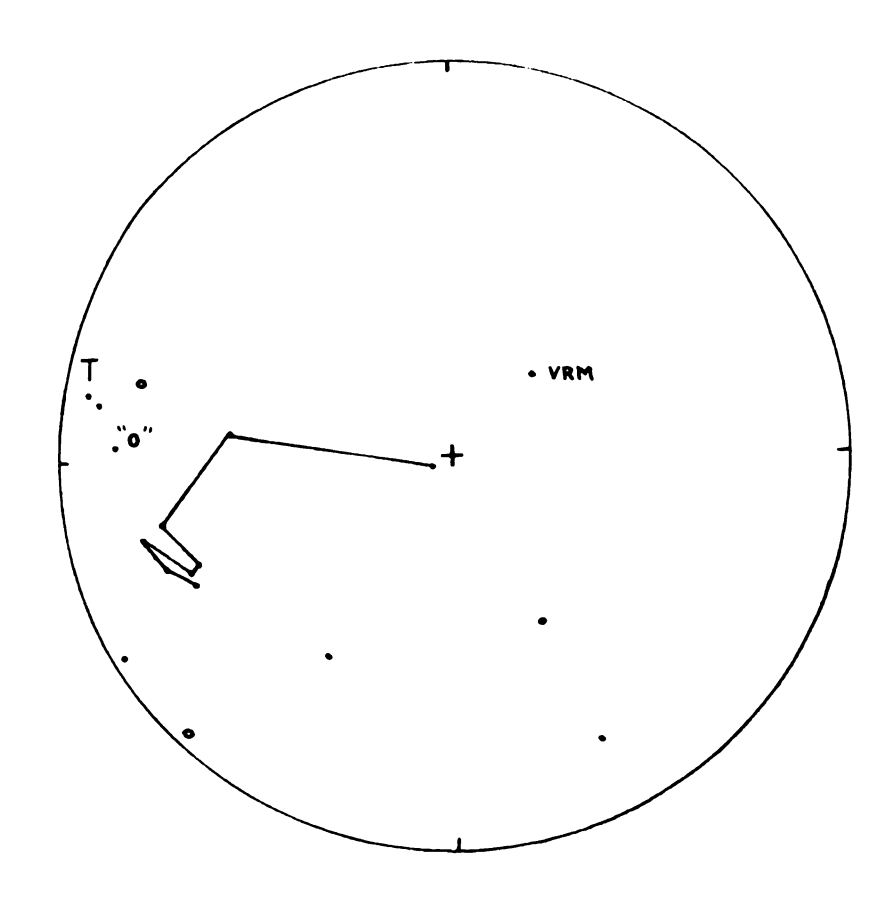


Figure 4-13c. Storage test and demagnetization of specimen VN-32B. Equal area projection.

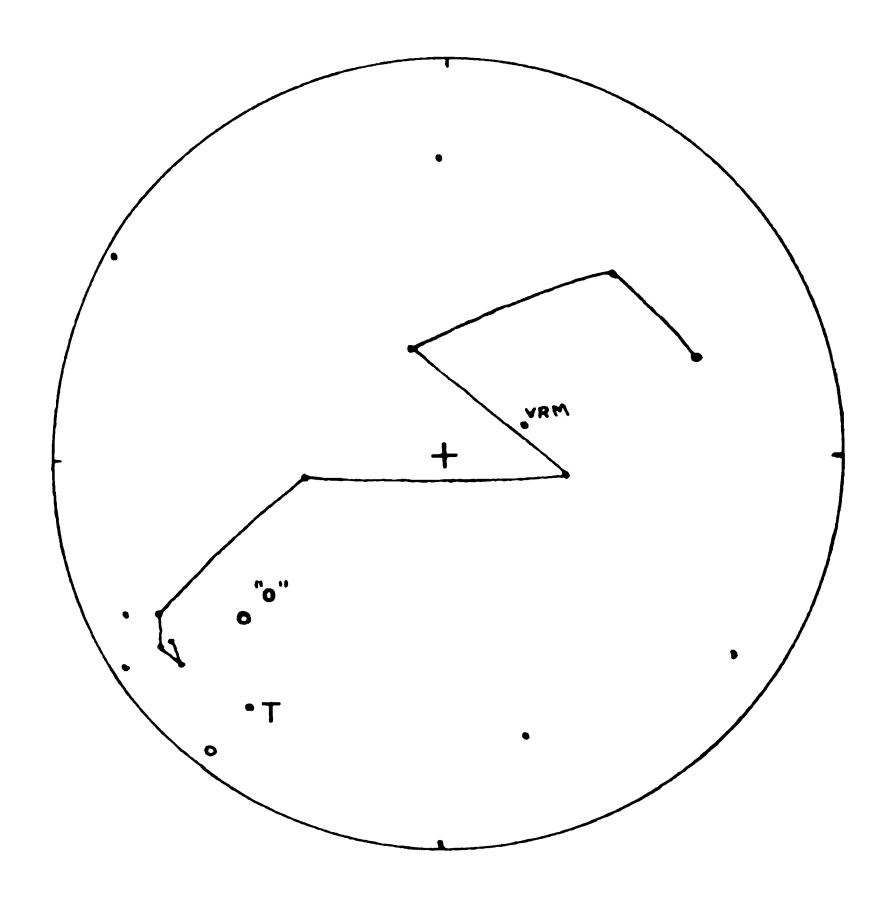


Figure 4-13d. Storage test and demagnetization of specimen VN-41B. Equal area projection.

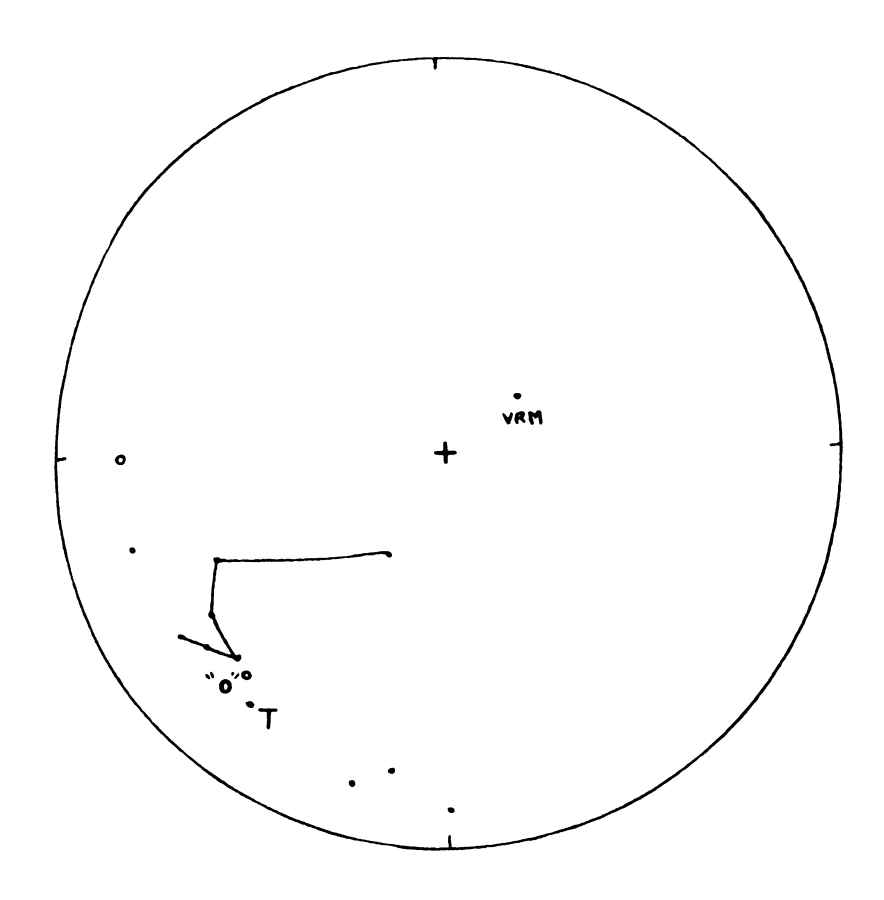


Figure 4-13e. Storage test and demagnetization of specimen VN-41C. Equal area projection.

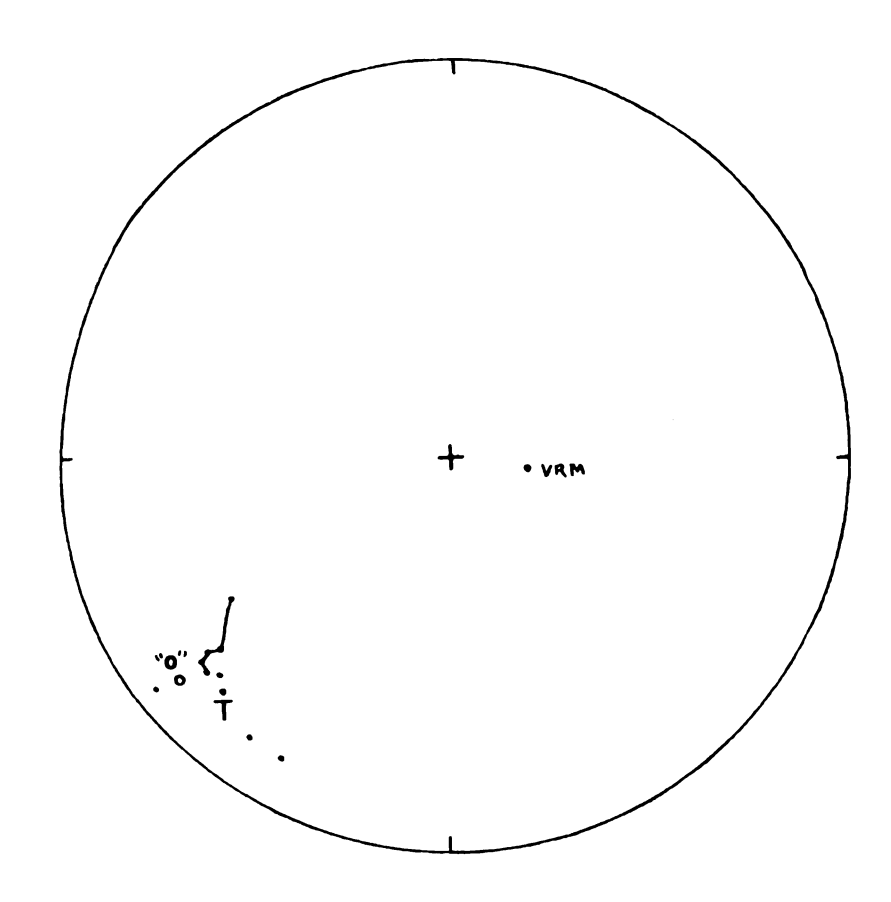


Figure 4-13f. Storage test and demagnetization of specimen VN-41D. Equal area projection.

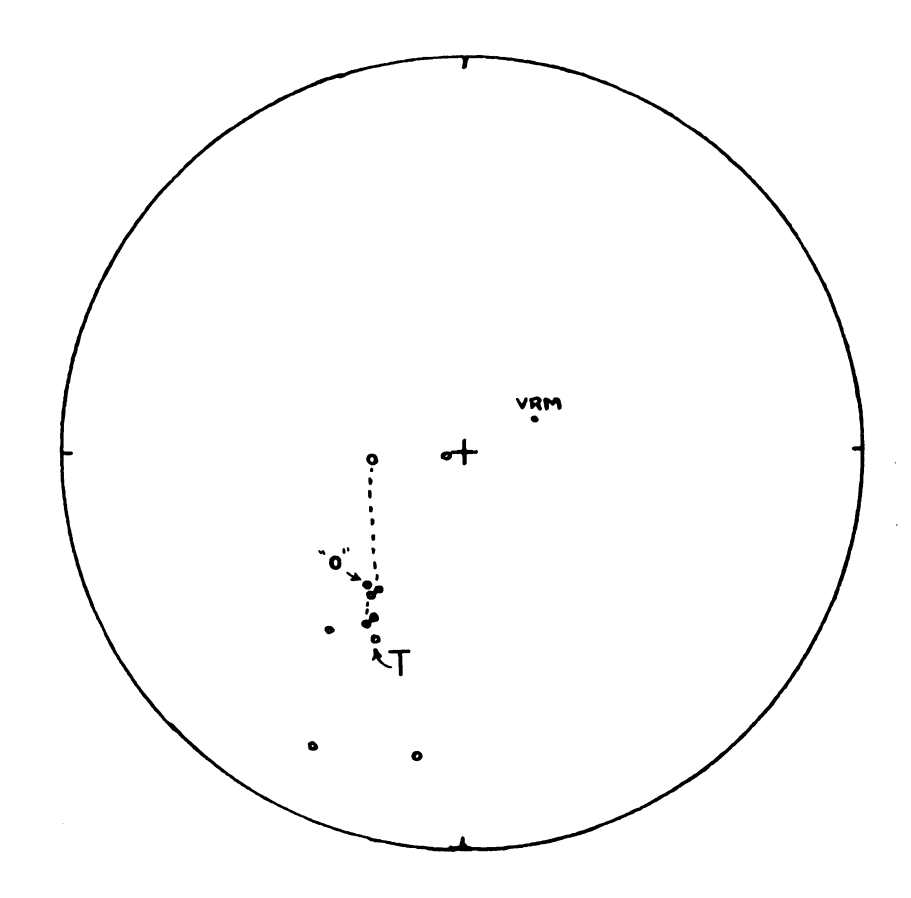


Figure 4-13g. Storage test and demagnetization of specimen VN-47A. Equal area projection.

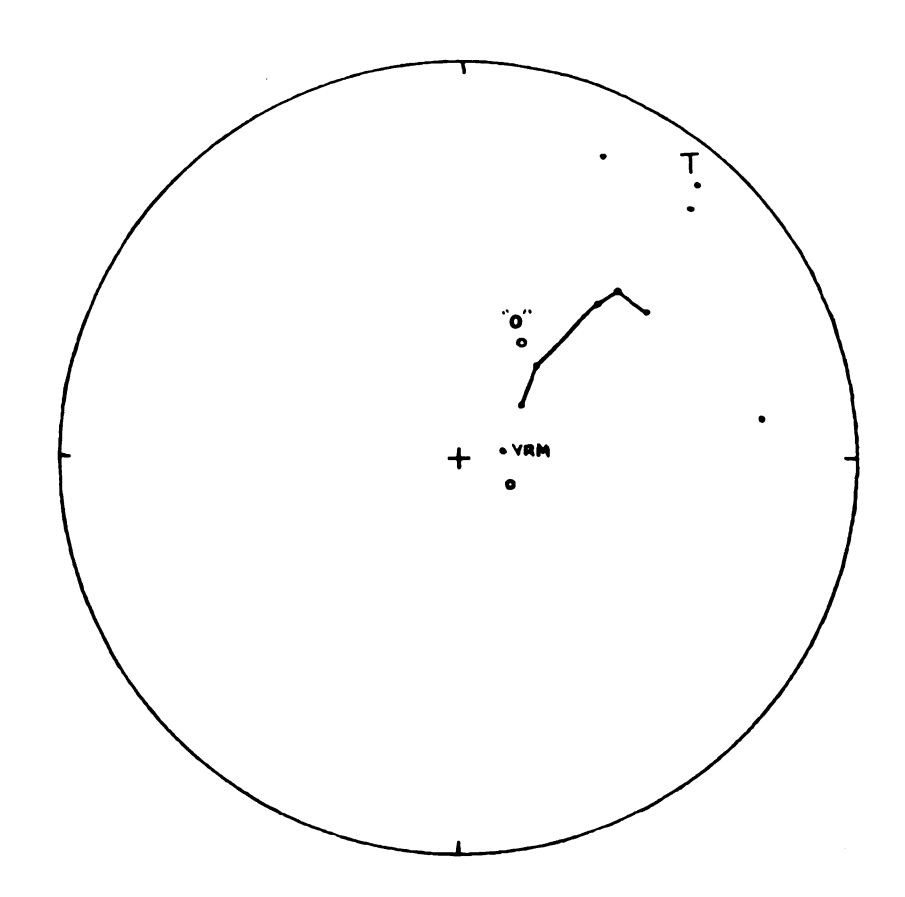


Figure 4-13h. Storage test and demagnetization of specimen VN-47D. Equal area projection.

demagnetization to be nearly in the same direction as the VRM direction. This indicates that at 20 oersteds the demagnetizing field had removed a component which was nearly parallel to the storage acquired VRM. The remaining four interval demagnetizations show reversely polarized components and, hence, would not be due to remanence attained during storage. The migration of the net component away from the ambient field direction shows that the effect of the recently acquired VRM is quickly and easily masked by remanence removed in the direction of the NRM. similar manner the remaining figures in the group can be inspected. All but two of the samples behave in a fashion as specimen VN-30A-A. Specimens VN-41D and VN-47A show little indication of having recently acquired a VRM. because the directions of the first components removed are near their respective NRM directions. Clearly the VRM of these two specimens was very soft. The demagnetization fields necessary to remove the storage VRM were estimated from orthogonal projection curves and the results are included in Table 4-7.

For a low inducing field, approximately 30 oersteds of demagnetization are necessary to remove the VRM acquired for each magnitude increase of storage time according to Rimbert's results. Applying this fact to the data of this study indicate that, if 20 oersteds of demagnetization remove the VRM of three months, then 55 oersteds should remove the VRM acquired in 30 months. The VRM picked up

by the 1968 specimens during two years of storage should have been removed by the demagnetization as carried out in this study.

As previously mentioned, it is generally thought that soft components of remanent magnetization, such as VRM, are removed in fields of 300 oersteds or less. This is particularly true with the coarse grained magnetite bearing rocks of this study. However, the amount of long term VRM acquired during "storage" in the field which was removed by the demagnetizing process is unknown. Generally, this can be determined by demagnetizing until a level is reached at which the remanence is stabilized. However, the demagnetization process leads to erratic results indicating that the remanence is very soft and easily distributed in spurious ways by the demagnetization apparatus. This is substantiated by the erratic results obtained from demagnetization of a few specimens to 800 oersteds.

4.5 Q-Ratios

Koenigsberger (1938) recognized the value of defining a ratio, Q, as the remanent to induced magnetization. The magnetic expression of a body is a composite of the remanent and induced components. Thus, the Q ratio expresses the relative importance of the two components to each other. Books (1962) has shown that the magnetic anomaly over volcanic buttes can be primarily due to remanent

magnetization. Characteristically, volcanic rocks have Q's greater than 1.0. On the other hand, in most intrusive igneous rock Q is less than 0.5. Thus, the remanent component is generally neglected in magnetic modeling of anomalies derived from plutonic rocks. It will be shown that there is good reason to consider remanence, even though it may be soft and unstable.

The Q ratios were calculated using an inducing field of 0.56 oersteds, the mean NRM, and susceptibility for each of the 34 in situ cored sites. The specimens with anomalously high remanence were eliminated. The results of the calculations are illustrated in Figure 4-14. The mean values of Q for the monzonite and quartz monzonite are 0.42 and 0.38 respectively. The remanence has been shown to be unstable and hence it would be very sensitive to mechanical, thermal, and magnetic disturbances. Lightning strikes, slight heating during drilling of the specimens, magnetic fields of the transporting vehicles and fields encountered during preparation will disturb the magnetism and may increase it. The Q ratio would increase because of the relatively constant value of magnetic susceptibility. The effects of weathering would decrease the susceptibility and remanence proportionately and hence have no appreciable affect on Q. This assumes the product of weathering to be the relatively nonmagnetic goethite.

The median value was chosen as the most representative Q value for each rock type. This was done because

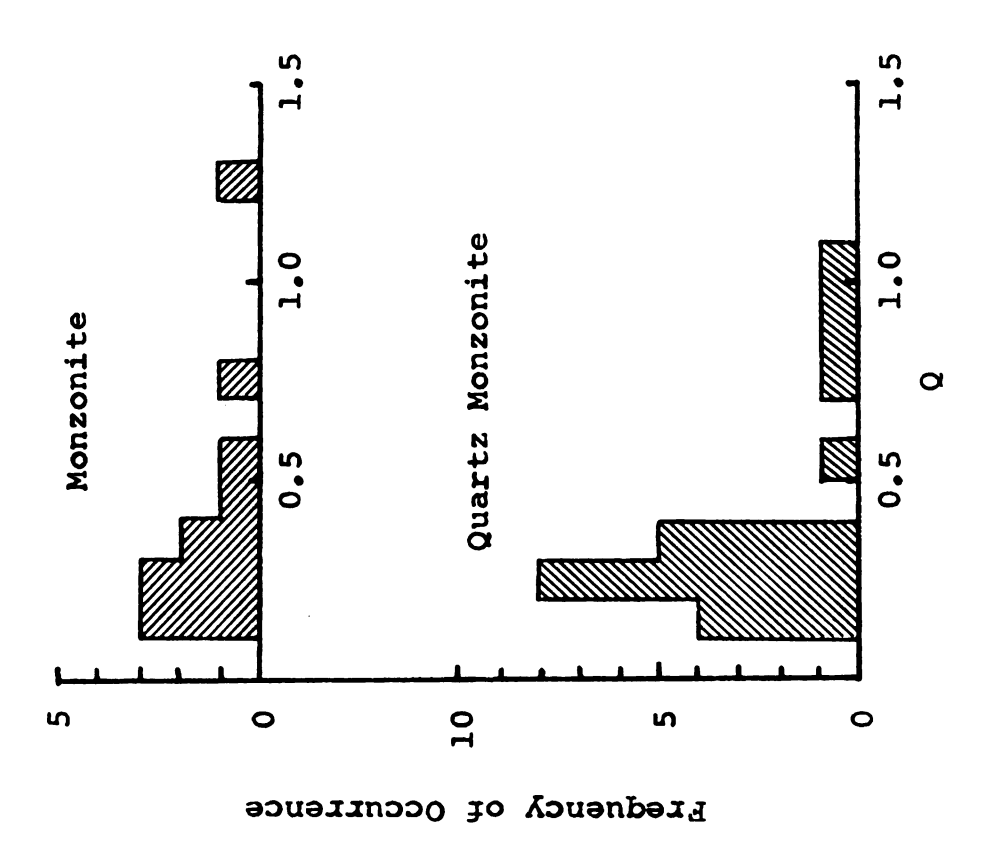


Figure 4-14. Distribution of Q ratios by rock type.

righthanded skewness of the histograms in Figure 4-14 is considered to reflect magnetic disturbances in the remanence. The median values are essentially the same, 0.28 and 0.29 with the monzonite being slightly larger.

Thus, the remanence is approximately one-fourth of the induced magnetization. Since the remanence is in the general direction of the earth's magnetic field, the total magnetization of the intrusive will be low by 25 percent if remanence is disregarded. For the quartz monzonite the induced magnetization is about 1.1 x 10^{-3} emu/cc and with the effects of remanence included this value rises to nearly 1.4 x 10^{-3} emu/cc. Similarly, corresponding values for the monzonite are 1.7 x 10^{-3} emu/cc and 2.1 x 10^{-3} emu/cc. This difference may be quite important in magnetic interpretation.

How much of this argument for including remanence in the total magnetization can be extended to other intrusive bodies is difficult to assess. However, it should be remembered that, even though the remanence may be soft and possess large VRM components, this magnetization will align itself with the direction of the earth's magnetic field and the ommision of this remanence will effectively lower the magnetization of the body.

A study of the effect of the intrusive's geometry on $\mathbb Q$ values indicates that there is little relation of the $\mathbb Q$ values of the quartz monzonite to the distance from the limestone-intrusive contact on the southern margin.

However, the monzonite (Figure 4-15) shows a decrease in Q away from the contact. As mentioned previously, the magnetic susceptibility shows no discernible relationship to the border of the intrusive. As a result, the trend shown in Figure 4-15 indicates a decrease in the remanence away from the contact. The data in the figure suggest that the Q values start leveling off at approximately onehalf mile from the contact. It is postulated that the magnetite fraction near the margin of the intrusive has a higher coercivity spectrum and hence, a more stable remanence of the TRM. In fact, those sites nearest the contact do show a more stable remanence than sites farther away from the contact, thereby suggesting higher blocking temperatures. This supports the view of the magnetite having an appreciably greater number of grains in the monodomain region near the contact. There are insufficient data from the magnetite grain size study to help verify this point. Thermal demagnetization would be helpful in revealing the blocking temperature spectrum.

If the monzonite were the first pluton to be intruded, it would have a significant thermal gradient with the country rock. This temperature differential could well explain a somewhat faster crystallizing margin than the interior of the pluton. As the cooling proceeds the country rock would be heated. Then, if the quartz monzonite was intruded into an already heated host rock, the temperature gradients would be less than within the

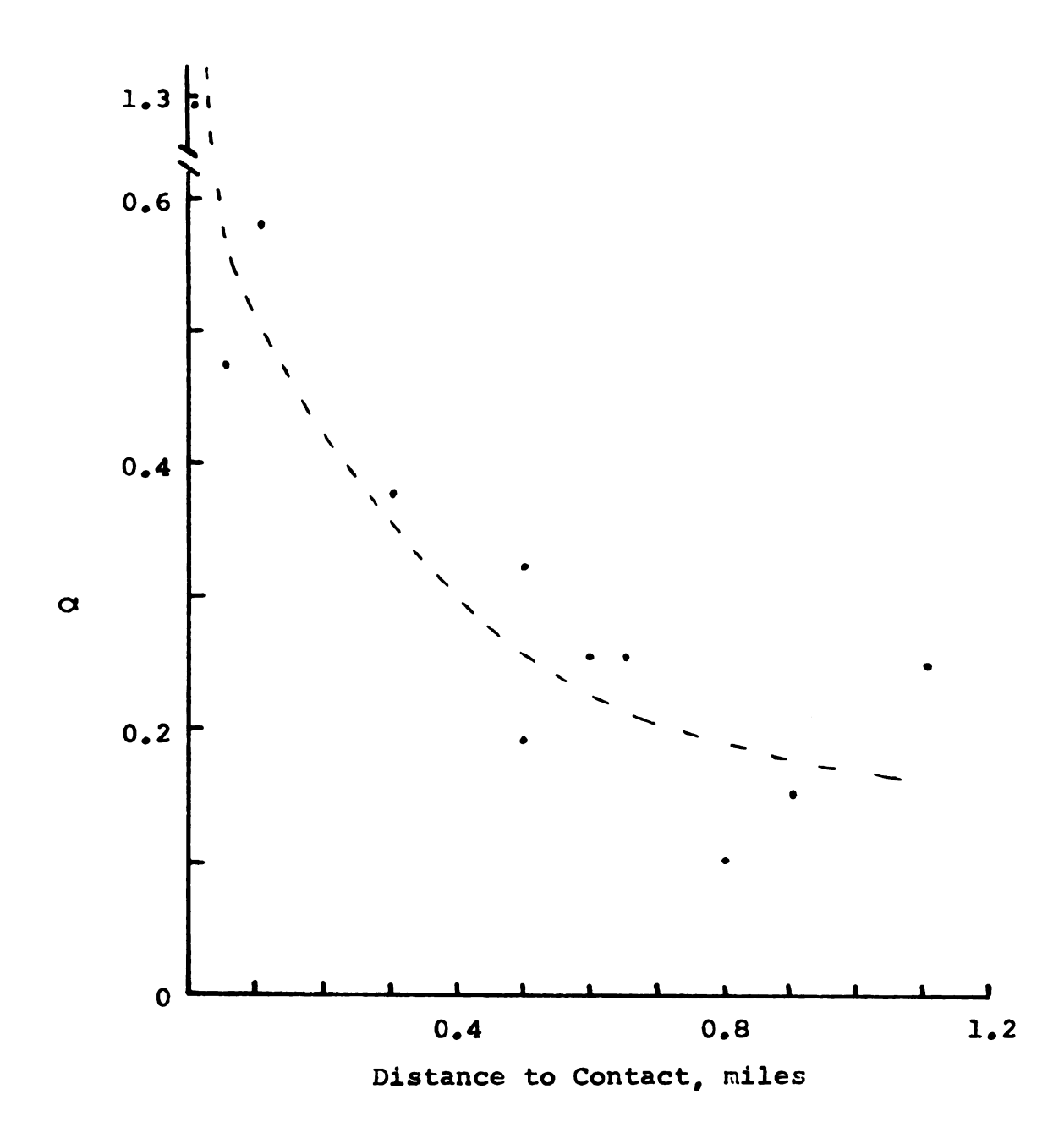


Figure 4-15. Q ratios versus distance from south contact in the monzonite pluton.

monzonite pluton at the time of crystallization. As a result the grain size of the magnetite would be more homogeneous, leading to homogeneity in the stability of the remanence, and more uniform remanence within the quartz monzonite as observed.

4.6 Paleomagnetism

The determination of paleomagnetic poles has allowed geophysicists, as well as geologists, to reconstruct past events. Paleo-poles can be used to date magnetic rock units if certain structural relationships are known, or they can be used to decipher the structural history, if the age of the magnetic rock unit is known.

The age of the Melrose Stock is known to be early Cretaceous, or perhaps late Jurassic. The position of the Cretaceous paleo-magnetic pole with respect to North America is fairly well defined at 180°W, 64°N (Strangway, 1970). The limited scattered paleomagnetic data from known Jurassic rocks suggests that there may be little difference in the pole positions of the two geologic periods.

With the age of the intrusive known, the tectonic movement (rotation) can be determined. The Melrose Stock is part of a horst which has a strike of N16°E. Snow (1963) has indicated that the fault block has been rotated approximately 15°, upthrown on the west side and downthrown on the east, which is based on the orientation of sediments overlying the intrusive. This evidence may not be

conclusive due to distortion of the beds when the intrusive was emplaced as readily seen by the upturned beds along the southern margin of intrusive. However, the fault, which nearly parallels the range on the east side (Figure 1-2) and repeats the volcanic-intrusive sequence in outcrop, indicates the east side to be downthrown.

The paleo-pole position of the Cretaceous period and the poles obtained from the 1970 data with structural rotation are shown in Figure 4-16 and the corresponding numerical values are listed in Table 4-8. These are calculated from the NRM values of specimens collected in 1970 (the demagnetized positions differ little from the NRM). The positions of the NRM poles after 10°, 15° and 20° of rotation about an axis of N16°E, the strike of the horst which includes the Melrose Stock, are shown in sequence. To obtain the pole positions shown in Figure 4-16, the NRM vector was rotated to the west or the horst was uplifted on the west in order for the pole position to approach the Cretaceous pole. Therefore, the horst was originally differentially uplifted on the east during the Basin and Range faulting.

Both rock unit poles prior to application of the rotation are approximately the same distance from the Cretaceous pole. A structural rotation of 15° brings the monzonite pole to within 4° of great circle arc of the Cretaceous pole position while the quartz monzonite and the average of 1970 site poles do not closely approach the

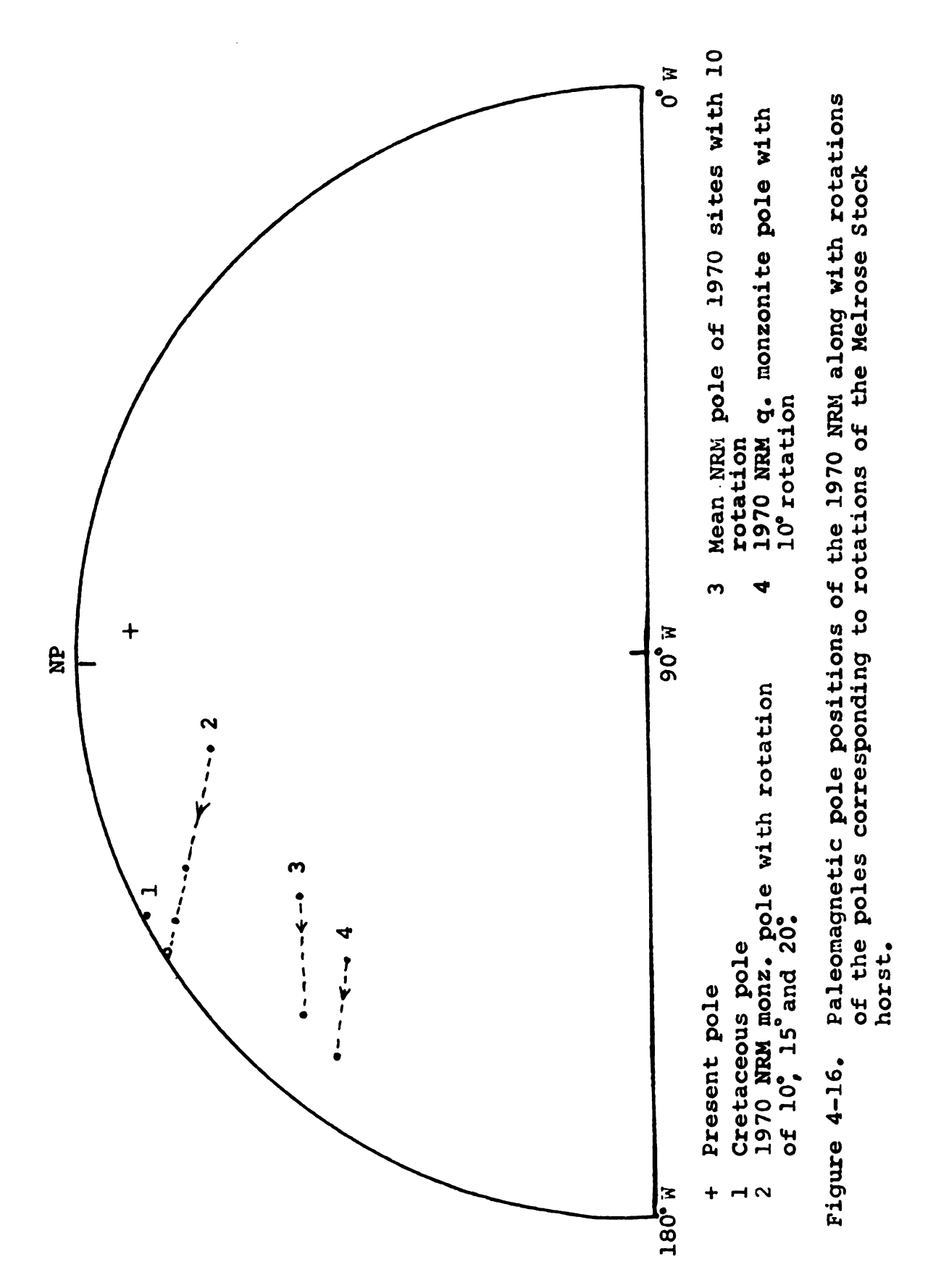


Table 4-8. Paleomagnetic poles determined from the 1970 NRM results.

Cretaceous	68n, 180w
1970 sites	48N, 139W
10° rotation	43N, 103W
1970 monzonite	65N, 115W
10° rotation	64N, 155W
15° "	61N, 171W
20° "	57N, 179E
1970 Q. monzonite	41N, 148W
10° rotation	38N, 168W

Cretaceous pole.

The position of the monzonite pole is nearly on a great circle with the quartz monzonite and present pole positions. This suggests migration of the poles due to VRM, although the storage tests do not indicate one rock type to be more susceptible to VRM than the other. Also, the monzonite pole is nearly in between the Cretaceous and the present magnetic pole positions. Unfortunately, no conclusive statement can be made regarding the position of the monzonite pole. It may have migrated from the Cretaceous pole position or the quartz monzonite position or it may represent its primary remanent magnetization position.

The different pole positions of the two major rock types of the stock may represent the magnetic field at two different times. The monzonite pole position with a 15° rotation nearly coincides with the established Cretaceous pole of North America. The quartz monzonite, which is thought to have been emplaced later, may have crystallized at a sufficiently different time to have taken on a different remanent direction. The age date of the Melrose Stock was determined on the monzonite pluton. In a composite batholith such as the Boulder Batholith, emplacement of individual plutons can take place over a time span of 10 m.y. (Tilling and others., 1968). It is not suggested that emplacement of the two exposed plutons in the Melrose Stock required that time interval. It

does, however, lend support to the suggestion that the relative position of the magnetic north pole may have changed. Secular variations of the field may be responsible for the difference between the two pole positions, however, the period of the secular variation is in the order of thousands of years and hence should be averaged out on the time scale for the emplacement and cooling of the Melrose Stock.

The structural rotation of the Melrose Stock as determined from the remanent magnetism is in the opposite sense to the geological interpretation by Snow. Both the paleomagnetic and Snow's method are subject to error and with the present data, the conflict cannot be resolved.

CHAPTER V

SUMMARY

As a result of this study a better understanding has been obtained of the many factors which play a role in determining the ultimate magnetic expression of an igneous intrusive. The Melrose Stock provided the evidence that permitted the answering of many questions and at the same time the evidence brought an awareness that there is much more work needed to be done on igneous intrusives. Hopefully, the Melrose Stock will serve as a representative model for future academic and commercial investigations of intrusives in the Basin and Range Province.

The Melrose Stock was emplaced into Permian sediments. The injection of magma into the host rock was forceful as evidenced by upturned sediments and cataclastic textures revealed microscopically. The magma must have been largely a crystal mush at the time of emplacement because of the minor reaction with the host and common occurrence of xenoliths. However, the assimilation of the carbonate host rock did modify the magma locally which is reflected in the iron oxides. The exposed portion of the Melrose

Stock shows it to be comprised of at least two plutons of monzonite and quartz monzonite compositions. A radiogenic age date of the monzonite pluton places it as very early Cretaceous and it is considered to be the older of the two plutons.

From the evidence of the association coefficient, it is surmised that the monzonite pluton had a shorter crystallization history than the quartz monzonite pluton. The magnetic minerals appear to have had a long history of formation. The growth of the magnetite was genetically related to the formation of the ferromagnesian minerals. Magnetite was found to have a much greater association to hornblende than any other constituent mineral in the rock. Magnetite formed by three processes as indicated by the association coefficients. These are direct preciptation, oxidation reactions and hydrothermal or deuteric alteration. The percentage of magnetite formed in these three ways can be estimated from the association parameter. The relative crystallization sequence of each pluton was portrayed from the evidence of the association coefficient and petrographic observations.

The important magnetic minerals found in the Melrose Stock are ilmenite, which in some cases has exsolved hematite, and a pure magnetite. The opaque content in the monzonite is 2.1 percent and 1.2 percent in the quartz monzonite. The ilmenite averages 10 percent of the opaque assemblage and is not preferentially distributed with

respect to rock type. In both rock types, the opaques associated with the ferromagnesian fraction have a larger grain size than the opaques associated with the quartz-feldspar fraction. In addition, the quartz monzonite has a larger grain size distribution than the monzonite. The larger size distributions are thought to reflect both the availability of iron and the time available for growth. The variation of the interstitial-inclusion index revealed that the relative intergranular nature of magnetite most likely changed in response to the viscosity of the consolidating magma.

The magnetic properties of the Melrose Stock were delineated by rock type. The magnetic susceptibility of the quartz monzonite is 2,000 x 10⁻⁶ cgs units and the monzonite is $3,200 \times 10^{-6}$ cgs units. These values are an average of values determined by in situ and specimen core methods. Both methods agree within 10 percent of each other. The susceptibility means are suspected to be lower than the true value. Weathering has reduced the susceptibility by an estimated 30 to 40 percent. The monzonite appears to be more susceptible to the effects of weathering than the quartz monzonite. The areal susceptibility distribution does not correlate with the aeromagnetic pattern. There are two notable areas within the stock where the susceptibility distribution in the subsurface is appreciably less than on the outcrop surface. This is not thought to be influenced by the remanent

magnetization.

The results of the remanent magnetization study were not totally satisfying. The remanence of these igneous rocks, not unexpectedly, was rather unstable and soft and possessed large components of VRM. Significant dispersion was added to the remanence by storage in the laboratory. However, a combination storage-demagnetization test revealed that a 50 oersted demagnetizing field to be sufficient for removing VRM acquired in the specimens stored for 18 months. Progressive demagnetization of nine sites showed 50 oersteds gave minimum dispersion of the site's remanent direction. When the site directions were statistically analyzed in various lithologic and time of collection combinations, it was found that the NRM results were as good or better than the demagnetized results. This reflects the unstable nature of the remanence that is commonly found in coarse grained granitic rocks. Hence, the reliability of the remanent magnetization for paleomagnetic interpretation is open to question.

Two remanent directions were obtained, one for each pluton of the stock. The remanent directions remained nearly stationary with demagnetization at 50 and 100 oersteds. The storage test showed the NRM to change by as much as 50 percent in three months and demagnetization to 100 oersteds removed approximately two-thirds of the NRM. This may indicate that a higher demagnetization

level is necessary to remove the VRM acquired through "geologic storage" in the field. Unfortunately, the specimens were very susceptible to picking up spurious moments of magnetization during demagnetization, especially at fields greater than 50 oersteds. If the two remanent directions are different, they may represent the position of the earth's magnetic field at different times.

The 1970 remanent data were used to determine the structural rotation of the horst of which the Melrose Stock is a part. The data indicate the Dolly Varden Range to be upthrown on the east and downthrown on the west side. This conflicts with the geological interpretation by Snow. Both interpretations are subject to error and cannot be resolved without further investigation.

The geometry of the intrusive has had a number of effects on the magnetic minerals of the Melrose Stock.

It was found that near the southern margin of the stock sphene was much more abundant than elsewhere in the stock. This is a result of the influence of the carbonate host providing calcium and the breakdown of ilmenite providing the titanium to form sphene. In the lowest portion of the stock and away from known contacts, ilmenite showed exsolution of hematite, presumably in response to slow cooling deep within the magma chamber. These two observations give the stock a zoned character and allow

conjecture to the size and amount of the stock removed by erosion.

Within the quartz monzonite pluton the interstitial-inclusion index increases with elevation, an observation presumably indicative of lower viscosity higher in the magma chamber. This is supported by a decreasing quartz content at higher elevations. Both the susceptibility and hornblende association also increase upwards in the quartz monzonite pluton. These are related to each other and are thought to represent the effects of a more oxidizing atmosphere higher in the magma chamber. The variation of the pO₂ with elevation could either reflect concentration of the volatile phase to the upper portions of the magma chamber or the assimilation of the sedimentary host rock.

The only expression of geometric effects within the monzonite pluton was on the Q ratios. Apparently the monzonite had a larger temperature differential with the host rock than did the quartz monzonite, for the former shows an exponential decrease of Q away from the southern margin contact.

There were sufficient data so as to permit suggestions regarding sampling guidelines for magnetic susceptibility. Susceptibility measurements were made both in situ and on specimen cores with a volume difference of eighty times.

Twice as many data were rejected as anomalous for

the specimen cores in comparison to the in situ method. The capacity to delineate magnetic units is in favor of the in situ method. This points out that the larger the sample volume, the greater the chances of having better quality data and of separating magnetic units. It was found that the number of sites sampled was more important than the number of samples per sites. Two or three in situ measurements per site was sufficient, but it involves little expenditure of time to take a few additional measurements. A site density of one site per square mile was determined to be sufficient in order to obtain a representative susceptibility for an intrusive such as the Melrose Stock. Also, this density gives the investigator the opportunity of detecting multiple pluton intrusives.

From the integrated approach of this thesis, it is believed that a significant amount of information was obtained which has led to a clearer picture of events in the history of the Melrose Stock than would have been possible by independent approaches of geophysics and petrology. Obviously, many points were not fully answered due to insufficient data and knowledge. Further insight would be gained by pursuing the geochemical aspects of this investigation. However, the scope of this investigation did reveal a much better understanding of the magnetic properties of an igneous intrusive.



REFERENCES CITED

- Armstrong, R.L., 1963, Geochronology and Geology of the Eastern Great Basin (Ph.D. thesis): New Haven, Yale University.
- As, J.A. and Zijderveld, J.D.A., 1958, Magnetic Cleaning of Rocks in Paleomagnetic Research: Geophys. Jour., v. 1, p. 308-319.
- Books, K.G., 1962, Remanent Magnetism as a Contributor to Some Aeromagnetic Anomalies: Geophys., v. 27, p. 359-375.
- Buddington, A.F., and Lindsley, D.H., 1964, Iron-Titanium Oxide Minerals and Synthetic Equivalents: Jour. Petrol., v. 5, p. 310-357.
- Carmichael, I.S.E., 1963, The Occurrence of Magnesian Pyroxenes and Magnetite in Porphyritic Acid Glasses: Mineral. Mag., v. 33, p. 394-403.
- Carmichael, I.S.E., 1967, The Iron-Titanium Oxides of Salic Volcanic Rocks and their Associated Ferromagnesian Silicates: Contr. Mineral. and Petrol., v. 14, p. 36-64.
- Carmichael, I.S.E. and Nicholls, J., 1967, Iron-Titanium Oxides and Oxygen Fugacities in Volcanic Rocks: Jour. Geophys. Research, v. 72, p. 4665-4687.
- Case, J.E., 1966, Geophysical Anomalies over Precambrian Rocks, Northwestern Uncompangre Plateau, Utah and Colorada: Bull. Amer. Assoc. Petroleum Geologists, v. 50, p. 1423-1443.
- Chikazumi, S., 1964, Physics of Magnetism: New York, John Wiley and Sons, Inc., 554p.
- Currie, R.G., Gromme, C.S., and Verhoogen, J., 1963, Remanent Magnetization of Some Upper Cretaceous Granitic Plutons in the Sierra Nevada, California: Jour. Geophys. Research, v. 68, p. 2263-2279.

- Czamanske, G.K. and Wones, D.R., 1970, Amphiboles as Indicators of Oxidation during Magmatic Differentiation: Geol. Soc. Am. Abs. with Programs, v. 2, p. 531.
- Doell, R.D., and Cox, A., 1967, Paleomagnetic Sampling with a Portable Coring Drill, in Collinson, D.W., Creer, K.M., and Runcorn, S.K., eds., Methods in Paleomagnetism: New York, American Elsevier Publ. Co., p. 21-25.
- Emmons, S.F., 1877, Descriptive Geology: Geological Exploration of the Fortieth Parallel, v. 2, p. 476-483.
- Fisher, R.A., 1953, Dispersion on a Sphere: Proc. Roy. Soc. London, v. 217, p. 295-305.
- Flinn, D., 1969, Grain Contacts in Crystalline Rocks: Lithos, v. 3, p. 361-370.
- Gromme, C.S., and Merrill, R.T., 1965, Paleomagnetism of Late Cretaceous Granitic Plutons in the Sierra Nevada, California: Further Results: Jour. Geophys. Research, v. 70, p. 3407-3420.
- Gromme, C.S., Merrill, R.T., and Verhoogen, J., 1967,
 Paleomagnetism of Jurassic and Cretaceous Plutonic
 Rocks in the Sierra Nevada, California, and
 Its Significance for Polar Wandering and Continental Drift: Jour. Geophys. Research, v. 72, p. 56615684.
- Hanna, W.F., 1969, Negative Aeromagnetic Anomalies over Mineralized Areas of the Boulder Batholith, Montana: U.S. Geol. Survey Prof. Paper 650-D p. D159-D167.
- Hanna, W.F., 1970, Personal Communication.
- Hill, S.M., 1916, Notes on Some Mining Districts in Eastern Nevada: U.S. Geol. Survey Bull. 648, p. 78-88.
- Irving, E., 1964, Paleomagnetism and Its Application to Geological and Geophysical Problems: New York, John Wiley and Sons, Inc., p. 399.
- Irving, E., Molyneux, L., and Runcorn, S.K., 1966, The Analysis of Remanent Magnetization and Susceptibilities of Rocks: Geophys. Jour., v. 10, p. 451-464.

- Koenigsberger, J.G., 1938, Natural Residual Magnetism of Eruptive Rocks, parts I and II: Terr. Mag. Atmos. Elec., v. 43, p. 119-127 and 299-320.
- Kretz, R., 1969, On the Spatial Distribution of Crystals in Rocks: Lithos, v. 2, p. 33-66.
- Larson, E., Ozima, M., Ozima, M., Nagata, T., and Strangway, D., 1969, Stability of Remanent Magnetization of Igneous Rocks: Geophys. Jour. Royal Astr. Soc., v. 17, p. 263-292.
- May, B.T., 1968, Magnetic Properties of Rocks Associated with the New Cornelia Porphyry Copper Deposit, Pima County, Arizona (Ph.D. thesis): Tucson, University of Arizona, 159 p.
- Mooney, H.M. and Bleifuss, R., 1953, Magnetic Susceptibility Measurements in Minnesota Part II: Analysis of Field Results: Geophysics, v. 18, p. 383-393.
- Nagata, T., 1961, Rock Magnetism: Tokyo, Maruzen Co. Ltd., 350 p.
- Opdyke, N.D. and Wensink, H., 1966, Paleomagnetism of Rock from the White Mountain Plutonic-Volcanic Series in New Hampshire and Vermont: Jour. Geophys. Research, v. 71, p. 3045-3051.
- Pothacamury, I., 1970, Magnetic Properties of the Boulder Batholith near Helena, Montana and their Use in Magnetic Interpretation (M.S. thesis): East Lansing, Michigan State University, 64 p.
- Rimbert, F., 1958, Thesis, University of Paris.
- Runcorn, S.K., 1967, Statistical Discussion of Magnetization of Rock Samples, in Collinson, D.W., Creer, K.M., and Runcorn, S.K., eds., Methods in Paleomagnetism: New York, American Elsevier Publ. Co., p. 329-339.
- Shandley, P.D. and Bacon, L.O., 1966, Analysis for Magnetite Utilizing Magnetic Susceptibility: Geophysics, v. 31 p. 398-409.
- Slichter, L.B., 1929, Certain Aspects of Magnetic Surveying: A.I.M.E. Trans, v. 81, p. 238.
- Snow, G.G., 1963, Mineralogy and Geology of the Dolly Varden Mountains, Elko County, Nevada (Ph.D. thesis): Salt Lake City, University of Utah, 153 p.

- Strangway, D.W., 1967, Magnetic Characteristics of Rocks, in Mining Geophysics, Volume II (theory): Tulsa, Soc. Explor. Geophysicists. p. 454-473.
- Strangway, D.W., 1970, History of the Earth's Magnetic Field: New York, McGraw-Hill Book Co., 168 p.
- Thellier, E., 1951, Propietes magnetiques des terres cuites et des roches: Jour. Physique et Radium, v. 12, p. 205-218.
- Tilling, R.T., Klepper, M.R., and Obradovich, J.D., 1968, K-Ar Ages and Time Span of Emplacement of the Boulder Batholith, Montana: Am. Jour. Sci., v. 266, p. 671-689.
- Verhoogen, J., 1962, Distribution of Titanium between Silicates and Oxides in Igneous Rocks: Am. Jour. Sci., v. 260, p. 211-220.
- Zietz, I., Bateman, P.C., Case, J.E., Crittenden, M.D. Jr., Griscom, A., King, E.R., Roberts, R.J., and Lerentzen, G.R., 1968, Aeromagnetic Investigation of Crustal Structure for a strip across the Western United States: Geol. Soc. Am. Bull., v. 80, p. 1703-1714.
- Zirkel, F., 1876, Microscopic Petrography: Geological Exploration of the Fourtieth Parallel, v. 6, p. 49, 166-167.



APPENDIX A

GENERAL REMARKS ON MAGNETIC PROPERTIES

APPENDIX A

GENERAL REMARKS ON MAGNETIC PROPERTIES

Magnetic Minerals

Most igneous rocks contain ferromagnetic minerals which lead to both induced and remanent magnetism. Ideally, the latter can be used to determine certain aspects of the rock's history providing this magnetism is sufficiently large and stable. The magnetic memory stored in a rock's remanent magnetization can be modified subsequent to acquisition; these modifications may or may not be desirable depending on the objectives of the particular investigation. Information is retrieved from the magnetic memory of the rock held in the iron-titanium oxides which are generally a minor constituent of the rock's total volume. The most important magnetic minerals fall into two crystallographic systems, the cubic and rhombohedral. According to their atomic and magnetic structures, these minerals are either ferromagnetic or antiferromagnetic.

The most common and important magnetic mineral is magnetite. Though it has the capacity to acquire

large amounts of remanent magnetism, it is not necessarily able to retain it, especially when coarse grained.

If titanium is available under proper physical-chemical conditions, it can reside in the inverse spinel structure which may form a solid solution with magnetite.

This gives rise to the titanomagnetite series with ulvospinel and magnetite as end members. The magnetic properties are diminished with increasing titanium content.

Also forming a series with magnetite is maghemite (Y Fe₂O₃), a low temperature variety of hematite which has an inverse spinel structure. It possesses magnetic properties similar to that of magnetite, but it is thermally unstable and reverts to the more stable but less magnetic hematite, the change involving a structural transition from the cubic to rhombohedral system.

Ilmenite and hematite occur in the rhombohedral crystal system and are end members of a continuous series. Hematite has no titanium in its structure, and it is much less magnetic than most titanomagnetites. However, it has a very strong coercive force and hence has a stable remanence. Ilmenite is an accessory to the magnetic properties of a rock for it is essentially non-magnetic, however, the physical relationship of ilmenite to magnetic minerals can affect their overall magnetic properties.

The hydrous iron oxide, goethite, generally a product of surface alteration of magnetite or ilmenite, can

carry a weak but stable remanence when cooled from moderate temperatures in the presence of a magnetic field. The magnetic susceptibility of goethite is negligible in contrast to that of magnetite.

The compositional relationship of the magnetic minerals to each other is shown in Figure A-1, the FeO-Fe $_2$ O $_3$ -TiO ternary system.

Remanent Magnetization

Natural remanent magnetism (NRM) is the remanence possessed by a specimen in its natural state in the field while the primary remanent magnetization is the magnetism that was acquired at the time of the rock's formation. The NRM and primary magnetization are not necessarily equivalent because of changes in the remanence following acquisition of the primary magnetization. Furthermore, the NRM can be altered subsequent to collection of the specimens. A brief outline of the various types of remanent magnetization that NRM can include follows.

The acquisition of remanent magnetism by cooling a mineral through its Curie point is referred to as thermo-remanent magnetization (TRM). The majority of the TRM is acquired near the Curie point, but due to a spectrum of blocking tempertures, the TRM is actually acquired over a wide range of tempertures below the Curie point. Thellier (1951) found that the TRM acquired in any temperature interval is independent of the TRM obtained in

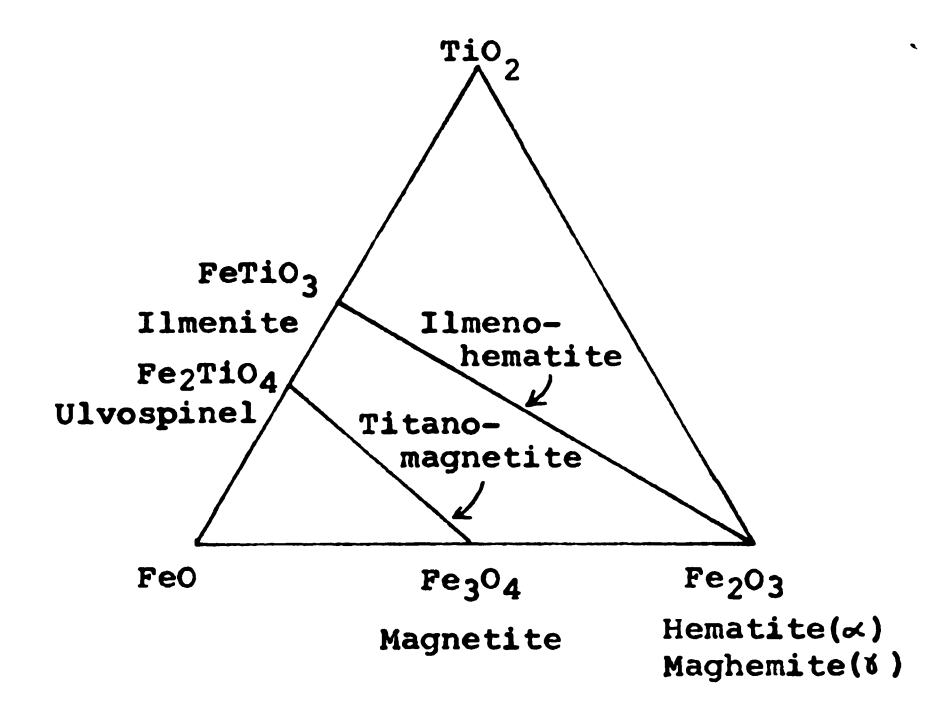


Figure A-1. Compositional relationships of the major magnetic minerals.

other temperature intervals. This led to the property of partial thermoremanent magnetization (PTRM) being simply an additive phenomenom. The stability of TRM appears to vary inversely with the size of the magnetic minerals in the rock.

Remanence obtained at a constant temperature gives rise to isothermal remanent magnetization (IRM). One variety of IRM is ARM, anhysteritic remanent magnetization, which is acquired by a magnetic material in the presence of an ambient field with a superimposed decaying alternating field. The acquisition of a component of remanent magnetization as a result of a specimen remaining in a constant magnetic field for a period of time is known as viscous remanent magnetization (VRM), the time dependent variety of IRM.

During a chemical reaction involving a magnetic mineral, a remanence can be acquired which is termed chemical remanent magnetization (CRM). A remanence also can be obtained from the deposition (DRM) of magnetic minerals in the genesis of a sedimentary rock.

In order to obtain the primary remanent magnetism of igneous rocks, which is generally TRM, it is necessary to magnetically "clean" the rocks. VRM is present in various proportions and can actually mask the original TRM direction so that the NRM direction is almost diametrically opposed to the TRM direction (Opdyke and Wensink, 1966). Two basic methods are available for the

recovery of the primary magnetization, alternating field (af) and thermal demagnetization. The af demagnetization technique was employed in this study for it is generally faster and easier and does not lead to mineralogic changes which may occur during heating of specimens. However, the thermal method can give an insight into the magnetic minerals present in the rock.

Magnetic Susceptibility

Induced magnetization is developed in a substance in response to an applied magnetic field and is lost upon removal of the inducing field. The intensity of magnetization (M) is related to inducing field (H) by the constant (k) which is the magnetic susceptibility;

M=kH

For inducing fields of less than a few oersteds, the magnetic susceptibility remains relatively constant. In magnetically isotropic material the direction of the induced magnetization is parallel to the inducing field and in anisotropic material the two vector quantities may be in slightly different directions.

Magnetic susceptibility is a function of a mineral's composition. Specifically, the presence of titanium in both iron-titanium series decreases the susceptibility. The rhombohedral and hydrous iron oxides contribute little to the overall susceptibility of a rock.

Even with a fixed composition and volume of magnetic

wary in a complex way with such factors as percent remanent saturation, grain size and exsolution. An increase in remanence in a rock is accompanied by a decrease in susceptibility (Shandley and Bacon, 1963). It is well known that as the grain size of the magnetite decreases so does the susceptibility. Shandley and Bacon (1963) determined a critical size limit dependence below 40 microns. In a closely related manner, exsolution tends to divide or partition a magnetic mineral into smaller subgrains which in turn expresses the behavior of many small grains.

The description of magnetic susceptibility and remanent magnetism presented here is quite brief, serving as only an introduction to this subject; for further information the reader is referred to several texts on the subject, (Nagata, 1961; Chikizumi, 1964; Strangway, 1967 and 1970).

APPENDIX B OPAQUE MINERAL SPECIES AND THEIR RELATIVE ABUNDANCE

APPENDIX B

OPAQUE MINERAL SPECIES AND THEIR RELATIVE ABUNDANCE

Table A-1. Opaque Data

Site	Magnetite	Ilmenite	Limonite	Hematite	Maghemite	Sphene
1	70	15	15	-	-	С
2	60	40	-	-	-	-
3	75	10	15	-	-	-
4	80	20	-	-	-	С
5	85	15	-	-	-	С
6	85	7	8	-	-	m
7	70	5	25	-	-	-
8	70	2	28	-		m
9	85	2	13	-	-	30 .
10	75	25	-	-	-	n
11	60	40	-	-	-	n
12	85	3	12	•		
13	75	15	10	-	-	m
14	-	-	100	-	-	c
15	80	2	18	-	-	m
16	78	x 15	5	2	-	M
17	75	x2 0	5	-	-	m
19	80	15	5	-	-	m
20	90	1	9	-	-	c
21	75	15	10	-	-	С

Site	Magnetite	Ilmenite	Limonite	Hematite	Maghemite	Sphene
22	80	10	10	-	-	C
23	85	x12	-	3	-	-
24	83	x10	5	2	-	-
25	92	x 3	5	-	-	C
26	80	x 15	5	-	-	m
27	85	x 10	5	-	-	c
28	83	x 2	3	10	-	-
29	82	x13	2	3	-	m
30	75	x 7	4	7	7	m
30A	80	x 10	5	5	m	m
31	75	x 7	3	15	-	m
32	70	5	15	10		-
33	99	-	-	1	-	c
34	93	5	-	2	-	C
40	90	8	2	-	-	m
41	85	15	-	-	-	-
42	78	20	2	-	-	С
43	85	5	10	-	-	m
44	95	2	2	1	-	С
45	80	x 20	-	-	-	-
46	89	x 8	-	3	-	m
47	90	10	-	-	-	m

x ilmenite with exsolution

c common or rich, approximately 1% m minor, approximately ½% - trace or absent

APPENDIX C

NRM RESULTS BY SITE

APPENDIX C

NRM RESULTS BY SITE

Table A-2. NRM Data

	Rejected to	Cir. con.		After removal of		
Site	total	before after		anomalous data		
	specimens	reje	ction	Dec.	Inc.	Int.
1	2/6	99.1	63.9	9.4	55.3	4.95
2	1/8	52.8	49.0	84.8	55.9	3.44
3	0/6	127.5	127.5	355.4	65.7	4.52
4	0/7	41.6	41.6	327.3	47.7	2.73
5	1/6	91.3	151.5	304.9	30.2	2.39
6	1/7	48.1	49.4	146.9	- 0.9	5.17
7	0/6	14.0	14.0	325.9	77.1	3.15
8	2/5	112.8	70.7	160.7	71.1	3.93
9	1/6	80.3	118.2	92.7	77.8	4.67
10	1/6	45.5	37.4	219.7	52.1	2.88
11	0/6	19.3	19.3	350.7	71.5	1.54
12	1/5	33.3	39.0	62.5	74.8	5.07
13	1/6	53.9	40.8	267.4	60.3	2.32
14	0/4	40.3	40.3	321.1	55.1	3.49
15	1/6	27.0	15.1	59.5	61.3	18.60
16	1/7	69.5	95.7	69.4	35.5	2.14
17	1/6	83.8	89.6	51.6	63.2	3.31
19	5/13	47.3	40.0	1.5	55.0	9.25

	Rejected to	Cir. Con.		After removal of		
Site	total	before after		anomalous data		
	specimens	rejec	tion	Dec.	Inc.	Int.
20	2/14	12.1	13.8	333.2	74.6	11.00
21	3/13	23.4	11.6	3.4	79.1	5.65
22	3/13	18.6	10.8	354.5	61.7	3.64
23	3/11	42.2	46.2	44.7	75.1	6.30
24	3/11	35.1	23.3	13.2	85.9	1.92
25	0/13	19.5	19.5	163.0	80.0	1.46
26	0/15	14.8	14.8	327.1	78.7	4.95
27	1/12	26.6	27.7	276.9	65.4	9.30
28	0/10	25.1	25.1	355.0	77.9	1.91
29	5/10	50.3	45.4	256.0	43.0	7.04
30	0/11	25.1	25.1	88.3	84.0	1.86
31	3/10	67.2	18.6	160.0	84.9	1.47
33	0/6	24.8	24.8	85.2	71.5	2.19
34	0/9	11.9	11.9	314.8	52.0	2.45
45	3/7	47.5	24.9	282.7	34.9	9.03
46	1/8	62.9	46.0	352.5	55.3	2.84

Intensity, $x 10^{-4}$ emu/cc

Circle of confidence, declination, and inclination in degrees

